

Doctoral thesis

Doctoral theses at NTNU, 2020:396

Noëmi Ambauen

Removal of organic pollutants from landfill leachate by electrochemical oxidation

Assessment of performance and applicability
in Northern Norway

NTNU
Norwegian University of Science and Technology
Thesis for the Degree of
Philosophiae Doctor
Faculty of Engineering
Department of Civil and Environmental
Engineering



Norwegian University of
Science and Technology

Noëmi Ambauen

Removal of organic pollutants from landfill leachate by electrochemical oxidation

Assessment of performance and
applicability in Northern Norway

Thesis for the Degree of Philosophiae Doctor

Trondheim, December 2020

Norwegian University of Science and Technology
Faculty of Engineering
Department of Civil and Environmental Engineering



Norwegian University of
Science and Technology

NTNU

Norwegian University of Science and Technology

Thesis for the Degree of Philosophiae Doctor

Faculty of Engineering

Department of Civil and Environmental Engineering

© Noëmi Ambauen

ISBN 978-82-326-5138-2 (printed ver.)

ISBN 978-82-326-5139-9 (electronic ver.)

ISSN 2703-8084 (online)

ISSN 1503-8181 (printed ver.)

Doctoral theses at NTNU, 2020:396

Printed by NTNU Grafisk senter

ABSTRACT

Landfill leachate treatment by advanced oxidation processes has gained much attention in the past decades. The removal of organic pollutants from landfill leachate in particular has been in focus due to their detrimental effects on the environment. This fact also leads to increasingly stringent regulations put in place by the authorities regarding the pollutant removal and adherence to treatment goals. More stringent regulations for landfill leachate treatment are also expected to be effective in Norway in the near future. The new regulations contain a list of priority substances that need to be removed below their detection limit in order to release the effluent after treatment into nearby waterbodies. An appropriate treatment process that is able to accomplish the treatment goals and takes the given local climate conditions into consideration is required. Low average temperatures in subarctic climates provide a significant challenge.

The motivation of the present thesis was to find a suitable landfill leachate treatment process that is able to remove priority substances while withstanding cold operating temperatures. An extended literature study was the basis for choosing electrochemical oxidation, an advanced oxidation process, as a suitable treatment process. The majority of electrochemical oxidation studies have been carried out at room or elevated temperatures, while there is a lack of focus on wastewater treatment in cold climates. Furthermore, none assessed the application of advanced oxidation processes. This thesis bridges this knowledge gap and contributes to the applied field of electrochemistry by assessing its applicability under cold operating temperatures. The work is therefore of great interest in light of the increased focus on the technology in arctic regions.

This thesis consists of three separate studies:

1. A mechanistic study that helps to understand the ongoing different oxidation processes during the electrochemical oxidation of organic pollutants.
2. A laboratory scale study with a model organic pollutant from the priority list where the influence of different parameters on its oxidation was assessed, with a special focus on temperature.
3. A laboratory scale study with pre-treated landfill leachate that contains the same model organic pollutant, where the matrix effect and more applied parameters were assessed under cold climate conditions.

The mechanistic study of the model pollutant salicylic acid confirmed that three different oxidation pathways take place during the electrochemical oxidation: Direct electron transfer from the pollutant to the electrode surface, electrochemical oxygen transfer reaction from hydroxyl radical to the organic pollutant, and mediated oxidation via an intermediately formed oxidant, such as active chlorine. Density functional and natural bond theory were able to successfully predict the salicylic acid intermediates that were formed during electrochemical oxidation.

In the second study, Bisphenol A (5 μM) was used as the model compound as it is listed on the Norwegian priority substance list. Complete removal of Bisphenol A was achieved at low temperatures (6 $^{\circ}\text{C}$) with the major drawback of extended treatment times. Besides temperature, pH also had a significant effect on the removal of Bisphenol A, and an alkaline pH (10) was found to be favourable. The anode material was found to have a major impact on the formation of disinfection by-products, favouring perchlorate formation on BDD anodes and trihalomethanes on Pt.

The final study confirmed increased treatment times at low operating temperatures (6 $^{\circ}\text{C}$). The study further showed that a relatively high current density (43 mA/cm^2) has to be applied in order to achieve complete Bisphenol A removal (5 μM) from the landfill leachate. The matrix effect of the landfill leachate disclosed lower Bisphenol A degradation rates compared to the ones obtained in the second study in clean electrolyte (3.3 mM NaCl & 0.3 mM Na_2SO_4). Formation of disinfection by-products increased with the application of higher current densities (10 – 86 mA/cm^2) and temperatures (6 – 20 $^{\circ}\text{C}$) while the anode material influenced their nature as previously.

The results of the three studies show that electrochemical oxidation is able to remove Bisphenol A from landfill leachate under cold operating temperatures. Treatment goals regarding Bisphenol A, given by the Norwegian authorities, were satisfied and indicate that results are transferrable to other organic compounds on the priority list. The major drawback are the increased treatment times, which subsequently result in higher energy demands, and ultimately in higher costs. Norway is a country driven by hydropower and lower electricity prices than the rest of Europe, so electrochemical oxidation is still a sustainable and economically feasible choice. Attention has to be paid to the choice of electrode material as they are a major matter of expense as well as influencing the disinfection by-products that are formed. This work sets

precedent with regards to applicability of electrochemical advanced oxidation processes under cold operating temperatures.

PREFACE

This thesis is submitted to the Norwegian University of Science and Technology (NTNU), Trondheim for partial fulfilment of the requirements for the degree of Philosophiae Doctor (PhD).

The work presented in the thesis is the result of a four-year PhD program, which was conducted at the Department of Civil and Environmental Engineering, NTNU, Trondheim. Ass. Prof. Thomas Meyn has been the main supervisor and Ass. Prof. Cynthia Hallé and Ass. Prof. Jens Muff (Aalborg University, Denmark) have been the co-supervisors.

The PhD project has been funded by the Norwegian University of Science & Technology (NTNU) and the Søndre Helgelands Miljøverk IKS (SHMIL), a waste management company located in Northern Norway (Åremma).

In accordance with the guidelines of the Faculty of Engineering Science and Technology, the thesis contains an introduction to, and includes, 3 scientific journal papers, 1 conference paper and 1 conference poster (listed on page xvii).

ACKNOWLEDGEMENTS

The past 5 years have been a roller coaster with many ups and downs. This journey brought me together with many different people in various fields and for various reasons. I am very grateful to have met all of them as they supported me in all kind of ways.

First and foremost, I would like to thank my main supervisor Ass. Prof. Thomas Meyn and my co-supervisor Ass. Prof. Cynthia Hallé at NTNU for their invaluable support throughout the past years. Both always had an open door and listen to my problems and offered their help wherever they could. They never spared a meeting discussing what seems to be a tiny problem for hours. Thomas, thank you for always fighting for my cause and for acquiring all the resources that I needed along the way in order to succeed. Cynthia, thank you for treating me like an equal rather than a student, this really lifted my confidence in myself and what I do.

I also would like to thank my co-supervisor Ass. Prof. Jens Muff at Aalborg University for always supporting me from afar and for his many invaluable inputs when I needed his expertise in the field of electrochemistry. Thank you, Jens, for giving me the opportunity to work in your group. Your passion for the field is perceptible and contagious. I really enjoyed my stay in Esbjerg. It was an amazing experience to be surrounded by many researchers from the same field, which made me feel less lonely in this big scientific world.

I am very grateful for the support from Dr. Kåre Andre Kristiansen, who patiently helped me to develop the right methods in the MS lab. Kåre, I felt like you were there during all day and night times and that there was no problem you could not solve. I still don't know how you endured all my questions and you always answered them patiently. I am sure you explained me 100 times how to properly switch on and off the UPLC/UPC² and how to clean the instrument and never were you annoyed once. Your expertise in the field of chromatography and drive for the simplest and best solution saved me a lot of time and provided me with the best possible results. Your help gave me hope and confidence that everything will work out in the end. I also want to thank Dr. Susana Villa Gonzalez who always was there when Kåre was not around. Susana, you always answered my questions, even during weekends and you always seem to know where the problem was. Finally, I also like to thank Dr. Zdenka Bartosova who helped me to develop the GC method. Zdenka, I never met a person that worked as precisely and was as well prepared as you. You make it look so easy to work with the GC and somehow it always worked out at the first try. Kåre, Susana and Zdenka, thank you for your warm welcome into

your lab, for the opportunity and for trusting me with the instruments and for our friendly chats and laughter while waiting for results. In addition, I also want to thank Dr. Markus Först for helping me with the pilot plant in Mosjøen. Even though I doubted to survive the travel to- and from Mosjøen with your style of driving, I enjoyed your company and the good times we had during the field trips.

I also like to thank Trine Margrete Hårberg Ness and Dr. Thuat Trinh from our analytical lab for their support in the lab and with IC and TOC measurement. Trine, thank you for always being there for me, for your moral support and listening to my struggles and giving me a hug when I needed it.

A huge thank you also goes to my students: Anna Gröhlich, Linda Bottesi, Julie Le Fol, Pauline Zimmermann and Clara Weber. This work would not have been possible without your support and commitment. Thank you for enduring many hours in the lab and on field trips with me. I really enjoyed your company and the good times we had together.

Ragnhild, Erle, Ana, Ganesh, Livia, Priska, and Blanca, thank you for sharing this exciting journey with me as friends and for making the time at the institute unforgettable. John, thank you for uncountable hours of running in the mountains to fuel energy and motivation. Kristin, thank you for countless trainings sessions and the many joyful trips we had together. Finally, Anne-Kathrin, Corine, Katrin and Saskia, I admire all of you for your intelligence, wit, and strength. It makes me the happiest that I can call you my friends and that our friendship defied the long distance in the past years.

Last but not least, I would thank my family who always encouraged me to pursue my dreams and who taught me to endure lows and fight for the highs. I am also grateful to have gained a second family that makes me feel at home here in Norway. Thank you Odd and Hanna for adding me to your family. And finally, Fredrik, I want to thank you for your unconditional support and patience during the past years. You believed in me more than I ever did, and this is the greatest support of all.

*«Dette har jeg aldri gjort før,
så det klarer jeg helt sikkert»*

Pippi Langstrømpe, Astrid Lindgren

TABLE OF CONTENT

Abstract	i
Preface.....	iv
Acknowledgements.....	v
Table of Content	ix
List of Figures	xi
List of Tables	xiii
List of Acronyms	xv
List of Publications	xvii
1 Introduction	1
1.1 Project Background & Motivation	1
1.2 Aims and Scope.....	2
1.3 Thesis Structure.....	2
2 Background.....	5
2.1 Legal Situation in Norway	5
2.2 Geographical Location	6
2.3 Landfill Leachate.....	7
2.3.1 Landfill site	7
2.3.2 Leachate Formation, Characteristics and Composition	8
2.4 Pilot Plant	12
2.5 Treatment Processes for Landfill Leachate	15
2.5.1 Biological Treatment	15
2.5.2 Advanced Oxidation Processes.....	16
2.5.3 Principles, advantages, and drawbacks of common AOP used for landfill leachate treatment	18
2.5.4 Selection of suitable advanced oxidation process.....	27
2.5.5 Disinfection by-product formation by electrochemical oxidation	29
3 Research Questions.....	31
4 Research Methodology	33
4.1 Field Work.....	33
4.2 Experimental Setup	33
4.2.1 Cyclic Voltammetry.....	33
4.2.2 Bulk Electrolysis.....	34
4.3 Sample analysis.....	35

4.3.1	Ultra-Performance Liquid Chromatography (UPLC – MS)	36
4.3.2	Ultra-Performance Convergence Chromatography (UPC ² – MS).....	36
4.3.3	Gas Chromatography Head Space Mass Spectrometry (GC – HS – MS).....	36
4.3.4	Ion Chromatography (IC)	37
4.3.5	Total Organic Carbon (TOC) Analyser	37
4.3.6	Hach-Lange Tests	37
4.4	Statistical analysis	38
4.5	Density Functional Theory simulations	38
4.6	Kinetic modelling.....	38
5	Summary of Key Findings of the Papers.....	41
5.1	Paper I	41
5.2	Paper II.....	42
5.3	Paper III.....	45
6	Discussion.....	47
6.1	Oxidation pathways & prediction of oxidation products (Q1).....	47
6.2	Impacts of landfill leachate pre-treatment (Q2).....	48
6.3	Effect of cold temperatures (Q3).....	49
6.4	Drawbacks & advantages (Q4)	51
6.5	Landfill leachate matrix effect (Q5).....	54
6.6	Adherence of treatment goals (Q6).....	56
7	Conclusions	59
7.1	Answers to the research questions	59
7.2	Conclusions	60
7.3	Outlook and Recommendations	61
	Bibliography	63
	APPENDIX A: Selected Papers.....	75
	APPENDIX B: Additional Data	125
	APPENDIX C: Permissions and Statements	135

LIST OF FIGURES

Figure 1: Geographical location of Mosjøen at the end of Vefsnfjorden and the landfill site (norgeskart.no).....	7
Figure 2: View on the local landfill site SHMI in Åremma, Mosjøen (picture: Shmil.no).....	8
Figure 3: Gas- and leachate quality development in leachate over time, adapted from [13] ..	10
Figure 4: Pilot plant on site for particle and turbidity removal.....	13
Figure 5: Leachate at different treatments steps in the pilot plant.....	14
Figure 6: a) direct anodic oxidation; b) oxidation via electrogenerated hydroxyl radicals; c) mediated oxidation via active chlorine; R: organic pollutant, P: oxidation product or CO ₂ ...	24
Figure 7: Structure of disinfection by-products	29
Figure 8: electrolytical cell; left: turbulence enhancing mesh; right: both anodes (Ti/Pt and Nb/BDD) with indicated active electrode area (10 cm ²).	34
Figure 9: top: Scheme of experimental set-up used; 1) solution tank, 2) peristaltic pump, 3) potentiostat, 4) electrochemical cell, 5) magnetic stirrer, 6) chiller incl. cooling coil; bottom: actual setup.....	35

LIST OF TABLES

Table 1: Common classification of pollutants contained in landfill leachate, source [13].....	9
Table 2: Summary of the landfill leachate composition from 2006 - 2019	10
Table 3: Summarized leachate composition before and after pilot plant.....	14
Table 4: Oxidation potential of common strong oxidation agents. Adapted from [15].....	17
Table 5: List of parameters that have to annually monitored in landfill leachate in Norway, from [8]	125
Table 6: List of Norwegian priority hazardous substances from [6], [9].....	127
Table 7: Complete list of parameters measured in the landfill leachate from 2006-2019.....	128

LIST OF ACRONYMS

AOP	Advanced oxidation process	N/A	Not available
BDD	Boron doped diamond	NBO	Natural bond theory
BOD	Biological oxygen demand	NTU	Nephelometric Turbidity unit
BPA	Bisphenol A	PAH	Polycyclic aromatic hydrocarbons
BTEX	Benzene, toluene, ethylbenzene, xylene	PCB	Polychlorinated biphenyls
COD	Chemical oxygen demand	Pt	Platinum
CV	Cyclic voltammetry	PCP	Pentachlorophenol
DBPs	Disinfection by-products	PP	Pilot plant
DET	Direct electron transfer	SA	Salicylic acid
DFT	Density functional theory	SBR	Sequencing batch reactor
DOC	Dissolved organic carbon	SHMIL	Søndre Helgeland Miljøverk IKS
EO	Electrochemical oxidation	SS	Suspended solids
EOTR	Electrochemical oxygen transfer reaction	THMs	Trihalomethanes
EEA	European Economic Area	TKN	Total Kjeldal Nitrogen
EU	European Union	TOC	Total organic carbon
GC	Gas chromatography	UASB	Upflow anaerobic sludge blanket
HRT	Hydraulic residence time	UPC²	Ultra performance convergence chromatography
HS	Head space	UPLC	Ultra Performance liquid chromatography
LL	Landfill leachate	WW	Wastewater
MBBR	Moving bed biofilm reactor		
MS	Mass spectroscopy		
N.D.	Not detected		

LIST OF PUBLICATIONS

Selected Papers:

1. Noëmi Ambauen, Thuat T. Trinh, Ngoc L. Mai, Jens Muff, Cynthia Hallé and Thomas Meyn. “Insights into the Kinetics of Intermediate Formation during Electrochemical Oxidation of the Organic Model Pollutant Salicylic Acid in Chloride Electrolyte.”
Water 2019, 11, 1322; doi:10.3390/w11071322
2. Noëmi Ambauen, Jens Muff, Franz Tscheikner-Gratl, Thuat T. Trinh, Cynthia Hallé and Thomas Meyn. “Application of electrochemical oxidation in cold climate regions – Effect of temperature, pH and anode material on the degradation of Bisphenol A and the formation of disinfection by-products.”
Journal of Environmental Chemical Engineering 2020; Volume 8, Issue 5, October 2020, 104183; <https://doi.org/10.1016/j.jece.2020.104183>
3. Noëmi Ambauen, Clara T. Weber, Jens Muff, Cynthia Hallé and Thomas Meyn “Electrochemical removal of Bisphenol A from Landfill Leachate under Nordic Climate Conditions.”
Journal of applied Electrochemistry 2020; doi:10.1007/s10800-020-01476-3.

Secondary Papers:

1. Javier Moreno-Andrés, Noëmi Ambauen, Olav Vadstein, Cynthia Hallé, Asunción Acevedo-Merino, Enrique Nebot and Thomas Meyn “Inactivation of marine heterotrophic bacteria in ballast water by an Electrochemical Advanced Oxidation Process.”
Water Research 140 (2018) 377-386, doi:10.1016/j.watres2018.04.061
2. Noëmi Ambauen, Cynthia Hallé and Thomas Meyn. “Electrochemical Treatment of Landfill Leachate under Cold Climate Conditions.”
In: 16th International Conference on Environmental Science and Technology, Rhodes, Greece, 2019

3. Ngoc Lan Mai, Noëmi Ambauen, Cynthia Hallé, Thomas Meyn and Thuat T. Trinh
“Initial degradation mechanism of salicylic acid via electrochemical process”

Under review: Chemical Physics

Posters:

1. Noëmi Ambauen, Cynthia Hallé and Thomas Meyn. “Electrochemical Oxidation of landfill leachate treatment under Nordic climate conditions.”

In: 5th European Conference on Environmental Applications of Advanced Oxidation Processes, Prague, Czech Republic, 2017

1 INTRODUCTION

This chapter gives a brief introduction to the motivation and background for this doctoral study. It further includes the aim and scope of the work, the research questions that were raised and addressed within the present research work. An overview of the thesis structure is given in section 1.3.

1.1 PROJECT BACKGROUND & MOTIVATION

Disposal of waste in landfills leads to the generation of landfill leachate (LL) through percolation of precipitated water through the soil. During this process, different environmental pollutants are leached from the disposed waste to the percolating water [1]. Drainage systems collect the percolating water in the landfill before it is discharged to a perceiving water body. Environmental pollutants found in the LL can be present as solid or dissolved, organic or inorganic and are highly persistent to biological degradation [2]. Therefore, regulations regarding pollutant concentrations in the LL to protect the aquatic environment are required. Consequently, adequate treatment processes to reach the treatment goals must be implemented.

As of spring 2020, no legal regulations or technical guidelines addressing these issues exist in Norway. However, a list of priority substance exists that serves as guidelines when it comes to the treatment of landfill leachate. It is awaited that this list of priority substances will be legally effective in the near future. The landfill age, the hydrogeology as well as the climate at the landfill site have a great impact on the formation and composition of the LL [3]. The climate influences the chemical equilibria of dissolution and degradation/transformation reactions, microbial activity, and metabolic processes that in the end determine the composition of the landfill leachate. Moreover, it greatly impacts the treatment process of LL by impacting the amount and form of precipitation that subsequently influences the LL formation. Furthermore, the climate also impacts the prevailing temperatures, which in turn affects treatment of LL by determining kinetics and in turn treatment times and costs. Finding an adequate treatment for LL that is tailored to the Norwegian environmental conditions and able to meet the future treatment goals is the incentive of this work.

1.2 AIMS AND SCOPE

This work has been aimed at the removal of organic pollutants from the LL. Anodic electrochemical oxidation (EO), a process belonging to the group of advanced oxidation processes (AOPs) was selected as the adequate treatment process (discussed in chapter 2.5). The overall goal was to assess the applicability of the anodic EO to remove organic pollutants and possibly other wastewater (WW) parameters under Nordic climate conditions.

Three different laboratory studies were carried out in order to accomplish the above mentioned goal. First, a mechanistic study of a simple model organic pollutant (salicylic acid) was performed to obtain a better understanding of the different degradation pathways during EO. Secondly, the EO of an organic pollutant listed on the Norwegian priority substance list (Bisphenol A) was evaluated under laboratory conditions. The focus has been laid on cold temperatures, pH and anode material and how those parameters affect degradation kinetics, treatment times and costs. Thirdly, the electrochemical degradation of Bisphenol A under laboratory conditions was linked to real LL. Bisphenol A degradation was studied along with common wastewater parameters, ammonium, nitrate, total organic carbon and chemical oxygen demand. Matrix effects of LL, effect of cold temperatures as well as current densities and anode materials were determined to get a comprehensive assessment for the applicability of EO for the removal of organic pollutants from LL.

1.3 THESIS STRUCTURE

Chapter 1 provides a brief introduction to the background and the topics that are addressed in this thesis. Chapter 2 describes the background in more detail and introduces the concepts of landfill leachate formation, the pilot plant on site as well as advanced oxidation processes in general and electrochemical oxidation in particular. Chapter 3 states the raised research questions and the papers that addressed the questions. Chapter 4 introduces the research methodology adopted and the experimental set-ups that were employed. Chapter 5 summarizes the research articles and their main findings which resulted from this work and answers to the raised research questions are given. Chapter 6 further discusses the main findings from the research articles. Chapter 7 summarizes the conclusion of this work and gives an overarching outlook and recommendations to future research and implementation of the technology. Appendix A encloses selected papers. Appendix B includes tables and figures that with

supporting information that are of minor importance to the thesis. Finally, Appendix C contains permissions and the co-author statements for the publication of this thesis.

2 BACKGROUND

This chapter encloses a detailed introduction into the project background and motivation. It describes the geographical location of the landfill along with the disposed waste, leachate formation and characteristics as well as the pre-treatment on site. An in-depth review of advanced oxidation and electrochemical oxidation is given together with elucidations of the challenges that accompany these processes.

2.1 LEGAL SITUATION IN NORWAY

The overall framework for regulations on landfills in Norway is defined by the European Union (EU). The most important regulation in this regard is the ‘Council Directive 1999/31/EC (1999) on the landfill of waste’ [4] which also applies in Norway under the name ‘Deponidirektivet’. This directive regulates among others, the categories of waste that can be disposed on landfills and the landfill leachate collection, treatment and control procedures during the operational and after-care phase [5]. Furthermore, it defines that the leachate must be collected at each point where leachate is discharged from the site. Monitoring of the surface water next to the landfill have to be performed at minimum two locations, one upstream and one downstream of the landfill. Additionally, the volume and composition of the leachate have to be measured in regular time intervals [5].

Another important statement of the directive [4] affects the required quality of the leachate. It states that the required water quality is subject to the national regulations and has to be defined according to the kind of waste that is disposed in the landfill. The parameters must be laid down in the permit of the landfill and must reflect the characteristics of the disposed waste [4]. The threshold values have to be defined for each landfill separately. For this reason, no national guideline for the treatment of landfill leachate has to be established by the states of the European Union and the European Economic Area (EEA) of which Norway is a member.

A further directive that not only applies for EU countries but also for Norway is the ‘directive 2008/98/EC of the European Parliament and the council of 19 November 2008 on waste and repealing certain Directives’ [6]. In this directive, several regulations and guidelines are specified. Furthermore, Norway has its own and most important guidelines on environmental risk assessments on landfill bottom liners and leachate collection TA-1995/2003 [7]. These guidelines aim to control the diffuse pollution from landfills and stipulate three levels of

investigation [7]. In addition, Norway also provides guidelines on the monitoring of landfill leachate TA-2077/2005, which ensure a controlled emission of landfill leachate [7]. An annual sampling program to measure 24 parameters in the leachate and 16 parameters in the leachate sediments are prescribed by the TA-2077/2005 guidelines [5]. Not all of these parameters have defined threshold values (APPENDIX B). However, Norway also released a list of priority substances whereby the compounds listed should be reduced to below the detection limit by 2020 [8]. The criteria of the priority substance list are that the pollutant is persistent, bio accumulative, has serious long-term health effects and is highly toxic for the environment [8]. Many heavy metals as well as organic pollutants such as PAHs, PCBs and Bisphenol A are subject of the priority list. A complete list can be found in Table 10 (APPENDIX B).

It is important to mention that the list of priority substances only sets goals for the reduction of emissions [5]. However, it is not a legal regulation and it is therefore not mandatory to meet the suggested treatment goals. Only the quality of drinking water is legally regulated by threshold values in Norway [9]. Aside from the fact that there are no official legal requirements, every county in Norway can still decide independently whether a certain basic or specific treatment of landfill leachate should be carried out and what kind of treatment goals should be reached. The local government of the Norland county (Norway) decided that from July 2011, the leachate of all four landfills in the county needs to be treated [5]. In conjunction with this decision, a study was carried out where the water qualities of the leachates were monitored over the period of two years. Based on this data, the different leachate could be analysed and compared. The treatment goals were then established by the operators based on the obtained data and with regards to the Norwegian list of priority substance and were finally approved as valid goals by the local government. Presently, the existing treatment on-site mainly consists of removing turbidity and heavy metals but does not account for the removal of e.g. persistent organic pollutants or ammonium.

2.2 GEOGRAPHICAL LOCATION

The landfill site (SHMIL IKS, Søndre Helgelands Miljøverk) is located in northern Norway in the Norland county, at 65°50'9.60" north and 13°11'26.74 east and its location is depicted in Figure 1. Being only about 100 kilometres from the polar circle (66 ° north), the prevailing climate is categorized as subarctic climate with long cold winters and rather short and cold or mild summers. Yearly precipitation is moderate with an average of 128 mm and monthly

minimum of 6 mm and maximum of 429 mm in the last ten years (2009-2019) [10]. The average yearly air temperature since 1961 is 3.6 °C varying from a monthly minimum of -6 °C to a maximum of 13.8 °C [10].

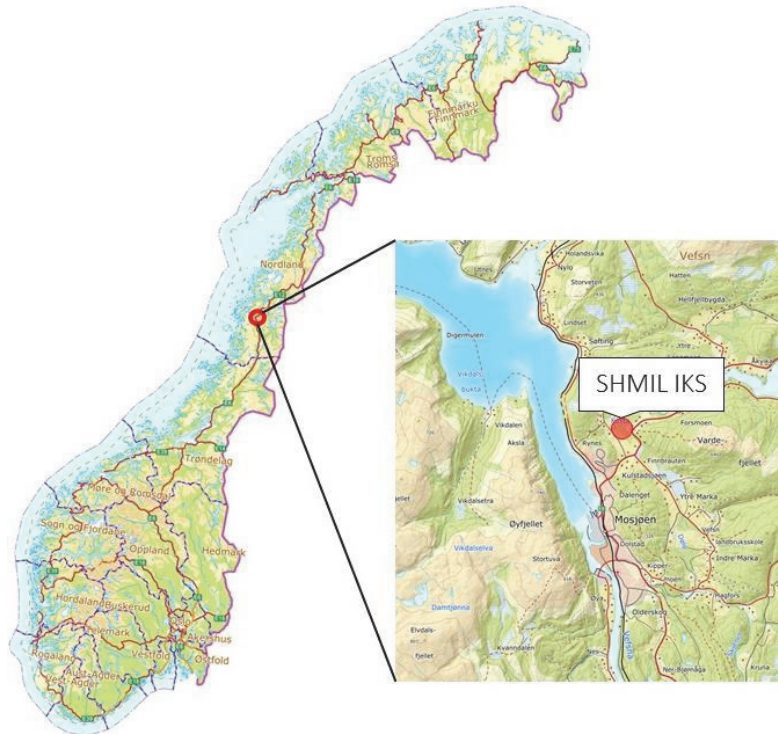


Figure 1: Geographical location of Mosjøen at the bottom of Vefsnfjorden and the landfill site (Norgeskart.no)

2.3 LANDFILL LEACHATE

2.3.1 Landfill site

The landfill site ‘Søndre Helgeland Miljøverk’ (SHMIL, Figure 2) not only consists of a landfill dump but also optically sorts municipal waste in order to recycle materials from plastic and metal packaging, bio waste, cardboard, glass and electronic waste [11]. Residual waste is incinerated in Sweden whereby thermal energy is used to generate power and teleheating. Waste that is actually disposed in the landfill are [12]:

- composted material, which does not fulfil quality requirements for conversion
- sand from sand traps (dewatered)

- slag from incinerators
- contaminated masses (below threshold values for hazardous waste)
- hazardous waste below certain threshold values, provided that it is stabilized and not reactive anymore, e.g.: pesticides, herbicides, organic solvents, heavy metals etc.

The landfill leachate used in the present study is contaminated from the materials such as listed above.



Figure 2: View on the local landfill site SHMIL in Åremma, Mosjøen (picture: Shmil.no)

2.3.2 Leachate Formation, Characteristics and Composition

Precipitation which percolates through the soil is the major transport phase for leaching and migration of pollutants [13]. The moisture that is contained in the dumped waste may also lead to leachate formation to a certain extent but the primary driver for leachate production is considered to be the rainfall which infiltrates into the soil [13]. Generally, the pollutants that are leached into the landfill can be divided in to four main categories; dissolved organic matter, inorganic macro components, heavy metals and xenobiotic compounds [14]. Table 1 provides an overview of those four groups:

Table 1: Common classification of pollutants contained in landfill leachate, source [14]

Dissolved organic matter	Inorganic macro components	Heavy metals	Xenobiotic organic compounds (XOCs)
<ul style="list-style-type: none"> • Dissolved organic carbon (DOC) • Volatile fatty acids • Refractory organic compounds (fluvic and humic-like compounds) 	<ul style="list-style-type: none"> • Calcium (Ca^{2+}) • Magnesium (Mg^{2+}) • Sodium (Na^+) • Potassium (K^+) • Ammonium (NH_4^+) • Iron (Fe^{2+}) • Manganese (Mn^{2+}) • Chloride (Cl^-) • Sulfate (SO_4^{2-}) • Hydrogen carbonate (HCO_3^-) 	<ul style="list-style-type: none"> • Cadmium (Cd^{2+}) • Chromium (Cr^{3+}) • Copper (Cu^{2+}) • Lead (Pb^{2+}) • Nickel (Ni^{2+}) • Zinc (Zn^{2+}) 	Among others: <ul style="list-style-type: none"> • (Poly) aromatic hydrocarbons • Phenols • Chlorinated aliphatics • Pesticides • Plastizers

Composition of the landfill leachate is different for every landfill site. It depends on the characteristics of the dumped waste as well as on the local climate and hydrogeological conditions [13]. The composition of a landfill leachate changes as it ages, meaning the leachate changes its properties and composition over time. The aging process can be divided into several phases, which are depicted in Figure 4. The initial aerobic phase only lasts for several days since oxygen is consumed rapidly and it occurs at neutral pH. Once all the available oxygen is depleted, the anaerobic phase begins where fermentation reactions start and thus the production of carboxylic acids and carbon dioxide (CO_2), this phase is also referred to as the acid phase [14]. The pH decreases during the acid phase and subsequently, the leachate becomes chemically more aggressive, which in turn will increase the solubility of a large number of compounds [14]. Usually, chemical oxygen demand (COD) and biological oxygen demand (BOD) exhibit the highest concentration along with a rather high BOD/COD ratio of 0.4 during the acid phase [14]. In the final methanogenic phase, the reaction products of the acid phase get converted into methane (CH_4) and CO_2 . On the basis of methane production, the acids are consumed and as a consequence, the pH starts to increase again. After reaching a peak in CH_4 production, initial methanogenic phase moves to the stable methanogenic phase or starts to decrease since the soluble substrates begins to deplete [14]. The remaining COD in the leachate

are mostly persistent organic compounds of xenobiotic nature or humic/fluvic like substances. During the operational phase of a landfill, the leachate consists of a mixture of different age characteristics since the leachate of older, already sealed, and covered landfill compartments is mixed with younger leachate.

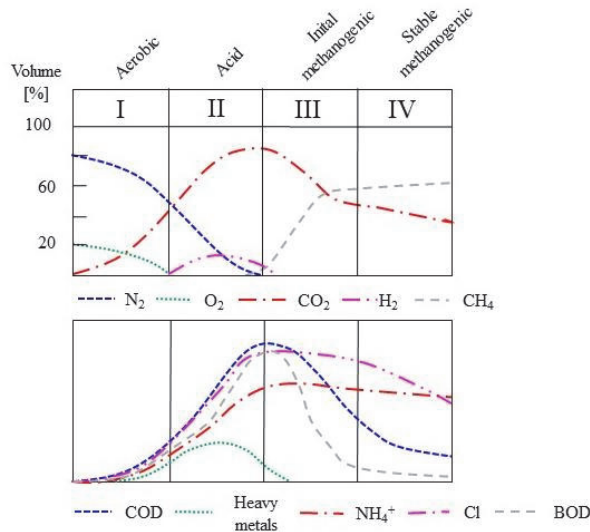


Figure 3: Gas- and leachate quality development in leachate over time, adapted from [14]

The landfill leachate coming from the SHMIL landfill was monitored continuously from 2006 until 2019. Samples are collected through drainage installations and partly analyzed on site and partly at an external accredited laboratory. The mean values of a curtailed list of parameters is given in Table 2. A full list of parameters is given in Table 11 (APPENDIX B).

Table 2: Summary of the landfill leachate composition from 2006 - 2019

	Acronym	Unit	Average	Min.	Max.
Common wastewater parameters:					
Acidity	pH	[-]	6.7	6.3	7.4
Temperature		⁰ C	22.4	21.0	24.8
Conductivity		mS/m	245.9	121.0	420.0
Suspended solids	SS	mg/l	82.6	27.0	360.0
Chemical oxygen demand	COD	mg/l	196.8	66.0	643.0
Biological oxygen demand	BOD ₅	mg/l	15.08	2.0	160.0
Total organic carbon	TOC	mg/l	55.7	3.0	136.0

Total nitrogen	N-tot	mg/l	97.8	43.0	200.0
Ammonium nitrogen	NH ₃ /NH ₄ ⁺	mg/l	90.4	27.0	210.0
Total phosphorus	P-tot	mg/l	0.5	0.1	2.3
Elements:					
Chlorine	Cl	mg/l	165.8	98.4	208.0
Iron	Fe	mg/l	30.1	3.9	78.5
Manganese	Mn	mg/l	1.3	0.6	2.0
Zinc	Zn	µg/l	69.0	26.7	440.0
Copper	Cu	µg/l	10.1	1.3	152.0
Lead	Pb	µg/l	1.7	0.6	6.1
Cadmium	Cd	µg/l	0.1	0.1	0.5
Nickel	Ni	µg/l	15.5	6.9	50.5
Chromium	Cr	µg/l	14.6	3.3	48.4
Arsenic	As	µg/l	4.0	2.2	10.0
Mercury	Hg	µg/l	0.0	0.0	0.0
Calcium	Ca	mg/l	137.1	86.0	184.0
Potassium	K	mg/l	77.5	33.4	187.0
Magnesium	Mg	mg/l	26.5	13.6	42.9
Aluminum	Al	µg/l	321.0	86.8	986.0
Barium	Ba	µg/l	122.0	74.7	243.0
Cobalt	Co	µg/l	4.8	2.8	12.2
Vanadium	V	µg/l	7.4	7.4	7.4
Organic compounds:					
Polycyclic aromatic hydrocarbons	PAH-16 Σ	µg/l	2.7	0.0	8.6
Monocyclic aromatic hydrocarbons	BTEX	µg/l	18.7	0.2	230.0
Bisphenol A	BPA	µg/l	13.8	4.5	23.0
Alkylated phenols (Σ)		µg/l	40.2	7.4	69.8

The SHMIL landfill was founded in 1995 and is still in use today (2020) and thus the leachate is a mixture of the old already covered landfill compartments and the younger leachate coming from newly filled compartments. Hence, arriving at the exact age of the leachate would be difficult owing to the complex chemical nature of the leachate samples (APPENDIX C, Table 11). The neutral pH indicates the leachate is still in the aerobic phase but the BOD/COD ratio of 0.08 suggests that the leachate is older and already in the stable methanogenic phase.

Leachates from different landfill sites show large variations for the basic parameters COD, BOD, pH, suspended solids (SS), ammonium nitrogen and total Kjeldal nitrogen (TKN). Table 12 in APPENDIX B gives an overview of these parameters for different landfill leachates from different countries. A comparison of the average leachate composition from SHMIL and from several countries adapted from Renou et al. [15] is given in Table 3. Compared to the average parameters from leachates from other countries, the leachate from SHMIL exhibits a low COD concentration and a low BOD₅/COD ratio. In addition, the nitrogen concentrations are also considerably below average compared to other countries, along with the content of suspended solids. The pH is slightly more acidic than the average given in Table 3. Further comparison with domestic wastewater shows that besides ammonium and total nitrogen, all parameters in the landfill leachate show lower concentrations than average domestic wastewater. In conclusion, the landfill leachate from SHMIL can be characterized as low strength wastewater. This basic landfill leachate characteristics of the leachate used in this study are important to keep in mind with regard to the choice of a suitable treatment process.

Table 3: Comparison of average parameter values from landfill sites around the world to the leachate from SHMIL Mosjøen, which was used in this work

	COD [mg/L]	BOD [mg/L]	BOD/COD [-]	pH [-]	SS [mg/L]	TKN [mg/L]	NH3-N [mg/L]
Landfill leachate (Renou et al. [15])	11'038	3'900	0.24	8	1'241	2'683	2'443
SHMIL, Mosjøen	196	15	0.08	6.73	83	97	90
Domestic WW (Henze et al. [16])	750	350	0.47	-	350	60	45

2.4 PILOT PLANT

On site, there is an existing pilot plant for the removal of turbidity and particles, which also included the removal of heavy metals (Figure 4). The Pilot plant feed water is directly pumped from the drainage tank of the leachate. First, the pH of the leachate is adjusted to about 10 with NaOH and simultaneously aerated. Following pH adjustments, the leachate decants into a rapid mixing tank where the coagulant (Ferric chloride, FeCl₃) is added. The positive charge of Fe³⁺ neutralizes negatively charged colloidal particles, which induces their destabilization. In the slow mixing tank, the neutralized particles are then given time to agglomerate due to van der

Waal forces to form larger flocs that can be removed by sedimentation [17]. This sedimentation is done by a lamella clarifier wherein the sludge is collected at the bottom of the tank and regularly drained to the pumping basin and eventually discharged to the fjord. The present pilot plant is only installed for experimental purposes and therefore the sludge as well as not collected supernatant are returned to the pumping basin. The supernatant from the lamella clarifier was collected, transported to the laboratory facilities and used within the experimental studies conducted in this work.

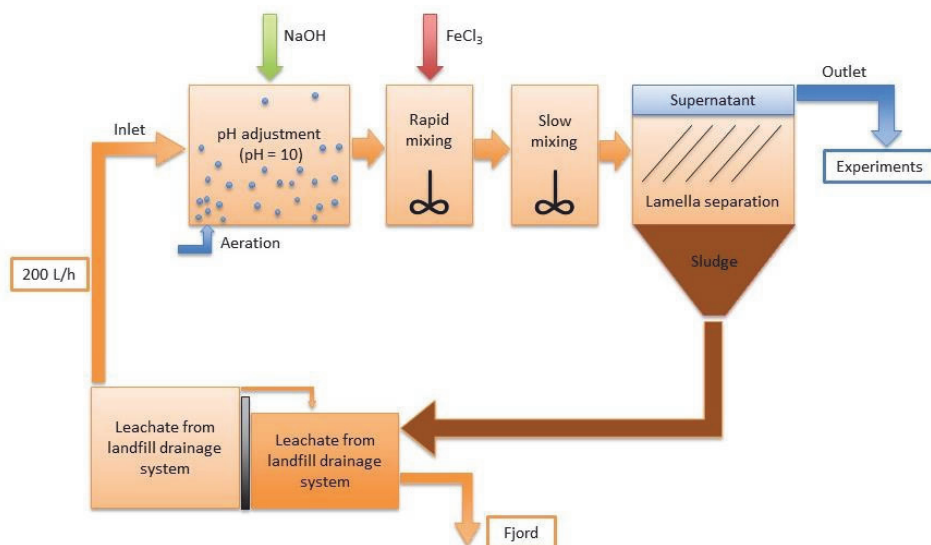


Figure 4: Pilot plant on site for particle and turbidity removal

The physical appearance of the leachate at different treatment steps in the pilot plant is depicted in Figure 5. The intense orange color in the slow mixing tank is due to the addition of the ferric chloride coagulant. After adding the ferric chloride, the Fe(III) concentration in the slow mixing tank corresponded to on average 35 mg/L and was removed again to below detection limit (0.2 mg/L) in the supernatant. Coagulation and the subsequent lamella separation thus removed more than 99 % of the Fe(III) that was added. It is furthermore visible from Figure 5 that a greater part of turbidity also could be removed by the pilot plant. Initial turbidity values ranged from 40 to 109 NTU and 83 % could be removed on average.

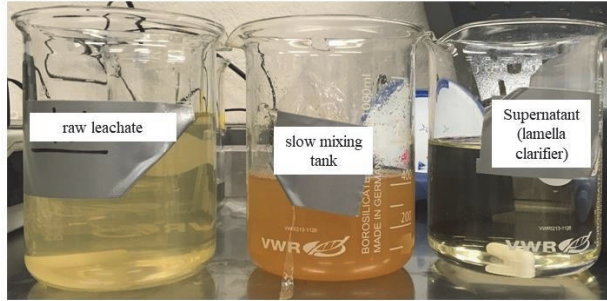


Figure 5: Leachate at different treatments steps in the pilot plant

Landfill leachate was collected three times in the course of this study. As described above, the leachate was collected after the pilot plant (supernatant) and is subsequently referred to as pretreated leachate. The leachate was collected two times during the summer, July 2018 and June 2019, and once in autumn in October 2018. Table 4 summarizes the properties of the leachate at the times collected before and after the treatment with the pilot plant. More data is available for the pretreated leachate than for the raw leachate. When looking at the different concentration of the measured parameters, it is apparent that the season at which the samples were gathered plays a role. The leachate collected in autumn exhibits lower concentrations in general, which can be attributed to higher precipitation in autumn that consequently leads to a dilution of the leachate due to more water percolating through the landfill.

Table 4: Summarized leachate composition before and after pilot plant (PP)

Parameter	Unit	Summer 2018		Summer 2019		Autumn 2018	
		before	after	before	After	before	After
		PP	PP	PP	PP	PP	PP
pH	-			6.7	9.9	6.5	10.6
COD	mgO/L		129.6	120.0	87.0	98.0	51.0
BOD5	mgO/L	N/A	N/A	57.0	< 10	N/A	42.0
TOC	mg/L		33.5	31.0	29.1	3	21.5
Turbidity	NTU	N/A	N/A	109	16	40.1	7.4
sum PAH	µg/L	N/A	N/A	< 0.19	0.32	N.D.	0.6
BTEX	µg/L	N/A	N/A	0.74	2.99	N.D.	1.4
Bisphenol A	µg/L	N/A	N/A	< 0.05	11	< 0.05	8.4
Ammonium (NH ₄ ⁺)	µg/L		83.7	73.3	72.8	48.7	32.4
Most abundant heavy metals:							

Ni	µg/L	N/A	N/A	N/A	N/A	6.5	24.2
Cr	µg/L	N/A	N/A	N/A	N/A	4.4	13.7
Zn	µg/L	N/A	N/A	N/A	N/A	93.1	13.2
Cu	µg/L	N/A	N/A	N/A	N/A	23.4	11.9
As	µg/L	N/A	N/A	N/A	N/A	4.0	1.6

2.5 TREATMENT PROCESSES FOR LANDFILL LEACHATE

2.5.1 Biological Treatment

Landfill leachate can be treated by conventional biological processes, which has been shown by several studies, summarized by Renou et al. [15] and Wiszniowski et al. [18]. Biological treatments both, aerobic and anaerobic, are designed to degrade dissolved organic compounds by microorganisms, which can use these compounds as energy source to live and reproduce [19]. The most common applied biological treatments for landfill leachate are activated sludge system, sequencing batch reactors (SBR), membrane biofilters, moving bed biofilm reactor (MBBR) and up-flow anaerobic sludge blankets (UASB) [15]. Detailed description of these processes can be found elsewhere, e.g. [17]. For biological treatment of wastewaters to be successful, they have to fulfil certain requirements [20]: A high biodegradability, expressed in a rather high BOD/COD ratio, preferably > 0.5 ; low toxicity of organic compounds, moderate temperatures at which the microbial community thrives and a preferred pH range from 6.5 – 8.5.

As landfill leachate ages over time it changes its composition. Young leachate has a higher BOD₅/COD ratio and is therefore better suited for biological treatment than medium age or old landfill leachate (Figure 3). Comparison of the landfill leachate used in this study to the average composition of the leachate in other countries (Table 3) and to domestic wastewater shows that the SHMIL leachate has low biodegradability (BOD₅/COD = 0.08) and a rather high nitrogen content. Low biodegradability is a poor prerequisite for a biological treatment process. In addition, leachate in general and also the one used in this study contain many refractory organic compounds (Table 4 and Table 11), which besides not being biodegradable can also be toxic to the microbial community [21]. Furthermore, the average leachate temperature of 6 °C is comparably low. Overall reaction rates for aerobic biological treatments are highest in the mesophilic range from 31.0 to 35.5 °C and about 80 % less at 4 °C [22]. The same applies for

anaerobic biological treatment where the ideal reactor temperature should be kept around 35 °C. Thus, the low average leachate temperature is a main obstacle that has to be overcome as it slows down the microbial metabolism, regrowth and consequently the degradation process. There are only a few studies that consider biological wastewater or leachate treatment at temperatures at low temperatures (< 12 °C). Bandara et al. [23] showed that low strength domestic wastewater treatment with an UASB reached less than 40 % COD removal during winter (6 °C) with no biogas production while COD removal was up to 71 % during summer (31 °C). Kettunen et al. [24] tested an USAB with landfill leachate and obtained a COD removal of up to 65 % at 11 °C and a hydraulic retention time (HRT) of 2 days, while COD removal was up to 70 % at 24 °C and an HRT of 10 hours.

The requirements for a successful biological treatment of the landfill leachate used in this study are not satisfied due to considerably low average biodegradability and the low average temperature. Nonetheless, prior to this work, a preliminary study using an MBBR was carried out on-site. Results show that it was not possible to steadily operate the MBBR to a satisfactory extent under the local conditions on site. MBBR carriers were obtained from the airport wastewater treatment plant (Gardermoen, Oslo, Norway) to conduct biological nitrification experiments. Initially, nitrification worked well but decreased from 34 % ammonium removal to 0 % with increasing experimental time (8 days). It was assumed that the aeration oxidized reduced metals that are contained in the landfill leachate (Table 2), which started to precipitate and formed a thick metal layer at the outside of the biofilm. In addition, the toxicity of the landfill leachate was suspected to have an adverse impact on the nitrification in the MBBR. Furthermore, the cold temperatures on site are also disadvantageous for the MBBR treatment. An overload of the reactor in terms of BOD was excluded as a possible cause to the decreasing nitrification performance.

Based on literature, the present leachate composition and on the results from this preliminary study, biological treatment was discarded as a possible treatment process for the landfill leachate in this work. Instead, the focus was laid on more advanced oxidation processes, which are discussed in the subsequent section.

2.5.2 Advanced Oxidation Processes

Advanced oxidation processes are often used as a polishing- or disinfection step after biological and/or physical treatment of different kind of wastewater or drinking water. Oxidation is the loss of an electron (e^-) by an atom. The ultimate goal of any oxidation process is to mineralize

an organic compound into harmless molecules like CO₂ or water (H₂O) [25]. Inorganic compounds can be oxidized as well whereby they reach a so-called higher oxidation state, e.g. Fe²⁺ is oxidized to Fe³⁺. Charge must be preserved, that is why every oxidation occurs together with a reduction reaction [26]. The standard enthalpy of formation ($\Delta_f H^\ominus$) of CO₂ (-393 kJ/mol) and H₂O (-285 kJ/mol) as oxidation products from organic compounds are thermodynamically favourable since a significant amount of energy is released via their formation by an exothermic reaction [25].

Some common strong oxidizing agents are summarized in Table 5 together with their corresponding standard reduction potentials. The higher the reduction potential, the more likely the oxidant is to reduce itself and thereby oxidizing other compounds. The standard reduction potential can be employed as a parameter to categorize different oxidizing agents after their oxidation power, it is a measure of the tendency of a compound to accept electrons. Naturally, the compounds listed in Table 5 can be seen to be associated with high electronegativity, the ability to attract pairs of electrons [26].

Table 5: Oxidation potential of common strong oxidation agents. Adapted from [25].

Species	Standard reduction potential [V]
Fluorine	3.03
Hydroxyl Radical (HO [•])	2.80
Atomic oxygen (O)	2.42
Ozone (O ₃)	2.07
Hydrogen peroxide (H ₂ O ₂)	1.78
Hypochlorous acid (HOCl)	1.49
Chlorine (Cl ₂)	1.36

Radicals such as hydroxyl radicals (HO[•]) have especially strong oxidation power since they have a single unpaired electron, which makes them highly reactive. Hydroxyl radicals are non-selective and therefore react with a broad range of organic compounds. They are also able to oxidize persistent organic pollutants into less hazardous compounds, ideally completely mineralizing them to CO₂ and H₂O [27]. This feature makes hydroxyl radicals a primary choice when it comes to the removal of organic pollutants from drinking water and wastewater via chemical oxidation [20].

Hydroxyl radicals react with organic compounds via the following three common reactions pathways: Hydrogen abstraction, addition to double bonds or aromatic rings and direct electron transfer [28]. Double bond addition is a faster reaction pathway than hydrogen abstraction [20]. As a consequence, different organic compounds are reacting at different rates with hydroxyl radicals, depending on their structure. Both organic compounds that were considered in this work are phenolic (salicylic acid and Bisphenol A). Phenolic compounds are likely to undergo an addition of the hydroxyl radical to the aromatic ring as a primary and rate determining step of the of the hydroxyl radical attack [29].

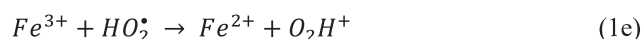
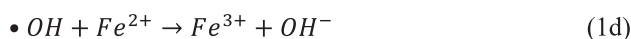
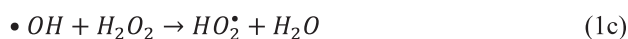
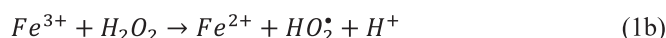
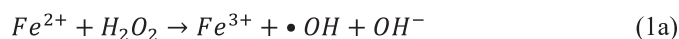
An oxidation process that can produce such highly reactive hydroxyl radicals is considered an AOP [30]. There are several ways to produce HO[•]. The most common ones are Fenton oxidation, ozonation, catalysis, electrochemical oxidation and photo-, electro- or ultrasound enhanced AOPs [25].

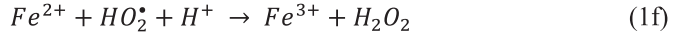
2.5.3 Principles, advantages, and drawbacks of common AOP used for landfill leachate treatment

The above mentioned AOPs were assessed for landfill leachate treatment in several studies. In the following, the principles, advantages, and drawbacks of three selected and commonly used AOP in wastewater/landfill leachate treatment are presented, compared and summarized in Table 6.

Fenton oxidation

One of the most the most thoroughly investigated processes for landfill leachate treatment is Fenton oxidation, which can be enhanced by ultrasound (sono), by UV light (photo) and by electrolysis (electro) or by a combination of different enhancements. The conventional Fenton process builds on a sequence of reactions (equation 1a – 1g) [31]:





Fe^{2+} : ferrous iron, H_2O_2 : hydrogen peroxide, Fe^{3+} : ferric iron, OH^- : hydroxide ion, HO_2^* : hydroperoxyl radical, O_2H^+ : protonated oxygen ion, O_2 : elementary oxygen

Ferrous iron (Fe^{2+}) is oxidized to ferric iron (Fe^{3+}) by hydrogen peroxide to form hydroxyl radicals, whereby Fe^{2+} acts as a catalyst and cycles between Fe^{2+} and Fe^{3+} . Both, hydroxyl- and hydroperoxyl radicals that are formed in this reaction sequence can react with organic compounds contained in the leachate, leading to their partial or complete oxidation. The net reaction of the Fenton process is the decomposition of H_2O_2 to H_2O and O_2 catalyzed by iron [31]. A simplified scheme for Fenton oxidation is shown in Figure 6.

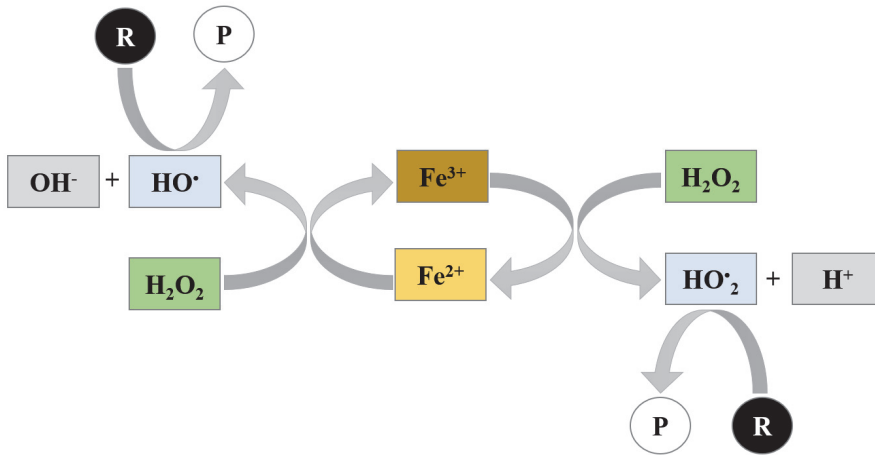


Figure 6: Simplified scheme for Fenton oxidation of organic compounds (R) to a product (P); adapted from [32].

The pH plays a very important role in Fenton processes because it influences the iron speciation and the H_2O_2 decomposition, its optimum is around pH 2 – 3 [33]. At a pH > 4, ferric salts start to precipitate as ferric hydroxide and ferrous salts are in a dissolved state at pH 7 [34]. Thus, Fenton oxidation requires strict acidic conditions (pH < 4) for effective wastewater treatment [35].

Fenton oxidation has the following advantages: Rather simple reactor design, which is commercially available and very low operational costs compared to other AOPs. Unfortunately, Fenton oxidation also comes with a set of drawbacks: The iron sludge production due to flocculation of the organic compounds and the catalyst, which requires

further sludge treatment and/or disposal. Furthermore, the addition of acid to lower the solution pH, the addition and storage of liquid H₂O₂ and the very narrow optimum pH range are other demerits that increase costs and risks of conventional Fenton oxidation. Some of these disadvantages can be avoided by the use of enhanced Fenton oxidation. Electro-Fenton is the combination of Fenton- with electrochemical oxidation, whereby H₂O₂ is generated on-site via the electrochemical reduction of O₂ at the cathode [36]. Additionally, Fe³⁺ is reduced at the cathode to Fe²⁺, which enhances the regeneration of Fe²⁺ and thus reducing the iron sludge production [36]. Combing Fenton oxidation with UV-irradiation is known as photo-Fenton oxidation. Light energy is used to enhance the reduction from Fe³⁺ to Fe²⁺ and direct photolysis of H₂O₂ leads to the production of hydroxyl radicals. Photo-enhancement also leads to a reduced iron sludge production and lower initial iron addition and increased hydroxyl radical production [36]. However, the design of a photo-reactor leads to increased costs. During sono-Fenton oxidation, the process is enhanced by ultrasound, which leads to direct degradation of organic compounds via sonication and an enhanced hydroxyl radical production via sonication of H₂O, which in turn increases the degradation of organic pollutants via hydroxyl radicals [37]. Sonication further enhances the regeneration of Fe³⁺ to Fe²⁺ and increases the contact time of hydroxyl radicals and organic pollutants due to improved mixing [37].

Fenton oxidation and enhanced Fenton oxidation have been successfully applied for the treatment of landfill leachate. Zang et al. [38] used electro-Fenton to remove COD from the landfill leachate and achieved removal efficiencies of more than 80 %. It was further observed that electro-Fenton was superior to conventional Fenton oxidation, both in terms of removal efficiency, which was below 50 % for conventional Fenton oxidation, and in economic terms. Applying Fenton oxidation at lower temperatures (10 and 13 °C) showed that COD removal decreased with decreasing temperatures [33], [39]. Decreasing the temperature from 37 to 13 °C decreased the COD removal from 56 to 42 %. Sono-Fenton of landfill leachate also showed very promising results with a COD removal efficiency of up to 95 % at pH 2 [40]. Despite the successful application of Fenton oxidation to treat landfill leachate, the above-mentioned drawbacks have to be kept in mind when comparing the process to other AOPs. In addition, Fenton oxidation of landfill leachate leads to the formation of unwanted halogenated disinfection by-products, like trihalomethanes, haloacetonitriles and halonitromethanes [41].

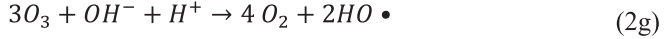
Ozonation

Along with Fenton oxidation, the application of ozonation has been considered as suitable advanced treatment process for landfill leachate [42], [43]. Hydroxyl radicals are hereby generated via ozone (O_3) as listed in the following reaction sequence (equation 2a – 2f) [20]:



OH⁻: hydroxide ion, O₃: ozone, HO₂⁻: hydrogen peroxide, O₂: elementary oxygen, O₃⁻•: ozone radical, HO₂[•]: hydroperoxyl radical, O₂⁻•: dioxide ion, HO₃[•]: trioxydanyl radical, H⁺: proton, HO•: hydroxyl radical

The net reaction and overall stoichiometry is given in equation (2g) below [20]:



The produced hydroxyl radicals are finally reacting with the organic pollutants contained in the landfill leachate, leading to their partial or complete oxidation. From equation (2a) it is visible that the pH plays an important role in the ozonation process. A high pH (≈ 11) is required for the reaction sequence to start with the hydroxide ions [20]. Unfortunately, deprotonated carbonate ions (CO_3^{2-}) are prevailing over bicarbonate ions (HCO_3^-) at a high pH, which act as hydroxyl radical scavenger. This leads consequently to lower reaction rates of hydroxyl radicals with organic pollutants. Despite the reaction of hydroxyl radicals with organic pollutants, ozone can directly react with them, leading to their degradation and formation of intermediate products. This is considered the direct pathway. Both pathways are illustrated in Figure 7.

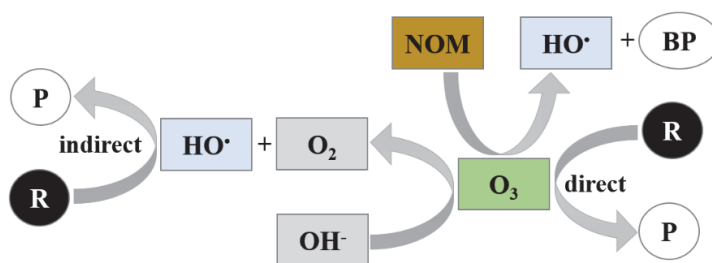
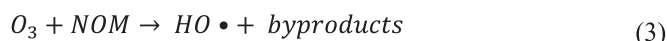


Figure 7: Simplified scheme for ozonation of organic compounds (R) to a product (P)

A third important pathway to produce hydroxyl radicals via ozonation is the reaction of ozone with NOM (equation 3) [20].



Quenching of the hydroxyl radicals produced via the reaction of NOM and ozone can in turn occur by NOM itself (equation 4). This quenching mechanism is usually more important than the one by carbonate [20].



If the direct or indirect ozonation pathway with organic compounds is dominating depends greatly on the nature of the organic compound [20]. Elovitz and von Gunten [44] state that the most important mechanism to destroy target compounds is via the reaction of ozone with NOM.

Ozonation, like Fenton oxidation, can be enhanced by different measures. The most common enhancement is via the addition of hydrogen peroxide or UV-irradiation. Hydrogen peroxide accelerates the transformation of ozone at pH > 6 when it is mainly present in its ionized form (equation 2b) [45]. The combination of ozonation with UV irradiation also enhances the formation of hydrogen peroxide via the photolysis of ozone [46].

Landfill leachate treatment by ozonation and enhanced ozonation has been reported in several studies [43], [47]–[49]. Wu et al. [43] used ozonation of landfill leachate as a post-treatment after coagulation by ferric chloride (FeCl₃), similar to the pre-treatment used in this work. They observed a significant increase in biodegradability by an increase of the BOD₅/COD ratio from 0.06 to 0.5. These findings apply for pure ozonation and hydrogen peroxide- and UV-irradiation enhanced ozonation. Furthermore, they achieved a color removal > 80 % for all ozonation processes. Poznyak et al. [42] also used ozonation as a post-treatment of landfill leachate after coagulation. Color was completely removed (100 %) after 5 min of treatment.

Toxic compounds were formed during ozonation, but were further degraded to aliphatic carboxylic acids, which are nontoxic and more readily biodegradable than the initial humic substances. Another study by Geenens et al. [50] conducted ozonation experiments with landfill leachate to reduce toxicity for a later activated sludge co-treatment with municipal wastewater. They applied a temperature between 5 and 10 °C during ozonation (non-regulated temperature) and achieved a COD removal up to 30 % while the BOD₅/COD increased from 0.06 to 0.17 after 2.2 hours residence time in the reactor. Other studies looked more specifically into the removal of certain organic pollutants from wastewaters, which is summarized in a review by Umar et al. [51]. The different studies report that ozonation is promising to remove Bisphenol A from wastewaters, with removal efficiencies between 58 and 100 % [52], [53].

Successful landfill leachate treatment with ozonation has been reported as stated above. The main advantages of ozonation are that when operated at a decently high pH (8 -10), the process does not require the addition of hydrogen peroxide or UV-irradiation [20] to produce hydroxyl radicals. In addition, ozonation processes are commercially available and have been established as a treatment step in many wastewater treatments plants in Europe and the in the US to remove organic (micro)pollutants [54] [55]. Furthermore, the process has been shown to be applicable at temperatures as low as 5 °C [50], which is important for treatment of landfill leachate under Nordic climate conditions. On the other hand, the main disadvantages are that ozone off-gas has to be removed, a fairly high pH has to be maintained for conventional ozonation and enhanced ozonation processes are expensive due to special reactor design. Furthermore, the formation of by-products has been observed during the ozonation of wastewaters, mainly aldehydes including formaldehydes, ketones and carboxylic acids were identified [56], [57]. Their formation increased with an increasing ozone concentration. If bromide is present, bromated by-products like bromoform can also be formed [58].

Electrochemical Oxidation

The third AOP, that was assessed in this work, is electrochemical oxidation. It uses the principle of electrolysis to produce powerful oxidants via anodic oxidation of water and ions contained in an aqueous solution. These oxidants react with organic pollutants and other water contaminants, leading to their partial or complete oxidation. A detailed description of electrolysis principles can be found elsewhere, e.g. [59].

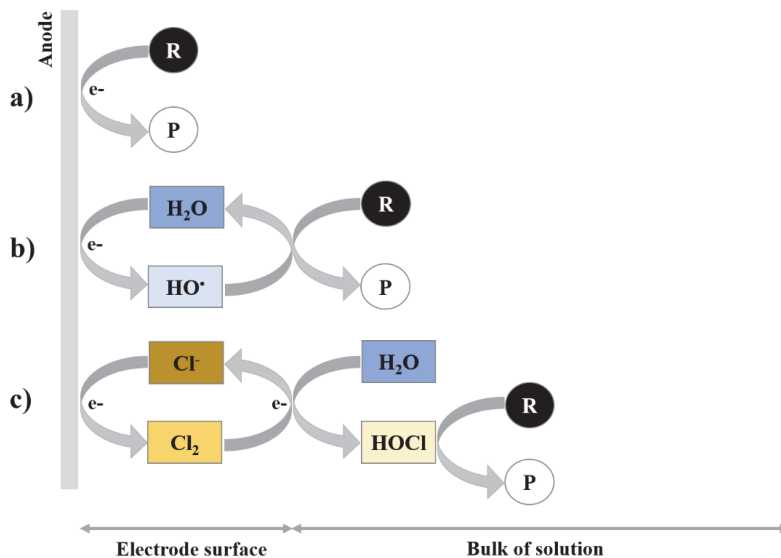
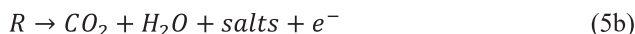
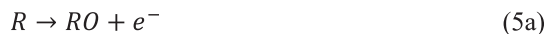


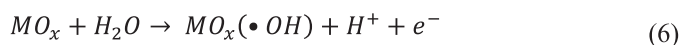
Figure 8: a) direct anodic oxidation; b) oxidation via electrogenerated hydroxyl radicals; c) mediated oxidation via active chlorine; R: organic pollutant, P: oxidation product or CO₂

Electrochemical oxidation of organic pollutants can occur via different oxidation pathways. These are distinguished based on oxidation via hydroxyl radicals produced from water discharge and direct and mediated (also called indirect) oxidation [60], [61]. The different electrochemical oxidation pathways are schematically illustrated in Figure 8.

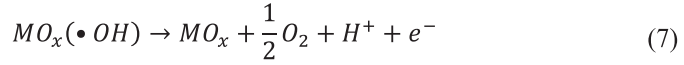
Direct anodic oxidation, as its name suggests, takes place directly at the anode surface (Figure 8a). The organic pollutant (*R*) is adsorbed and oxidized at the anode surface by passing on an electron (e^-) to the anode resulting in an oxidized organic pollutant (*RO*) (equation 5a) or in complete combustion to CO₂ and H₂O (equation 5b) [62].



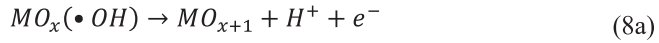
Electrochemical oxidation via the transfer of oxygen from the water (H₂O) results in reaction products, which under an ideal scenario would be CO₂, i.e. complete mineralization [61]. For water to be able to transfer an oxygen atom, it needs to be activated first. Electrolytic discharge of water in the electrochemical cell results in the formation of adsorbed hydroxyl radicals (equation 6, Figure 8b) [61]:



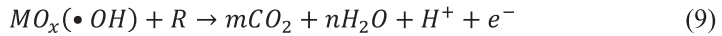
A competing side reaction may occur during the electrolytic discharge of water, called oxygen evolution (equation 7) [61]:



The occurrence of oxygen evolution is subject to the oxygen evolution over-potential of the anode material. In the same way, the transfer of oxygen from the adsorbed hydroxyl radicals to the organic compound (R) depends on the anode material [63]. Commonly, two different electrochemical oxygen transfer reaction (EOTR) mechanisms are distinguished [61]. The first EOTR mechanism takes place at anodes that have a low oxygen evolution over-potential, known as active anodes (e.g., platinum, Pt) [61]. Herein, the adsorbed hydroxyl radical reacts with the anode surface, forming higher oxides (MO_{x+1}), which in turn react with the organic pollutant R (equation 8a and 8b) [61]:

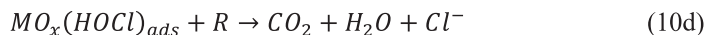
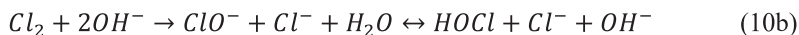


where MO_{x+1}/MO_x is the surface redox couple, called “active oxygen”. The second EOTR mechanism takes place at anodes with high oxygen evolution over-potential, known as non-active anodes (e.g., boron doped diamond, BDD). Herein, no formation of higher oxides occurs. Instead, the adsorbed hydroxyl radicals react directly with the organic compound, which in a best case scenario leads to its complete combustion to CO_2 and H_2O (equation 9):



Depending on the anode material, the active oxygen is termed chemisorbed (active anodes) or physisorbed (non-active anodes). To be able to conduct electrochemical oxidation, the sole presence of an organic pollutant and water molecules is not sufficient. Electrolytes need to be present to transfer the charge across the electrochemical cell. Nearly all wastewaters contain electrolytes of different natures and thus facilitate the treatment via electrochemical oxidation. However, electrolytes do not only transfer charges. Electrochemically active electrolytes may also undergo oxidation at the anode surface. Halide electrolytes will form active halide species, for example, NaCl will react to active chlorine ($HOCl/OCl^-$, pH depending). These active species also react with the organic pollutants, resulting in their partial chemical oxidation, a process known as mediated or indirect oxidation (Figure 8c) [64]. Bonfatti et al. [65] proposed

the following mechanisms (equation 10a – 10d) for active chlorine mediated electrochemical oxidation:



Halogenated organic pollutants however are not favoured reaction products, since they are generally more toxic than the mother compound and thus disadvantageous for the treatment process [66]. They are often referred to as “disinfection by-products” (DBPs) because active chlorine is used for water disinfection.

Electrochemical oxidation of landfill leachate has been shown to be a powerful technology, despite its energy consumption and potential to produce halogenated DBPs [67]. Anglada et al. [68] successfully operated a pilot plant scale electrochemical oxidation process and report a COD removal of more than 90 % within 8 hours of treatment on BDD anodes. An increasing removal was observed with an increasing applied current. Bashir et al. [69] reported 70 % COD removal after 4 hours of treatment on graphite carbon electrodes but they did not observed a significant increase in biodegradability (BOD₅/COD). Furthermore, Moraes et al. [70] report similar findings for the removal of total organic carbon (TOC) (57 %), COD (73 %), BOD₅ (71%) and ammonium (NH₄-N, 49 %) from landfill leachate. That electrochemical oxidation is a promising treatment step for ammonium removal from landfill leachate has also been shown by Cabeza et al. [71]. They report total ammonium removal after 6 hours of treatment on BDD anodes, whereby almost 50 % was oxidized to nitrate (NO₃-N). However, no study was found where temperatures below 10 °C were investigated for treatment of landfill leachate, which are common for the Nordic climate. Only recently (2020), Pei et al. [72] investigated the electrochemical removal of phenolic pollutants at 8.5 °C in clean electrolyte. They report a satisfactory pollutant removal at low temperature which is comparable to the one obtained at room temperature (23.5 °C) due to the effect of Joule heating, which results in higher interfacial temperatures at the anode surface. Despite this very recent study, Panizza et al. [73] tested temperatures between 25 and 50 °C, which showed that COD removal was accelerated with increasing temperatures. Similar results are reported by the same group for the treatment of Tannery wastewater [74]. A major reported disadvantage is the formation of DBPs during

electrochemical oxidation of landfill leachate. Another work of Anglada et al. [75] reports the formation of the following disinfection by-products on BDD anode: chloroform, dichloroacetonitrile, 1,2-dichloroethane and 1,1-dichloroacetone. They further state that at an applied current of 8.4 A and 12 A resulted in the same concentration profile whereas operation at 18 A resulted in much higher concentrations. These findings indicate that the DBPs formation can be controlled by the applied current. In addition, a study for electrochemical treatment of latrine wastewater by Jasper et al. reports the formation of perchlorate formation on BDD anode.

2.5.4 Selection of suitable advanced oxidation process

The advantages and drawbacks of Fenton oxidation, ozonation and electrochemical oxidation are summarized in Table 6.

Table 6: Advantages and drawbacks of commonly used AOPs for landfill leachate treatment

	Advantages	Drawbacks
Fenton oxidation	<ul style="list-style-type: none"> • Commercially available • Easy to enhance with electrochemical or UV-processes • Low operational costs 	<ul style="list-style-type: none"> • Low pH required (2 – 3) • Storage of dangerous chemicals • Extra costs for chemicals • Produced sludge requires further treatment • Formation of halogenated disinfection by-products
Ozonation	<ul style="list-style-type: none"> • Commercially available • Well established process • Operates at high pH • Tolerates low temperatures • No addition of chemicals other than ozone 	<ul style="list-style-type: none"> • Off – gas has to be removed • Complex process & operation • Ozone generation requires high energy input • High operational costs • Formation of recalcitrant oxidation products
Electrochemical oxidation	<ul style="list-style-type: none"> • Commercially available • Low operational costs • Low space requirements • No addition of chemicals • Simple equipment 	<ul style="list-style-type: none"> • High Acquisitions costs (BDD) • Formation of disinfection by-products • Electrode fouling • Replacement of electrodes

-
- Low pressure and temperature requirements
 - No residual sludge
 - Short retention times -> large volumes can be treated
-

One aspect that was not taken into consideration yet is the acquisition- and operational costs of the three different AOPs. Cañizares et al. [76] compared the costs of electrochemical oxidation with the ones for Fenton oxidation and ozonation. The operational costs for the removal of 1 kg O₂ were estimated to 2.4 – 4.0 €/kgO₂ for electrochemical oxidation, 8.5 – 10.0 €/kgO₂ for ozonation and 0.7 – 3.0 €/kgO₂ for Fenton oxidation. Comparison of the acquisition costs also concluded that ozonation is the most expensive investment. A considerable matter of expense for electrochemical oxidation is the purchase of BDD electrodes (15'000 €/m²), but it is assumed that prices drop in the near future. The same study also compared the effectiveness of the three processes for the removal of certain organic pollutants in synthetic and real wastewater. Only electrochemical oxidation achieved complete removal of the organic pollutants in all cases and the removal efficiencies for Fenton oxidation and ozonation strongly depended on the nature and concentration of the pollutant.

In order to select the most suitable AOP for the treatment of landfill leachate in this study it is important that the following criteria are fulfilled:

- ▶ Low space requirements
- ▶ Operation at high pH (after coagulation where pH is adjusted to ≈ pH 10)
- ▶ Effective at low average temperatures (< 6 °C)
- ▶ Simple operation and equipment
- ▶ Cost effective
- ▶ High removal efficiency for organic pollutants

Based on this criteria, the local climate conditions, and the advantages that the different considered AOPs have to offer, it was decided that electrochemical oxidation was the most suitable process to remove organic pollutants from the leachate for the given conditions. Fenton oxidation was quickly excluded due to the major drawback of a low operational pH and the sludge production that would require further treatment and costs. Ozonation appeared to be a suitable choice, especially the high operational pH. However, ozonation was excluded due to

high operational costs and rather complex operation that would require specialized personnel on site. Finally, electrochemical oxidation was chosen as the suitable process for landfill leachate treatment under Nordic climate conditions because it fulfils all of the requirements listed above. However, one important drawback of electrochemical oxidation is the formation or halogenated disinfection by-products, whose formation is further discussed in the next section.

2.5.5 Disinfection by-product formation by electrochemical oxidation

In this thesis, the focus was laid on the formation of two different DBPs. The formation of perchlorate (ClO_4^-) and trihalomethanes (THMs). The latter is a group of four different compounds: trichloromethane (chloroform, CHCl_3), bromodichloromethane (CHBrCl_2), dibromochloromethane (CHBr_2Cl) and tribromomethane (bromoform, CHBr_3). Their structures are shown in Figure 9.

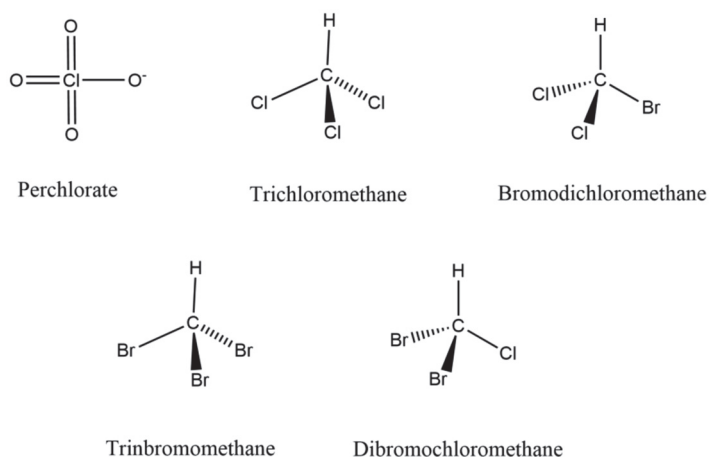
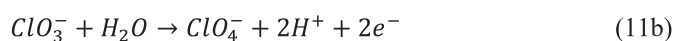
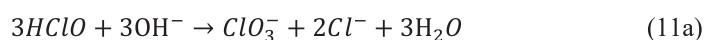


Figure 9: Structure of disinfection by-products investigated in this study.

Perchlorate is an anion that is highly soluble in water and relatively stable in surface- and groundwaters [77]. It is similar in size to iodide (I^-) and can be taken up in place of it by the mammalian thyroid, causing thyroid cancer [78]. Due to its persistence and toxic effect, perchlorate is an unwanted DBP, which is formed via further oxidation of active chlorine (HClO) to chlorate (ClO_3^-) and finally to perchlorate (ClO_4^-) (equation 11a and 11b):



THMs are volatile compounds and are adsorbed in the human body mainly by inhalation and through the skin. Chloroform affects the central nervous system, liver and kidneys when exposed to it over a longer period [79]. Bromoform and dibromochloromethane and bromodichloromethane have the same toxic effect on the human health as chloroform, causing liver and kidney damage [80]. The formation of THMs occurs via the reaction of i.a. active chlorine with organic compounds. Gallard et al. [81] found that CHCl_3 is formed from mono-, di-, tri- and tetrachlorinated phenols, which are incorporated by up to 12 % to CHCl_3 . Which THMs are formed depends on the electrolytes present in the aqueous solution.

There are many important matters to look at: No legal regulations in place, finding an adequate treatment process to adhere to suggested treatment goals and the formation of DBPs that are detrimental to the aquatic and human environment. This project is aimed at bridging these knowledge gaps and adding to the state of the art knowledge in the field of applied electrochemistry.

3 RESEARCH QUESTIONS

This chapter lists the research questions that were raised and gives an overview of the study themes (Paper I – III) designed at addressing these issues.

The following research questions (Q1 – Q6) were identified and answered in order to evaluate the suitability of EO for landfill leachate treatment under the given cold temperatures that dominate Scandinavia.

- Q1:** Which electrochemical oxidation pathways take place during the electrochemical oxidation of organic pollutants? Is it possible to predict oxidation derivatives of the pollutant?
- Q2:** In which way does the existing pre-treatment of the landfill leachate impact the electrochemical degradation of organic pollutants? What does this mean for its application?
- Q3:** How do cold temperatures that are predominant in Northern Scandinavia affect the electrochemical removal of organic pollutants from landfill leachate?
- Q4:** What major drawbacks and advantages accompany the electrochemical oxidation of landfill leachate? Are there ways to overcome or reduce them?
- Q5:** To what degree does the landfill leachate matrix impact the removal (efficiency) of organic pollutants?
- Q6:** Can the future treatment goals for landfill leachate regarding organic pollutants be met by electrochemical oxidation in Scandinavia where cold temperatures dominate?

The research questions are addressed in the following papers:

Paper I: Insights into the Kinetics of Intermediate Formation during Electrochemical Oxidation of the Organic Model Pollutant Salicylic Acid in Chloride Electrolyte

Research outcomes disseminated as part of *Paper I* address research question 1 (Q1). It includes the investigation of the three different oxidation pathways via cyclic voltammetry and bulk electrolysis of the organic model pollutant salicylic acid. Further, the influence of electrolyte composition and the anode material used on the manifestation of the three oxidation pathways were assessed as part of *Paper I*. Density functional theory and natural bond theory

along with a kinetic model were employed to predict oxidation derivatives of the model pollutant.

Paper II: *Application of electrochemical oxidation in cold climate regions – Effects of temperature, pH and anode material on the degradation of Bisphenol A and the formation of disinfection by-products*

Research outcomes disseminated as part of *Paper II* address research questions 2 - 4 (Q2 – Q4). Bulk electrolysis experiments were carried out with an organic model compound (salicylic acid) listed on the list of priority substance in otherwise pure electrolyte, with concentrations resembling the real landfill leachate. Cold experimental temperatures were applied and pH of solution equal to the one before and after pre-treatment. The formation of disinfection by-products was also monitored as part of the experimental testing program.

Paper III: *Electrochemical removal of Bisphenol A from Landfill Leachate under Nordic Climate Conditions.*

Research outcomes disseminated as part of *Paper III* address research questions 4 - 6 (Q4 – Q6). Bulk electrolysis experiments were carried out with real pre-treated landfill leachate spiked with the same organic model pollutant as in *Paper II*. Cold temperatures were applied and an overall assessment of the process applicability under cold operating temperature was performed. Results from *Paper III* were juxtaposed with *Paper II* to estimate the influence of the landfill leachate matrix on the removal of electrochemical oxidation of the model pollutant. Additionally, the formation of disinfection by-products continued to be monitored.

4 RESEARCH METHODOLOGY

This chapter describes the applied research methods. It summarizes the experimental set-ups and analytical methods that were used to obtain the answers to the raised research questions.

4.1 FIELD WORK

Field work was carried on site of the landfill in Mosjøen, Northern Norway. The previously mentioned pilot treatment plant was out of order when no field landfill leachate was collected for this study. The main field work consisted in operating the pilot plant and collecting the landfill leachate for further experiments in the laboratory. Three different sampling campaigns were carried out in the course of ca one year. Summer (August) 2018, Autumn (October) 2018 and Summer (June) 2019. Sampling during winter and spring was not possible due to frozen soil and consequently, due to no landfill leachate runoff during this time of the year.

4.2 EXPERIMENTAL SETUP

4.2.1 Cyclic Voltammetry

Cyclic voltammetry (CV) was used to partially answer *research questions 1 – 2*. CV experiments were carried out with an μ AUTOLABIII/FRA2 (Metrohm, Switzerland) using a $7.07 \times 10^{-6} \text{ m}^2$ platinum rotating disc electrode (Pt-RDE, Metrohm), a $1.24 \times 10^{-5} \text{ m}^2$ boron doped diamond rotating disc electrode (BDD-RDE, neoCoat) and a $1.19 \times 10^{-4} \text{ m}^2$ glassy carbon rod (GC-rod) electrode (Metrohm). A Pt wire was used as an auxiliary electrode. Figure 10 depicts the CV set-up. The speed of the rotating disc electrode was set to 100 rpm for all experiments. A platinum wire served as a counter electrode and an Ag/AgCl (3.0 M) was used as a reference electrode. All experiments were performed at room temperatures (20 °C) using 25 mL electrolyte. The scanning rate was 1 V/s and 5 consecutive scan cycles were run at the time and the potential was swept between -1 and 2 V. CV results were analyzed using NOVA 2.0 software (Metrohm).

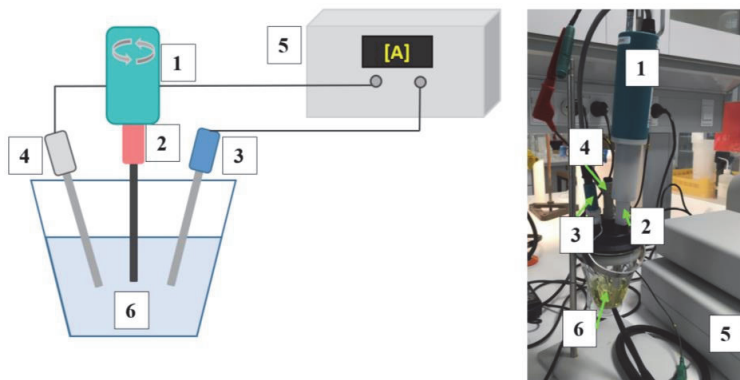


Figure 10: Set-up for cyclic voltammetry; 1) rotating mechanism, 2) working electrode, 3) auxiliary electrode, 4) reference electrode, 5) potentiostat, 6) electrolyte

4.2.2 Bulk Electrolysis

Bulk electrolysis experiments were used to partially answer *research questions 1 – 7*. Electrochemical oxidation was carried out with a micro flow cell (ElectroCell Europe AS, Denmark). In general, two different anode materials were used: Platinum (Pt) with titanium (Ti) as supporting material and boron doped diamond anode (5 microns on both sides) on 2 mm niobium (Nb) as supporting material. A stainless-steel cathode (AISI 316) was used along with both anode materials. Both the cathode and anode have active areas of 10 cm². Two polytetrafluoroethylene turbulence-enhancing meshes were placed between the anode and cathode (4 mm inter-electrode cap). The electrolytic cell is shown in Figure 11.

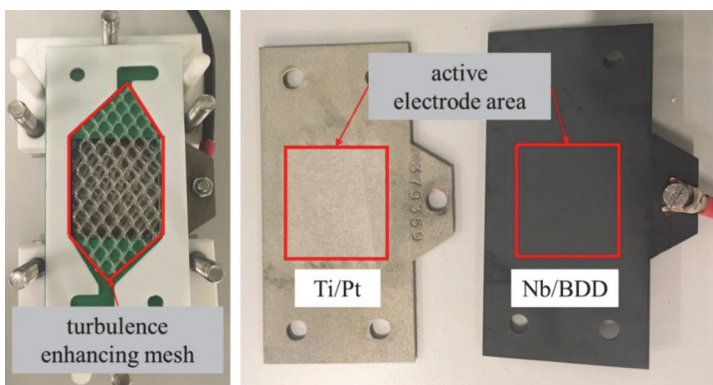


Figure 11: Electrolytic cell; left: turbulence enhancing mesh; right: both anodes (Ti/Pt and Nb/BDD) with indicated active electrode area (10cm²).

The set-up (Figure 12) was placed in a fume hood since gaseous chlorine and other volatile compounds were produced during the experiment, which could be compromising for the human

health. The working- and counter electrodes were cooled from the rear side during the experiment with a tap water stream (ca. 7 °C). The solution (2500 mL) in the glass tank was magnetically stirred and pumped with a peristaltic pump (Masterflex, Cole-Parmer Instrument Co, USA) via Teflon tubing to the micro flow cell with a flow rate of 380 mL/min. A cooling coil (stainless steel) immersed into to the solution and connected to a chiller (FP50-ME, Julabo GmbH, Germany) assured stable operating temperatures. All experiments were carried out in a galvanostatic mode (constant current) with a default applied current of 43 mA/cm². For some experimental batches, the applied current was varied between 10, 43 and 86 mA/cm².

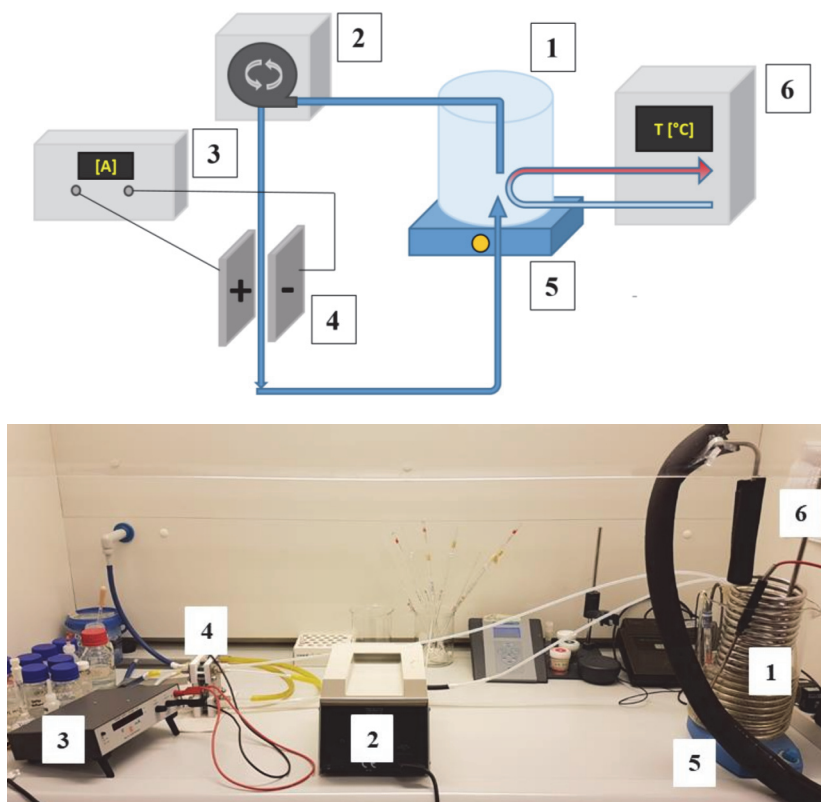


Figure 12: top: Scheme of experimental set-up used; 1) solution tank, 2) peristaltic pump, 3) potentiostat, 4) electrochemical cell, 5) magnetic stirrer, 6) chiller incl. cooling coil; bottom: actual setup

4.3 SAMPLE ANALYSIS

The subsections below (4.3.1 - 4.3.6) are a summary of the sample analysis methods. A more detailed description can be found in the corresponding papers (APPENDIX A: Selected Papers

4.3.1 Ultra-Performance Liquid Chromatography (UPLC – MS)

Samples containing salicylic acid and dihydroxy benzoic acids (*Paper I*) obtained from bulk electrolysis were analysed using an UPLC (Waters, USA) with XEVO TQ-XS triple quadrupole mass spectrometer (Waters) with a 2.1 mm × 100 mm high strength silica HSS T3 column (Waters). The UPLC-MS/MS was operated in multiple reaction monitoring (MRM) mode using electrospray ionization (ESI). A solution of water (HPLC grade, VWR) with 2 mM ammonium formate (Sigma-Aldrich, Merck, Germany) and 0.1% formic acid (VWR International LLC, USA) was used as solvent A and acetonitrile (HPLC grade, VWR) with 2 mM ammonium format (Sigma-Aldrich) and 0.1% formic acid (VWR) was used as solvent B. A flow of 0.4 mL/min was constantly maintained. Data processing was carried out using the ‘Targetlynx’ software (Waters).

4.3.2 Ultra-Performance Convergence Chromatography (UPC² – MS)

Bisphenol A content in samples (*Paper II & III*) was quantified by UPC² (Waters, USA) with XEVO TQ-S triple quadrupole mass spectrometer (Waters) with an Aquity UPC² BEH 1.7 μm column (Waters). Measurements were conducted in multiple reaction monitoring mode using electrospray ionization. The mobile phases were compressed CO₂ (solvent A), methanol containing 10 mM ammonium acetate (solvent B) and 100 % methanol as makeup solvent. A flow rate of 2.5 mL/min and a makeup flow rate of 0.8 mL/min were applied. The automated backpressure was set to 1500 psi. The initial solvent gradient was 95 % A and 5 % B, hold for 0.3 min, increased to 70 % A and 30 % B from 0.3 to 1.3 min and hold for 0.4 min, then decreased to 95 % A and 5 % B from 1.7 min to 1.8 min and hold for 0.7 min. Samples were dried under vacuum (SpeedVac, Thermo Fischer Scientific, USA) at 45 °C and reconstituted in isopropanol prior to analysis. Masslynx (Waters) and Targetlynx (Waters) where the software used for measurements and data analysis respectively.

4.3.3 Gas Chromatography Head Space Mass Spectrometry (GC – HS – MS)

THMs (*Paper II & III*) were identified and quantified using a headspace injector (Tekmar HT3, Teledyne Technologies, USA) coupled to a GC-MS (GC/MS Triple quad 7000, Agilent, USA). The samples or standards (10 mL) were placed in 20 mL headspace vials together with 20 μL of internal standard (dichloromethane), and sealed with a crimp cap. A trap column (Purge/Trap K Vocab® 3000, Supelco, USA) and a DB-624 UI GC column (Agilent) with a length of 30 m, 0.25 mm diameter and 1.40 μm film thickness was used for the headspace GC analysis. The

oven program for the GC started at 35 °C hold for 3 min followed by a ramp of 30 °C/min up to 125 °C, hold for 1 min, followed by a second ramp of 50 °C/min up to 250 °C and a final hold of 4 min. Masshunter (Agilent) was the software used for data gathering and Masshunter Quant (Agilent) software was used for further data processing.

4.3.4 Ion Chromatography (IC)

Chloride (Cl⁻) and perchlorate (ClO₄⁻) anions (*Paper II & III*) were measured using an ion chromatography 940 Professional IC Vario (Metrohm, Switzerland) together with an 858 Professional Sample Processor (Metrohm) and a 10 mL 800 Dosino (Metrohm). A high-performance separation column Metrosep. A Supp5 (Metrohm) was used with polyvinyl alcohol with quaternary ammonium groups as column substrate and column dimensions of 250 x 4.0 mm and 5 µm particle size. Sodium bicarbonate Na₂CO₃ 3.2 mM and sodium carbonate NaHCO₃ 1 mM (Sigma Aldrich) with 20 % acetone with HPLC grade (VWR Chemicals) was used as eluent. The suppressor solution was 0.1 M sulfuric acid (Merck, USA) and 0.1 M oxalic acid (Sigma Aldrich) in ultra-pure water. The flow rate was set to 0.7 mL/min and the thermostat to 40 °C. MagIC Net 3.2 software (Metrohm) was used for measurements and sample analysis.

4.3.5 Total Organic Carbon (TOC) Analyser

TOC (*Paper III*) was measured with the TOC analyser Apollo 9000 (Tekmar). Prior to measurement, samples were diluted 10 times and preserved by adding an adequate amount of concentrated phosphoric acid to obtain a final sample pH between 2 - 3. Measurement procedure followed the Norwegian standard NS EN 1484 [20] and had an LOQ of 0.5 mgC/L.

4.3.6 Hach-Lange Tests

Cuvette tests from Hach (Hach Co., USA) were used to measure the following parameters (*Paper III*): ammonium NH₄⁺/NH₃ (LCK 303, 2- 47 mgNH₄-N/L), nitrate NO₃⁻ (LCK 339, 0.23- 13.5 mgNO₃-N/L) and chemical oxygen demand COD (LCK 314, 15- 150 mgO₂/L). The cuvette tests were analysed with a Hach DR3900 laboratory spectrophotometer for water analysis. Free chlorine (HClO/ClO⁻) in samples (*Paper I -III*) was measured with a with a Hach Pocket Colorimeter™ II, using the N,N-diethyl-p-phenylenediamine (DPD) method with a LOQ of 0.1 mgCl₂/L.

4.4 STATISTICAL ANALYSIS

The experiments (*Paper II & III*) followed a full factorial design with three factors (A, B, C) at two or three levels. The investigated factors were: Temperature, electrode material and pH (*Paper II*) and temperature, electrode material and applied current (*Paper III*). A linear regression model (equation 12) was used to estimate the intercept (b_0), the model constants (b_1 - b_7), where Y is the response and factors A to C assumed to be independent variables. The regression model also accounts for the product terms of the independent variables to model a possible interaction between two or three factors.

$$Y = b_0 + b_1A + b_2B + b_3C + b_4AB + b_5AC + b_6BC + b_7ABC \quad (12)$$

Since the full factorial included replicates ($r=2$), the model has 8 degrees of freedom ($(r-1)2^k$). The experimental order was randomized and analysis of variance (ANOVA) was done using Minitab. The null hypothesis (H_0) stated that no effect is significant ($\text{Effect}_j = 0$) and alternative hypothesis (H_1) assumed at least one effect is significant ($\text{Effect}_j \neq 0$). A significance level of 5 % ($\alpha = 0.05$) was chosen.

4.5 DENSITY FUNCTIONAL THEORY SIMULATIONS

Density functional theory (DFT) simulations (*Paper I*) were performed to study the relative stability of different products, as well as the electronic property of SA in reaction. All calculations were done with the Gaussian 09 package [82]. Unrestricted spin calculation using Lee-Yang-Parr (B3LYP) [83] functional and def2-TZVPP basis set [84], [85] were employed. An implicit solvation model for water was considered using a solvation model based on the quantum mechanical charge density (SMD) [86]. Natural bond theory (NBO) [87] was used to analyse the spin and charge density of the molecules. The default values of Gaussian 09 were used for the convergence of energy and force in the DFT calculations. A similar set up was successfully employed to study the electro-chemical reaction [88].

4.6 KINETIC MODELLING

Mathematical models (*Paper I – III*) predicting the degradation or formation of different compounds were applied. First order (equation 13) or zero order (equation 14) kinetics were assumed depending on the fit of the experimental data to the integrated rate law.

$$-\frac{d[A]}{dt} = k \quad \text{integrated: } [A] = [A]_0 - kt \quad (13)$$

$$-\frac{d[A]}{dt} = k[A] \quad \text{integrated: } [A] = [A]_0 * e^{-(kt)} \quad (14)$$

A: concentration at time t, A₀: initial concentration, k: rate constant, t: time

Computations of reactions rates were done both in Matlab (Mathworks, USA) and in RStudio (RStudio, USA). An ordinary differential equation solver (Runge-Kutta) was used to find the numerical solution of the set of differential equations. Rate constants were determined by fitting the experimental data to the model using the least square method.

5 SUMMARY OF KEY FINDINGS OF THE PAPERS

This chapter gives an overview of the main research outcomes from three journal articles that were published or forthcoming in international and relevant research journals. The focus lays on the main findings which answered the research questions that were identified in Chapter 3.

5.1 PAPER I

Insights into the Kinetics of Intermediate Formation during Electrochemical Oxidation of the Organic Model Pollutant Salicylic Acid in Chloride Electrolyte

Contribution to research questions 1:

Electrochemical oxidation of organic compounds/pollutants is an intricate process and is generally divided into three distinct oxidation pathways [61], [63]. The direct electron transfer from the organic pollutant to the anode surface, the oxidation via electrochemical oxygen transfer reaction (EOTR) from water and the indirect oxidation via a mediating oxidizing species. *Paper I* was aimed at identifying these three oxidation pathways with the help of the organic model pollutant salicylic acid. A priori density functional theory (DFT) simulation was done in order to foresee which salicylic acid derivatives would be formed. EOTR is expected to form hydroxylated salicylic acid derivatives since EOTR occurs via hydroxyl radicals ($\bullet OH$). Indirect oxidation depends on the electrolyte used and the consequently formed oxidizing species. Direct electron transfer was identified via cyclic voltammetry experiments. EOTR and indirect oxidation were investigated by bulk electrolysis experiments. The latter one strongly depends on the supporting electrolyte (NaCl or Na₂SO₄) while EOTR depends more on the used anode material (Platinum, Pt or boron doped diamond, BDD). Therefore, both mentioned electrolytes and anode materials were evaluated. Further, a kinetic model was developed to model the EOTR and indirect oxidization pathways and was validated by comparison to the experimental data.

Results showed that salicylic acid was directly oxidized at the Pt anode surface while no direct electron transfer was observed at the BDD anode. Hydroxylated salicylic acid derivatives (2,3-dihydroxybenzoic acid and 2,5-dihydroxybenzoic acid) were identified and confirmed EOTR of salicylic acid (Figure 13b and d). This oxidation pathway was identified independently of anode material or electrolyte. Indirect oxidation of salicylic acid was determined by the

observation of chlorinated salicylic acid derivatives, 3-chlorosalicylic acid, 5-chlorosalicylic acid and 3,5-dichlorosalicylic acid (Figure 13a and c). Their formation was observed in the NaCl electrolyte. As a consequence of the absent NaCl, chlorinated salicylic acid derivatives were not present in Na₂SO₄ electrolyte. The observed chlorinated and hydroxylated salicylic acid derivatives matched the ones predicted by DFT simulations. Apart from DFT simulations, the kinetic model also predicted the formation of the hydroxylated and chlorinated derivatives to a satisfactory extent (Figure 13a-d).

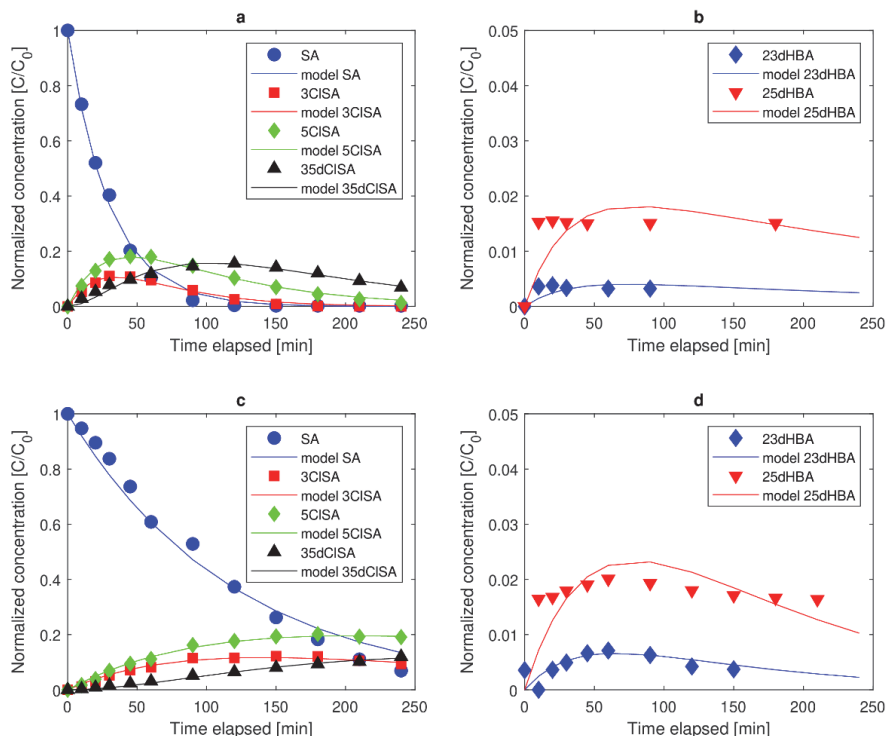


Figure 13: Key figure Paper I; Salicylic acid degradation via intermediate oxidation (active chlorine) to chlorinated salicylic acids on BDD anode (a) and Pt anode (c). Salicylic acid degradation via EOTR to dihydroxybenzoic acids on BDD anode (b) and Pt anode (d) from Ambauen et al. [89].

5.2 PAPER II

Application of electrochemical oxidation in cold climate regions – Effects of temperature, pH and anode material on the degradation of Bisphenol A and the formation of disinfection by-products.

Contribution to research questions 2-4:

Nordic climate is generally characterized by a lot of precipitation (2000 mm/year) and cold average yearly temperature (3.6 °C). The latter greatly affects the kinetics of chemical and biological reaction rates. Consequently, treatment times and costs are generally presumed to be negatively affected as well. The adverse impacts of cold temperatures on reaction rates, treatment times and costs of electrochemical oxidation of the organic model pollutant Bisphenol A has been addressed in this study. Bisphenol A is both originally contained in the landfill leachate and listed on the Norwegian list of priority substances to be removed from landfill leachate. Bulk electrolysis was applied in an electrolyte composition resembling the real landfill leachate with a solution pH equal to the one after the landfill leachate pre-treatment (pH = 10). The identification and formation of the unwanted disinfection by-products, perchlorate and trichloromethane (chloroform) was monitored and quantified. The study was carried out after a full factorial design, which also included a full set of replicates. Three factors were investigated: Temperature (6/20 °C), anode materials (Ti/Pt & Nb/BDD) and pH (7/10). Their influence on the Bisphenol A degradation and disinfection by-product formation was assessed and conclusions were drawn, particularly for cold temperatures and alkaline pH.

Findings from this study demonstrated that cold applied temperatures (6 °C) significantly impacted the electrochemical oxidation of Bisphenol A (99 % removal) (Figure 14a). Longer treatment times (up to 71 %) and higher energy consumption (up to 21%) were observed, which ultimately are associated with higher costs. Furthermore, it showed that a high pH (≈ 10) is beneficial for the electrochemical oxidation of Bisphenol A because at pH 10 Bisphenol A is present as bisphenolate ion ($pK_a = 9.6$), which is more prone to electrophilic attack than Bisphenol A. Consequently, a faster degradation of Bisphenol A was achieved. Another active chlorine species was formed at higher pH (OCl^-) than at neutral pH ($HOCl$) and Bisphenol is present in its deprotonated form, which lead to a more efficient oxidation. The formation of the disinfection by-products was strongly influenced by the anode material. Perchlorate was only formed on BDD anodes (Figure 14c) while trichloromethane was formed faster on Pt than on BDD anodes (Figure 14b). Temperature only significantly affected the formation of trichloromethane but not the formation of perchlorate. It could be concluded from *Paper II* that by accepting longer treatment times and energy consumptions and by choosing an appropriate anode material, electrochemical oxidation can be a suitable choice for organic pollutant removal in Nordic climate areas.

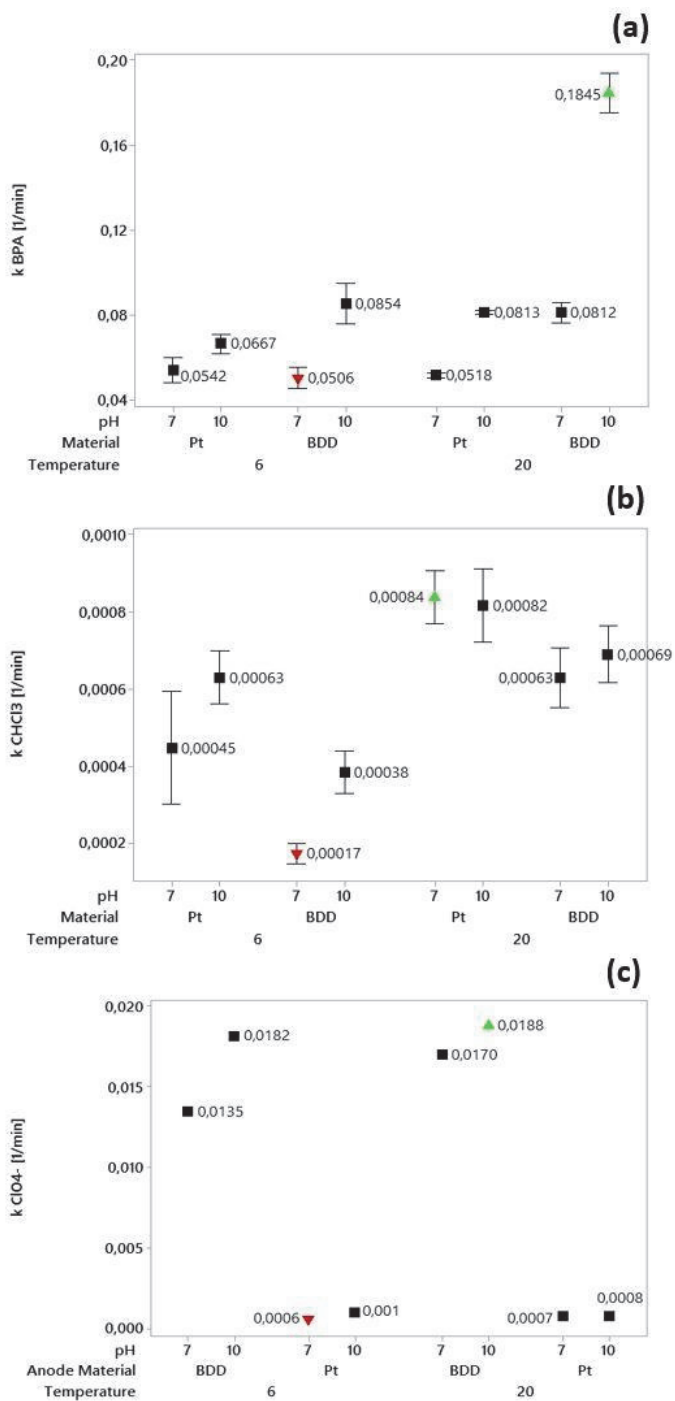


Figure 14: Key figure Paper II, from [90]: Interval plots for the average degradation/ formation rates [1/min] of a) Bisphenol A, b) trichloromethane and c) perchlorate; respective parameter settings can be read from the x-axis

5.3 PAPER III

Electrochemical removal of Bisphenol A from Landfill Leachate under Nordic Climate Conditions

Contribution to research questions 4 – 6:

The final paper of this thesis investigated the applicability of electrochemical oxidation for landfill leachate treatment under simulated real local conditions. Pre-treated landfill leachate was spiked with the organic model pollutant Bisphenol A, which is naturally present in the landfill leachate and listed on the Norwegian list of priority substances. This list itemizes substances that will have to be removed from the landfill leachate to below detection limit in the near future. The electrochemical oxidation of Bisphenol A from the landfill leachate was monitored over time (4 hours), along with several common wastewater parameters. Formation of disinfection by-products was monitored in addition. A full factorial design was applied, with 3 factors: temperature (6/20 °C), anode material (Ti/Pt & Nb/BDD) and current density (10, 43 and 86 mA/cm²). Obtained results were finally compared to the findings from *Paper II*, in order to assess the effect of the landfill leachate matrix on Bisphenol A removal efficiency, treatment time and energy consumption.

The paper shows that Bisphenol A could also with the leachate matrix present be removed to > 99 % within the given treatment time (4 hours), provided that a current of at least 43 mA/cm² is employed (Figure 15). Comparing the degradation of Bisphenol A in landfill leachate (Figure 15b) revealed that removal is always faster (50 – 68 %) in the pure electrolyte. This was attributed to competing reactions caused by the matrix of the landfill leachate, which contains a large number of unknown compounds. Slower degradation kinetics of Bisphenol A in the landfill leachate consequently leads to longer treatment times and higher energy consumption and costs. The average energy consumption for 99 % Bisphenol A removal was found to be 35 % higher at 6 °C compared to 20 °C. However, this study showed that the priority substance Bisphenol A can efficiently be removed from the landfill leachate by electrochemical oxidation even when Nordic climate temperatures apply. TOC was constant throughout all experiments which indicates no complete mineralisation of the organic content. Up to 23 % COD was removed, mostly at higher temperature and increased applied current. Trihalomethanes were mainly formed on Pt anodes in the ppb range, while perchlorate was primarily formed at BDD

anodes in the ppm range. Their formation increased with increasing applied current and temperature.

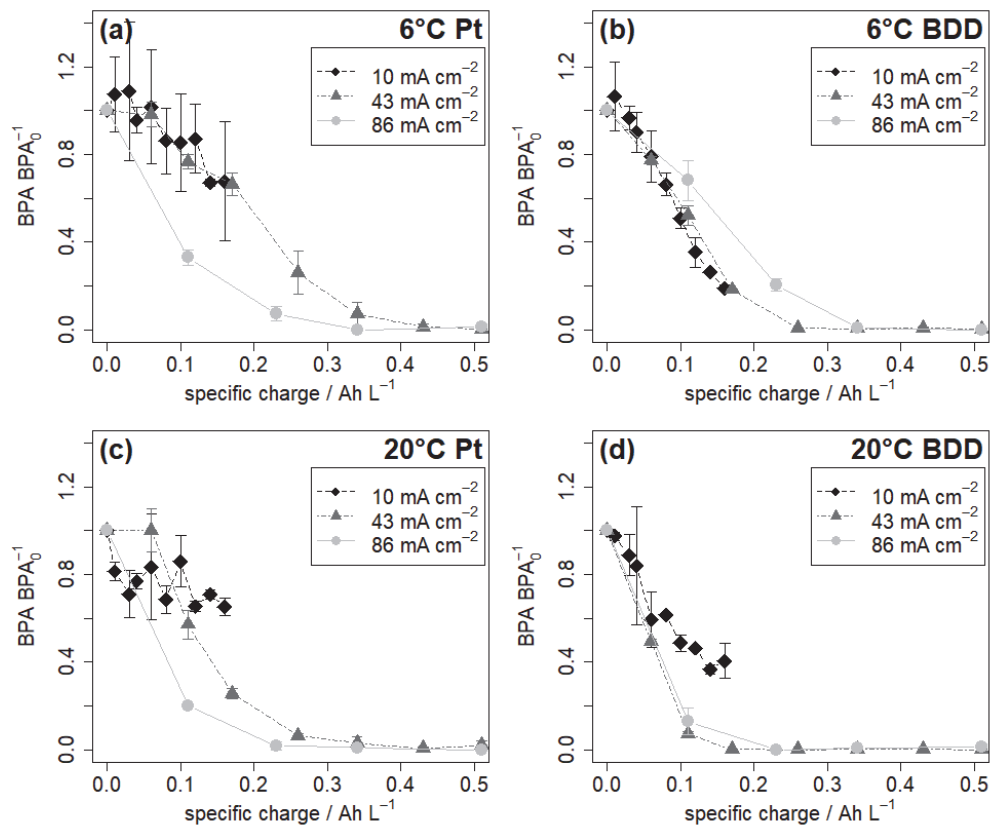


Figure 15: Key figure Paper III: removal of Bisphenol A at different temperatures, anode materials and current densities: a) 10 mA/cm², b) 43 mA/cm², c) 86 mA/cm² (Paper II). Attention must be paid to the different x-axis values. Error bars depict the standard deviation of the replicate experiments. From Ambauen et al.[91].

6 DISCUSSION

The raised research questions are discussed in this chapter based on results obtained from Paper I – III.

6.1 OXIDATION PATHWAYS & PREDICTION OF OXIDATION PRODUCTS (Q1)

As discussed in Section 2.5.3.3, three different oxidation pathways can take place during the electrochemical oxidation of an organic compound/pollutant. Cyclic voltammetry confirmed the oxidation of the organic model pollutant salicylic acid via direct electron transfer (DET) at the anode surface. DET was only confirmed at the “active” platinum electrode but not at the “non-active” BDD electrode. The absence of DET of salicylic acid on BDD anode was attributed to its low affinity towards organic compounds contained in the solution. Oxidation of salicylic acid via electrochemical oxygen transfer reaction, i.e. via the reaction of hydroxyl radicals, was observed by identifying hydroxylated salicylic acid derivatives. Similarly, intermediate oxidation via a mediating oxidizing agent, i.e. active chlorine, was confirmed by identifying chlorinated salicylic acid derivatives.

DFT simulations along with natural bond theory (NBO) to analyse the spin and charge density were able to predict the derivatives of the electrochemical oxidation of the organic model pollutant salicylic acid. Both, hydroxylated and chlorinated derivatives of salicylic acid were adequately predicted by DFT and NBO. The predicted derivatives were later observed during the bulk electrolysis of salicylic acid. The simple first order kinetic model satisfactorily predicted the degradation kinetics of salicylic acid via the a priori predicted derivatives. A better model fit was observed for the chlorinated salicylic acid derivatives than for the hydroxylated ones. This can be partly explained by the fact that the model assumed first order kinetics which is not clearly exhibited in the hydroxylated derivatives. In addition, the hydroxylated derivatives were formed to much lower extent than the chlorinated ones.

The application of DFT and NBO coupled with a kinetic model to predict the degradation behaviour of an organic model pollutant during electrochemical oxidation has been done for the first time in this study. It appeared to be a suitable tool kit for the accurate prediction of organic pollutant derivatives formed via electrochemical oxidation. This method can be transferred to any organic pollutant. It allows to foresee derivatives and helps to make evaluations of the harmfulness of such derivatives, which often are more hazardous than their

parent compound, e.g. [92]. Thus, it can be concluded that electrochemical oxidation of organic pollutants can be predicted to a satisfactory extent by simulations and modelling.

6.2 IMPACTS OF LANDFILL LEACHATE PRE-TREATMENT (Q2)

The existing pre-treatment on the landfill site consisted of aeration, coagulation/flocculation, and lamella clarification). The pH of the landfill leachate was adjusted with sodium hydroxide (NaOH) in order to achieve proper coagulation (coagulant: ferric chloride, FeCl₃). This led subsequently to an elevated pH (≈ 10). The natural pH of the landfill leachate corresponds to on average 6.7 (Table 2). It was anticipated that the pH increase may impact the electrochemical oxidation of organic pollutants contained in the landfill leachate. The pre-treatment was installed with the intention to remove particulate matter, part of the organic matter and heavy metals by chemical precipitation, to provide a higher quality feed water for the subsequent electrochemical oxidation. It is further assumed that pre-treatment of the landfill leachate is beneficial for the subsequent electrochemical oxidation with regard to electrode fouling due to depositions on the electrodes, scaling of Ca²⁺ or Mg²⁺, and clogging of the electrolytical cell. This work did not investigate these aspects, but it is recommended to include them into further research, especially when testing a large-scale pilot plant under more applied conditions.

With the on-site pre-treatment, the majority of the initial turbidity could be removed from the landfill leachate. On average, 83 % of the initial turbidity for the leachate batches collected in Autumn 2018 and Sommer 2019 was removed. The pre-treatment also removed a greater part of the heavy metals that are contained in the landfill leachate. Zinc (Zn), copper (Cu) and arsenic (As) were removed to 86 %, 49 % and 60 % respectively (Table 4). According to the residual concentration of Zn, Cu and As in the pre-treated leachate, the values would classify the leachate as Class III - Moderate for As, Class IV - poor for Zn, and Class V - Very poor for Cu [93]. This means that with regard to heavy metals, the leachate after pre-treatment would still have toxic effects on the environment. In addition, the settled sludge from the lamella clarifier contains a moderate concentration of heavy metals and thus requires appropriate disposal. Up to now, the pre-treatment was not in full use and only operated intermittent to test its capacity and treatment efficiency, and the sludge was returned to the leachate collector system after pre-treatment.

Results obtained in *Paper II* demonstrated that a higher pH clearly influences the formation of the active chlorine species that are formed. Active chlorine is present to 100 % as ClO^- at pH 10. At pH 7, the pH comparable to the one of the untreated landfill leachate, active chlorine is present to 77.2 % as HClO and to 22.8 % as ClO^- . The organic model pollutant, Bisphenol A, was also affected by the augmented pH. Bisphenol A has a pK_a of 9.6, which entails that at alkaline pH it is present in its deprotonated form as bisphenolate ion [94]. The higher pH was found to be beneficial for the electrochemical degradation of Bisphenol A. The benefits can be attributed to a combination of two different events. First, ClO^- (pH 10) lead to faster degradation rates of Bisphenol A than the combination of ClO^- and HClO (pH 7), whereby HOCl was predominant. This identifies ClO^- to be the stronger oxidant to oxidize Bisphenol A. Second, the deprotonated form of Bisphenol A has been demonstrated by others [94] to be more prone to electrophilic attack by hydroxy radical on the aromatic ring.

The electrochemical oxidation was designed as final treatment step with the main goal to remove persistent organic pollutant from the landfill leachate. The finding from *Paper II* shows that the existing pre-treatment, which results in an alkaline solution pH is affecting the electrochemical oxidation of the organic model pollutant Bisphenol A in a beneficial way. It can therefore be concluded that the pre-treatment has a positive impact on the subsequent application of electrochemical oxidation.

6.3 EFFECT OF COLD TEMPERATURES (Q3)

The temperature at which the experiments were carried out corresponds to the average landfill leachate temperature (6 °C) and room temperature (20 °C). Removal of 5.0 μM Bisphenol A was investigated at both temperatures and in pure electrolyte (0.0033 M NaCl & 0.0003 M Na_2SO_4) as well as in landfill leachate. The law of Arrhenius describes the temperature dependence of chemical reaction rates (k). Based on that, it was anticipated that a cold applied temperature results in slower degradation kinetics of Bisphenol A.

Results clearly show that the a priori made anticipation can be confirmed. In all tested cases with an applied current of 43 mA/cm^2 or higher, removal of Bisphenol A to below detection limit was observed at cold temperature (6 °C) within the experimental time of 240 min. In pure electrolyte, Bisphenol A degradation rates were on average 37 % faster at 20 °C than at 6 °C. In landfill leachate, the average degradation rates were 49 % faster at 20 °C than at 6 °C. Treatment times for 90 % removal of 5.0 μM Bisphenol A were on average 37 % (26 min) and

23 % (8 min) longer at cold temperature compared to room temperature for landfill leachate and pure electrolyte respectively. These findings were specific for the case of the investigated organic model pollutant Bisphenol A.

Degradation rates of COD were on average 25 % slower at 6 °C than at 20 °C. Slower degradation kinetics lead to longer treatment times, higher energy consumption and finally operating costs. The average non-household electricity price in Europe (2019) is 0.1306 €/kWh, while it is 0.0829 €/kWh in Norway [95]. Electricity is on average 36 % cheaper in Norway than in the rest of Europe. In addition, 97.8 % of electricity in Norway is produced by renewable energy (hydropower and wind power) [96]. The relatively low electricity prices along with the sustainable electricity production can justify the application of electrochemical treatment of landfill leachate under cold temperatures with regards to increased energy demand. Moreover, all in chapter 2.5.2 considered AOPs require a certain energy input, which most likely will also increase at low temperatures. Particularly ozonation requires an additional high energy input for the generation of ozone, 6 -13 kWh/kgO₃, depending on the input gas [97], [98]. Thus, an increased energy demand for EO at low temperatures can be put into perspective compared to other advanced oxidation treatment options.

Furthermore, it has to be considered that this study was conducted on a laboratory scale with a recirculating batch reactor. Upscaling to a pilot plant or full-scale reactor would mean that several electrodes have to work in parallel to provide a large enough total electrode area. Anglada et al. [99] implemented such a parallel electrode system on a pilot scale. In their study, rainwater was used to cool the leachate in order not to overheat the electrolytic cell above a critical temperature of 35 °C. There is heat development that naturally occurs in the electrolytic cell due to electrical resistance. This heat development in the cell may be beneficial for the electrochemical oxidation of cold temperature landfill leachate. Warmer leachate leads to faster reaction rates and consequently to lower energy consumption and costs. It is however difficult and was beyond the scope of this work to estimate to what extent the heat development would warm up the cold landfill leachate in a large-scale set-up. It may also be likely that the heat development in the cells can increase the solution temperature to an extent where electrode cooling would be required. A large-scale study on site is required to evaluate the heat development within the electrolytic cell and to estimate to what extent it would be beneficial for cold temperature leachate treatment.

6.4 DRAWBACKS & ADVANTAGES (Q4)

The results from *Paper II & III* show that electrochemical oxidation of a chloride containing solution results in a considerable disadvantage. The formation of active chlorine species via the Cl^- oxidation leads to the formation of unwanted DBPs. Experiments in pure electrolyte have shown that perchlorate as well as chloroform are formed. Chloroform belongs to the group of THMs, volatile halogenated compounds. The same was observed during the electrochemical oxidation of landfill leachate and besides chloroform other chlorinated and bromated THMs were identified. Perchlorate was only formed on BDD anodes and its formation was negligible on Pt anodes. THMs on the other hand were mainly formed on Pt anode and to a much lesser extent on BDD anodes. This behaviour was attributed to the fact that more organic compounds are completely mineralized on BDD anodes, while only partial oxidation takes place on Pt anodes. The partially oxidized organic compounds further react with active chlorine or bromine to form THMs. These findings are in line with the literature provided in Chapter 2.5.5. The formation of those DBPs is a major drawback since they are harmful to the environment [79], [100]. It is difficult to argue which anode material is the better choice with regards to the formation of DBPs. Both, THMs and perchlorate are compromising for the health of living organisms by affecting the thyroid, kidney, liver and central nervous system (Chapter 2.5.5). Perchlorate is very stable in the water while THMs are volatile compounds and are likely to volatilise into the air. Shorter treatment times on BDD anodes will limit the formation of perchlorate. Toxicity tests of both, perchlorate and chloroform show that chloroform is toxic for fish (rainbow trout) and crustacean (*daphnia magna*) at lower doses than perchlorate. The lethal concentrations (LC) at which 50 % of the *daphnia magna* population dies (LC_{50}) are estimated to 29 – 65 mg/L for chloroform [101], [102] and 490 mg/L for perchlorate [103]. The values were obtained for an exposure of 48 hours in a flow through reactor. Corresponding LC_{50} values for an exposure of 96 hours for the rainbow trout are 36 mg/L for chloroform [102] and 2 mg/L for perchlorate [103]. Maximum perchlorate concentration that was reached on BDD anode was 237 mg/L and 16 mg/L on Pt anode. The maximum chloroform concentration reached on BDD anode was 15 $\mu\text{g/L}$ and 136 $\mu\text{g/L}$ on Pt anode. This implies that the perchlorate LC_{50} for fish was exceeded on both anode materials but was much higher on the BDD anode. The perchlorate LC_{50} for *daphnia magna* was not exceeded at neither BDD nor Pt anode. The chloroform LC_{50} was neither exceeded for *daphnia magna* nor for fish at both anode materials. Thus, it is assumed that perchlorate causes more toxic harm to the aquatic environment and therefore Pt anode would be a favourable choice over BDD. One option to minimize the

production of perchlorate is the application of graphite cathodes, which are known for high cathodic hydrogen peroxide (H_2O_2) production [104]. The cathodic reduction of oxygen (O_2) leads to the formation of H_2O_2 which is able to inhibit perchlorate formation [105][106]. Perchlorate production is minimized by scavenging of the precursors HOCl/OCl^- by H_2O_2 whereby chloride (Cl^-), H_2O and O_2 are formed [107].

Table 7 summarizes the advantages and disadvantages associated with the anode material. The different electrode materials (BDD & Pt) did not only have an impact on the formation of DBPs but also showed to be significantly influencing the degradation kinetics of the organic model pollutant Bisphenol A (*Paper II & III*). The use of BDD anodes lead to an overall faster degradation of Bisphenol A than the use of the Pt anode. On one hand, faster oxidation of organic pollutants means shorter treatment times when comparing both anode materials with the same anode area. On the other hand, it means that the total anode surface area could be reduced when BDD anodes are used instead of Pt anodes due to the more effective degradation on BDD anodes. At first, this implies that BDD would be the anode material of choice when implementing a large scale treatment. However, anode material costs cannot be ignored and neither their lifetime. Cañizares et al. [76] compared the operational costs of electrochemical oxidation of wastewaters with ozonation and Fenton process. It was found that Fenton process is the cheapest process with 0.7 – 3.0 € per kgO_2 removed followed by electrochemical oxidation (BDD) with 2.4 – 4.0 € per kgO_2 removed and finally ozonation with 8.5 – 10.0 € per kgO_2 removed. It was further stated that the operational costs are mainly higher for electrochemical oxidation than for Fenton process due to the high costs of conductive BDD electrodes which are estimated to 15'000 €/m². The support material of BDD anode that was used in this study, niobium (Nb), is also very expensive and has been replaced by silicon (Si) for large scale applications by the market leader WaterDiam (former: Adamant Technologies). The cost for platinum coated titanium electrodes are estimated to be around a factor 2.5 lower than for BDD electrodes. ElectroCell Europe AS [108] states an electrode price for their laboratory scale electrochemical flow cell for Ti/Pt (0.001 m²) of 238 € while the same size Nb/BDD anode costs 600 €. It is thus assumed that the electrode price difference for large scale electrochemical flow cells differs by the same factor. Both, BDD and Pt anodes are known to have high conductivity, chemical stability and a long service life [109]. BDD anode is additionally popular due its low adsorption property which resists a polymer layer formation [110]. Keeping the price and the development of DBPs in mind, Pt anode is the more feasible material when it comes to a possible large-scale implementation of the electrochemical process.

Table 7: Overview of anode materials and their associated advantages and disadvantages

Material	Advantages (+)	Disadvantages (-)
<i>Boron doped diamond (BDD)</i>	<ul style="list-style-type: none">• fast degradation kinetics• negligible THMs formation• shorter treatment times• lower energy costs	<ul style="list-style-type: none">• production of perchlorate• more expensive material• toxic concentrations of DBPs• DET not detected for model compound SA
<i>Platinum (Pt)</i>	<ul style="list-style-type: none">• negligible perchlorate formation• less expensive material• nontoxic concentrations of DBPs• DET of model compound SA	<ul style="list-style-type: none">• slower degradation kinetics• production of THMs• longer treatment times• higher energy costs

As mentioned above, Fenton process is the most economical AOP, but comes with a major drawback, which is the production of iron sludge. This sludge needs further treatment or disposal which again is associated with more costs and which also is a secondary source of pollution [111]. Electrochemical oxidation on the other hand has the major advantages that no residual waste is produced and no O₂ has to be fed to the cathode like for the Electro-Fenton process and only a clean reagent, the electron, is used [112], [113]. This includes also that the storage of potentially dangerous chemicals can be avoided, which increases the process safety [114]. Similar to electrochemical oxidation, ozonation does not require the addition of chemicals. However, the production of ozone as well as the treatment of off-gas to remove hazardous residual ozone before release, add additional costs and risks to the process. In addition, ozonation is a more complex process than electrochemical oxidation that requires complicated equipment and reactor design [115]. The afore mentioned production of mediating oxidizing agents is another advantage compared to other AOPs, as they improve the overall oxidation efficiency [114]. This advantage has to be put into perspective to the formation of DBPs. Finally, a last disadvantage of electrochemical oxidation includes the fact that the process is not easily scalable, which requires extensive pilot studies prior to implementation [114]. All AOPs come with advantages and disadvantages. The most suitable process depends therefore on: Power availability and costs, sludge disposal, space on site, safe chemical storage and personnel that can handle the process complexity. With regard to the oxidation efficiency

and DBPs formation, the leachate composition is most important. It will also decide if electrochemical oxidation will be a standalone process or a polishing step [114]. In this study, the advantages of electrochemical oxidation as discussed here and in Chapter 2.5.3 outweighed the disadvantages. The most significant advantages of electrochemical oxidation compared to other AOPs are: No sludge production, no chemical addition, and the possibility of successful operation at low temperatures. In retrospective, more weight should have been given to possible by-production formation, based on the water composition in order to choose the most suitable treatment process.

6.5 LANDFILL LEACHATE MATRIX EFFECT (Q5)

Juxtaposing the results from *Paper II & III* allows to draw conclusions about the effect of the landfill leachate matrix on the electrochemical degradation of the model organic pollutant Bisphenol A. In *Paper II*, 5.0 μM Bisphenol A was degraded in clean electrolyte containing similar amount of NaCl and Na₂SO₄ as the landfill leachate. In *Paper III* the same initial amount of Bisphenol A was degraded in landfill leachate. The remaining parameter settings, applied current (43 mA/cm²), temperature (6 & 20 °C), anode material (BDD & Pt), pH (10) and the flow rate (384 mL/min) were maintained at the same levels in both studies. Reaction rate constants of Bisphenol A (k_{BPA}) were compared for both applied temperatures (6 and 20 °C) and both anode materials. Table 8 summarizes the effect of the matrix on the degradation kinetics of Bisphenol A [116]:

Table 8: Landfill leachate matrix effects on the degradation kinetics (k_{BPA}) of Bisphenol A, adapted from Ambauen et al. [116].

	clean electrolyte	landfill leachate	Reduction
	k [1/min]	k [1/min]	Δk [%]
6 °C/Pt	0.072	0.023	68
6 °C/BDD	0.097	0.044	55
20 °C/Pt	0.087	0.036	59
20 °C/BDD	0.187	0.093	50

Larger differences of k_{BPA} in the two different matrices were observed when the temperature was low or on Pt anode. The presence of hydroxyl radical scavengers in form of inorganic anions such as Cl⁻ and bicarbonate lead to a decelerated oxidation of Bisphenol A. The

scavenging effect of the inorganic anions also contributes to slower degradation kinetics k_{BPA} . There are also unknown constituents in the landfill leachate which compete with Bisphenol A for oxidants, which could also slow down the degradation of Bisphenol A. The degradation over time of Bisphenol A in landfill leachate and clean electrolyte is shown in Figure 16.

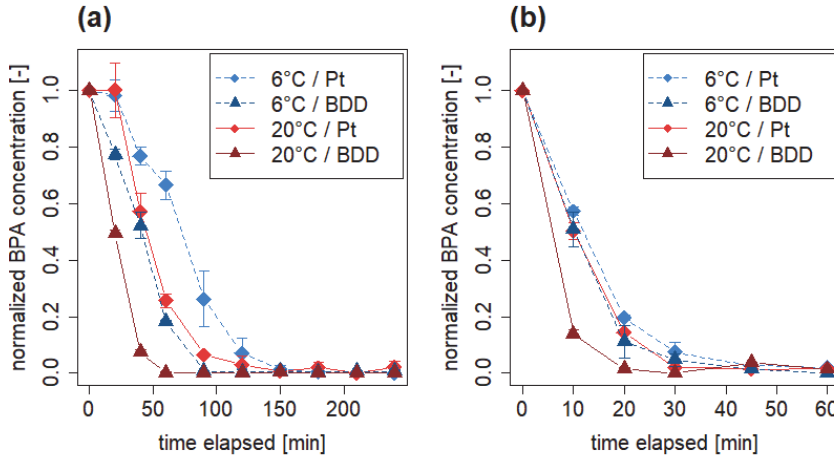


Figure 16: Comparison of Bisphenol degradation in landfill leachate (a) and clean electrolyte (b), adapted from Ambauen et al. [117] & Ambauen et al. [116]. Error bars show the standard deviation of replicate experiments.

It can be seen that the degradation pattern of Bisphenol A was similar in both solutions. In landfill leachate (Figure 16a), degradation only starts immediately at BDD anode while a small time delay is observed on Pt anodes. In clean electrolyte (Figure 16b) degradation started immediately on both anode materials. The matrix effect decreased the degradation speed but the different parameter settings (temperature & anode material) lead to the same order of k_{BPA} from slowest to fastest (Table 8). The initial delay in landfill leachate matrix is caused due to the slower formation of active chlorine in the landfill leachate which results in less mediated oxidation.

Not only is Bisphenol A facing competition during oxidation but also chloride ions have to compete during electrochemical oxidation with other leachate constituents. The landfill leachate matrix also affected the formation of chloroform on Pt anode, but in the opposite way. Formation of chloroform is the result of the reaction between an organic compound and active chlorine [81]. The presence of many unknown organic compounds along with Bisphenol A leads therefore to the formation of more chloroform than in the clean electrolyte. Besides, the leachate most likely contains compounds that readily react with active chlorine to form

chloroform, while Bisphenol A first has to be partially oxidized before reacting to form chloroform. For perchlorate, the opposite than for chloroform was observed. The landfill leachate matrix affected the perchlorate formation on BDD anode in a positive way in the sense that about 96 % less perchlorate was formed in landfill leachate compared to clean electrolyte. Perchlorate (ClO_4^-) is the highest oxidation state of Cl^- which is formed via the intermediate formation of active chlorine (or ClO^- at pH 10). Since there is more scavenging of active chlorine in the landfill leachate, the active chlorine is used for mediated oxidation and only a small part is further oxidized to perchlorate.

Thus, the landfill leachate matrix decelerates the oxidation of Bisphenol A due to the competition with other unknown constituents. This leads consequently to longer treatment times and costs to remove the same amount of Bisphenol A from the two different solutions. This competition also has a negative effect when it comes to the formation of chloroform, a THM and DBP, since its formation is higher than in clean electrolyte. On the other side the competition caused by the matrix effect reduces the formation of perchlorate, which is beneficial with regard to effluent toxicity.

6.6 ADHERENCE OF TREATMENT GOALS (Q6)

Adherence of treatment goals was assessed based on the results from *Paper II & III*. As mentioned in Chapter 2.1, the goal of an adequate treatment is to remove compounds listed on the Norwegian list of priority substances (Table 10, APPENDIX B) to below their detection limit. In the case of the organic model compound (Bisphenol A) used in this study, which is listed on the Norwegian priority substance list, the detection limit was found to be 5.0 nM (1.1 $\mu\text{g/L}$) with the applied UPLC-MS² method. The removal of 5.0 μM Bisphenol A from landfill leachate to below detection limit within the given experimental time of 4 hours was successful as long as an applied current of at least 43 mA/cm^2 was maintained. For lower currents (i.e. 10 mA/cm^2) 4 hours of treatment were not enough for any applied temperature or anode material used.

The initial Bisphenol A concentration was spiked by a factor 100 to be able to better follow its degradation over time. In the pre-treated landfill leachate, a Bisphenol A concentration of 11 $\mu\text{g/L}$ (50 nM) was found, while it was increased to 1.1 mg/L (5000 nM) for the purpose of this study. Taking this fact into consideration, means that the treatment time to remove Bisphenol A below its detection limit may be much shorter in practice. The real treatment times can be

roughly estimated by using the obtained reaction rate constant for the different experimental settings. Such estimations show that treatment times to remove Bisphenol A to below detection limit would approximately be 66 % reduced. Consequently, operational costs to remove Bisphenol A would be reduced accordingly.

Under the challenging conditions of the Nordic climate in the subarctic climate zone, electrochemical oxidation showed to be a suitable process to successfully remove the chosen model compound to below its detection limit. Thus, electrochemical oxidation was able to adhere to the given treatment goals. However, this study only focused on one particular organic pollutant, yet many other organic pollutants are found on the Norwegian list of priority substances (APPENDIX B, Table 10) and of course also in the leachate matrix (APPENDIX B, Table 11). Based on the behaviour of Bisphenol A, it is expected that electrochemical oxidation also is a suitable AOP to remove organic pollutants in general from the landfill leachate. Nonetheless, treatment times may vary a lot based on the complexity of the other organic compounds. The ultimate goal is to remove all the compounds from the Norwegian list of priority substances to below detection limit. To get an appropriate estimate of corresponding treatment times and costs, it is suggested to measure sum parameters (e.g. PAH, BTEX) for the different organic compounds. The above made suggestion were not investigated in this study because setting up chromatographic methods for e.g. PAH is very time consuming and costly and could not be covered by the project funding. The same applies for the identification of heavy metals. One time analysis of raw and pre-treated landfill leachate was done in an external lab and gave an idea of the content of organic sum parameters and heavy metals (Table 4).

7 CONCLUSIONS

This chapter summarizes the answers to the identified research questions, the contribution of the study and discloses the common thread for this thesis. It also states the limitations and questions for further research.

7.1 ANSWERS TO THE RESEARCH QUESTIONS

In the following the 6 research questions are recommenced and concisely answered:

- Q1:** *Which electrochemical oxidation pathways take place during the electrochemical oxidation of organic pollutants? Is it possible to predict oxidation derivatives of the pollutant?*
- A1:** Oxidation via direct electron transfer from the organic compound to the anode, direct oxidation via oxygen transfer reactions and mediated oxidation via an intermediate oxidant are the three identified pathways. It was possible to predict the formation of hydroxylated and chlorinated oxidation derivatives of the organic model compound via density functional theory simulations along with natural bond theory.
- Q2:** *In which way does the existing pre-treatment of the landfill leachate impact the electrochemical degradation of organic pollutants? What does this mean for its application?*
- A2:** The alkaline pH after pre-treatment affects the dissociation of the organic model pollutant and the dominating active chlorine species. Both factors have a beneficial effect on the degradation kinetics.
- Q3:** *How do cold temperatures that are predominant in Northern Scandinavia affect the electrochemical removal of organic pollutants from landfill leachate?*
- A3:** Colder temperatures lead to longer treatment times and consequently to higher energy demands and ultimately to higher costs. Despite the higher energy consumption and higher operating costs, a satisfactory removal of the target model compound could be achieved. The all-renewable energy production in Norway delivers comparably cheap power, which justifies a higher energy consumption and thus the application of the process in Northern Scandinavia.

Q4: *What major drawbacks and advantages that accompany the electrochemical oxidation of landfill leachate? Is there a way to overcome or reduce them?*

A4: The major disadvantage is the formation of unwanted disinfection by-products, perchlorate and trihalomethanes. Their formation can be reduced by either choosing a rather low applied current or by specifically choosing an anode material. Perchlorate is primarily formed on BDD anodes while trihalomethanes were mainly formed on Pt anodes. The major advantages of electrochemical oxidation of landfill leachate is its relatively simple application and its effectiveness to degrade the target compound to below the detection limit.

Q5: *To what degree does the landfill leachate matrix impact the removal (efficiency) of organic pollutants?*

A5: The landfill leachate contains scavenging compounds that lead to reduced kinetics of the electrochemical oxidation of the target compound. The matrix effect of the landfill leachate slowed down the degradation of the target compound between 50 % and 68 %, depending on the applied current and temperature. The degradation pattern of the target compound at different applied currents and anode materials was however the same for both clean electrolyte and landfill leachate matrix.

Q6: *Can the future treatment goals for landfill leachate regarding organic pollutants be met by electrochemical oxidation in Scandinavia where cold temperatures dominate?*

A6: Yes, future treatment goal can potentially be met by the application of electrochemical oxidation, but further studies need to be conducted to get an appropriate estimate of treatment times and costs.

7.2 CONCLUSIONS

The incentive of this work was to find and assess an adequate treatment for landfill leachate that meets the challenging Norwegian environmental conditions and that is able to comply future treatment goals. Different research questions were formulated and subsequently answered by three separate studies. The aims and objectives were addressed by laboratory studies combined with kinetic modelling. Field work on the landfill site was also a relevant part of this study.

The findings of this thesis show that the Nordic climate, i.e. the cold operating temperatures significantly affect the electrochemical treatment of landfill leachate. A major effect and disadvantage are the increased treatment times and the subsequent higher energy demand ultimately leading to higher operational costs. However, the study also shows that the landfill leachate can be treated successfully by electrochemical oxidation under the given conditions. The organic model pollutant was successfully removed to below the detection limit and thus adhering to the constituted treatment goals. Further, this implies that the process is also suitable for the removal of other organic compounds, listed on the Norwegian list of priority substances. The study also stresses the importance of individual process parameters, whereas the applied current as well as the anode material were identified as paramount when it comes to disinfection by-product formation and operational matters of expense.

The findings of this thesis contribute to the field of applied electrochemistry and the general emerging interest of different technologies in arctic regions. A novel cornerstone for advanced oxidation treatments and their application under cold operating temperatures could be set with this study, which is of great profit for any future application under similar environmental conditions. Furthermore, the present study is a valuable contribution to help to evaluate and estimate process performance and associated costs, which is indispensable for future design, implementation, and operation. This makes the findings of this study not only interesting for suppliers of electrochemical oxidation- or advanced oxidation systems in general, but also for the operators of landfills or wastewater treatment plants that are compelled to meet the future more stringent treatment goals in Norway.

This thesis could successfully answer all the objectives and research questions, yet it also encountered its limitations. Focus was given to the removal of organic pollutants while the landfill leachate contains a lot of other pollutants such as heavy metals and inorganic compounds. The latter ones were not addressed in this study, except during the pre-treatment on site. The study was also limited to lab-scale experiments and thus neglected the importance of a pilot plant, which is important for design optimization for a later large-scale implementation.

7.3 OUTLOOK AND RECOMMENDATIONS

There is room for future work on the application of electrochemistry to treat landfill leachate. This study mainly focused on the removal of one specific organic pollutant and on the

formation of disinfection by-products. However, the landfill leachate consists of a very complex matrix containing a lot of unknown and only few known compounds. In addition, all studies in this work were carried out in a lab scale unit in a very controllable environment. Very few large scale studies are found up to date that investigated the application of electrochemical oxidation for landfill leachate of wastewater in general. Future work that would complement this thesis could include the investigation of the following points:

- Focus on the removal of compounds other than organic pollutants, with a special focus on the removal of heavy metals and nitrogen.
- Implementation of large scale units on site to assess the proper configuration and design such as parallel units or units in series.
- Attention to the heat development within large scale applications that may be favourable towards the challenge of the cold leachate temperatures.
- Comparison to other advanced oxidation processes such as ozonation to be able to find the most suitable advanced oxidation process, also with regard to the removal of heavy metals and nitrogen.
- Possible change of composition and concentrations due to change in disposed waste or climate change that may affect the landfill leachate matrix.

This study did roughly estimate the energy costs to remove the organic model pollutant from the landfill leachate. However, a proper assessment of a potential large-scale unit that includes energy consumption, material costs, maintenance and life expectancy would be of interest as well for future work. Last but not least, an environmental impact analysis could help in the decision making process of finding the appropriate landfill leachate treatment for Nordic climate areas.

BIBLIOGRAPHY

- [1] T. A. Kurniawan, *Treatment of Landfill Leachate*. LAP Lambert Academic Publishing, 2011.
- [2] Z. Salem, K. Hamouri, R. Djemaa, and K. Allia, “Evaluation of landfill leachate pollution and treatment,” *Desalination*, vol. 220, no. 1–3, pp. 108–114, 2008.
- [3] R. B. Brennan, M. G. Healy, L. Morrison, S. Hynes, D. Norton, and E. Clifford, “Management of landfill leachate: The legacy of European Union Directives,” *Waste Manag.*, vol. 55, pp. 355–363, 2016.
- [4] “COUNCIL DIRECTIVE 1999/31/EC of 26 April 1999 on the landfill of waste,” *Off. J. Eur. Communities*, no. 10, 1999.
- [5] A. Gröhlich, “Evaluation of landfill leachate treatment , considering water quality , legal aspects and site specifics,” 2015.
- [6] “DIRECTIVE 2008/98/EC OF THE EUROPEAN PARLIAMENT AND OF THE COUNCIL of 19 November 2008 on waste and repealing certain Directives,” *Off. J. Eur. Union*, pp. 3–30, 2008.
- [7] K. Harstad, *Handling and Assessment of Leachates from Municipal Solid Waste Landfills in the Nordic Countries*. Norden, 2006.
- [8] Norwegian Environment Agency, “List of priority substances.” [Online]. Available: <https://www.environment.no/topics/hazardous-chemicals/list-of-priority-substances/>.
- [9] LOVDATA, “Forskrift om vannforsyning og drikkevann (drikkevannsforskriften),” 2016. [Online]. Available: <https://lovdata.no/dokument/SF/forskrift/2016-12-22-1868>.
- [10] Norwegian Meteorological Institute, “eklima,” 2019. [Online]. Available: eklima.met.no.
- [11] Søndre Helgeland Miljøverk IKS, “SHMIL,” 2019. [Online]. Available: <http://shmil.no/>.
- [12] M. Torsvik and H. Rasmussen, “Tillatelse til mottak , sortering og behandling av avfall gitt til Søndre Helgeland Miljøverk IKS,” 2009.

- [13] F. G. Pohland, S. R. Harper, K.-C. Chang, J. T. Dertien, and E. S. K. Chian, "Leachate generation and control at landfill dipsoal sites," *Water Qual. Res. J.*, 1985.
- [14] P. Kjeldsen, M. A. Barlaz, A. P. Rooker, A. Baun, A. Ledin, and T. H. Christensen, "Present and Long-Term Composition of MSW Landfill Leachate: A Review," *Crit. Rev. Environ. Sci. Technol.*, vol. 32, no. 4, pp. 297–336, 2002.
- [15] P. E. Payandeh, N. Mehrdadi, and P. Dadgar, "Study of Biological Methods in Landfill Leachate Treatment," *Open J. Ecol.*, vol. 07, no. 09, pp. 568–580, 2017.
- [16] M. Henze, *Biological wastewater treatment: principles, modelling and design*. IWA publishing, 2008.
- [17] I. Metcalf & Eddy, G. Tchobanoglous, F. Burton, and H. D. Stensel, *Wastewater Engineering: Treatment and Reuse*. McGraw-Hill Education, 2002.
- [18] J. Wiszniowski, D. Robert, J. Surmacz-Gorska, K. Miksch, and J. V. Weber, "Landfill leachate treatment methods: A review," *Environ. Chem. Lett.*, vol. 4, no. 1, pp. 51–61, 2006.
- [19] N. Rani, P. Sangwan, M. Joshi, A. Sagar, and K. Bala, "Chapter 5 - Microbes: A Key Player in Industrial Wastewater Treatment," M. P. Shah and S. B. T.-M. W. T. Rodriguez-Couto, Eds. Elsevier, 2019, pp. 83–102.
- [20] J. C. Crittenden, R. R. Trussell, D. W. Hand, K. J. Howe, and G. Tchobanoglous, *MWH's Water Treatment: Principles and Design*. John Wiley & Sons, 2012.
- [21] S. Plotkin and N. M. Ram, "Multiple bioassays to assess the toxicity of a sanitary landfill leachate," *Arch. Environ. Contam. Toxicol.*, vol. 13, no. 2, pp. 197–206, 1984.
- [22] H. A. O. Alisawi, "Performance of wastewater treatment during variable temperature," *Appl. Water Sci.*, vol. 10, no. 4, pp. 1–6, 2020.
- [23] W. M. K. R. T. W. Bandara *et al.*, "Anaerobic treatment of municipal wastewater at ambient temperature: Analysis of archaeal community structure and recovery of dissolved methane," *Water Res.*, vol. 46, no. 17, pp. 5756–5764, 2012.
- [24] R. H. Kettunen, T. H. Hoilijoki, and J. A. Rintala, "Anaerobic and sequential anaerobic-aerobic treatments of municipal landfill leachate at low temperatures,"

Bioresour. Technol., vol. 58, no. 1, pp. 31–40, 1996.

- [25] S. Parsons, *Advanced oxidation processes for Water and Wastewater treatment*. Cornwall, UK: IWA publishing, 2004.
- [26] M. M. Benjamin, *Water Chemistry*, Second edi. Waveland Press Inc., 2015.
- [27] A. R. Ribeiro, O. C. Nunes, M. F. R. Pereira, and A. M. T. Silva, “An overview on the advanced oxidation processes applied for the treatment of water pollutants defined in the recently launched Directive 2013/39/EU,” *Environ. Int.*, vol. 75, pp. 33–51, 2015.
- [28] V. Radim, A. Machulech Jr., S. C. Oliveira, and M. E. Osugi, *Organic Pollutants - Monitoring , Risk and Treatment*. Rijeka, Croatia: InTech, 2013.
- [29] M. Anbar, D. Meyerstein, and P. Neta, “The reactivity of aromatic compounds toward hydroxyl radicals,” *J. Phys. Chem.*, vol. 70, no. 8, pp. 2660–2662, 1966.
- [30] R. Andreozzi, V. Caprio, A. Insola, and R. Marotta, “Advanced oxidation processes (AOP) for water purification and recovery,” *Catal. Today*, vol. 53, no. 1, pp. 51–59, Oct. 1999.
- [31] Y. Deng and J. D. Englehardt, “Treatment of landfill leachate by the Fenton process,” *Water Res.*, vol. 40, no. 20, pp. 3683–3694, 2006.
- [32] R. Romero, D. Contreras, M. Sepúlveda, N. Moreno, C. Segura, and V. Melin, “Assessment of a Fenton reaction driven by insoluble tannins from pine bark in treating an emergent contaminant,” *J. Hazard. Mater.*, vol. 382, no. July 2019, p. 120982, 2020.
- [33] H. Zhang, J. C. Heung, and C. P. Huang, “Optimization of Fenton process for the treatment of landfill leachate,” *J. Hazard. Mater.*, vol. 125, no. 1–3, pp. 166–174, 2005.
- [34] A. Morone, P. Mulay, and S. P. Kamble, “8 - Removal of pharmaceutical and personal care products from wastewater using advanced materials,” M. N. V. Prasad, M. Vithanage, and A. B. T.-P. and P. C. P. W. M. and T. T. Kapley, Eds. Butterworth-Heinemann, 2019, pp. 173–212.
- [35] A. D. Bokare and W. Choi, “Review of iron-free Fenton-like systems for activating

- H₂O₂ in advanced oxidation processes,” *J. Hazard. Mater.*, vol. 275, pp. 121–135, 2014.
- [36] M. hui Zhang, H. Dong, L. Zhao, D. xi Wang, and D. Meng, “A review on Fenton process for organic wastewater treatment based on optimization perspective,” *Science of the Total Environment*. 2019.
- [37] S. Adityosulindro, L. Barthe, K. González-Labrada, U. J. Jáuregui Haza, H. Delmas, and C. Julcour, “Sonolysis and sono-Fenton oxidation for removal of ibuprofen in (waste)water,” *Ultrason. Sonochem.*, vol. 39, no. December 2016, pp. 889–896, 2017.
- [38] H. Zhang, D. Zhang, and J. Zhou, “Removal of COD from landfill leachate by electro-Fenton method,” *J. Hazard. Mater.*, vol. 135, no. 1–3, pp. 106–111, 2006.
- [39] F. J. Rivas, F. J. Beltrán, O. Gimeno, and P. Alvarez, “Optimisation of Fenton’s reagent usage as a pre-treatment for fermentation brines,” *J. Hazard. Mater.*, vol. 96, no. 2–3, pp. 277–290, 2003.
- [40] A. Krzysztozek and J. Naumczyk, “Landfill leachate treatment by Fenton, photo-Fenton processes and their modification,” *J. Adv. Oxid. Technol.*, vol. 15, no. 1, pp. 53–63, 2012.
- [41] S. M. Iskander, T. Zeng, E. Smiley, S. C. Bolyard, J. T. Novak, and Z. He, “Formation of disinfection byproducts during Fenton’s oxidation of chloride-rich landfill leachate,” *J. Hazard. Mater.*, vol. 382, no. September 2019, p. 121213, 2020.
- [42] T. Poznyak, G. L. Bautista, I. Chaírez, R. I. Córdova, and L. E. Ríos, “Decomposition of toxic pollutants in landfill leachate by ozone after coagulation treatment,” *J. Hazard. Mater.*, vol. 152, no. 3, pp. 1108–1114, 2008.
- [43] J. J. Wu, C. C. Wu, H. W. Ma, and C. C. Chang, “Treatment of landfill leachate by ozone-based advanced oxidation processes,” *Chemosphere*, vol. 54, no. 7, pp. 997–1003, 2004.
- [44] M. S. Elovitz and U. von Gunten, “Hydroxyl Radical/Ozone Ratios During Ozonation Processes. I. The Rct Concept,” *Ozone Sci. Eng.*, vol. 21, no. 3, pp. 239–260, 1999.
- [45] J. Staehelin and J. Holgné, “Decomposition of Ozone in Water: Rate of Initiation by Hydroxide Ions and Hydrogen Peroxide,” *Environ. Sci. Technol.*, vol. 16, no. 10, pp.

676–681, 1982.

- [46] E. Reisz, W. Schmidt, H. P. Schuchmann, and C. Von Sonntag, “Photolysis of ozone in aqueous solutions in the presence of tertiary butanol,” *Environ. Sci. Technol.*, vol. 37, no. 9, pp. 1941–1948, 2003.
- [47] C. Tizaoui, L. Bouselmi, L. Mansouri, and A. Ghrabi, “Landfill leachate treatment with ozone and ozone/hydrogen peroxide systems,” *J. Hazard. Mater.*, vol. 140, no. 1–2, pp. 316–324, 2007.
- [48] D. M. Bila, A. Filipe Montalvão, A. C. Silva, and M. Dezotti, “Ozonation of a landfill leachate: Evaluation of toxicity removal and biodegradability improvement,” *J. Hazard. Mater.*, vol. 117, no. 2–3, pp. 235–242, 2005.
- [49] S. Cortez, P. Teixeira, R. Oliveira, and M. Mota, “Ozonation as polishing treatment of mature landfill leachate,” *J. Hazard. Mater.*, vol. 182, no. 1–3, pp. 730–734, 2010.
- [50] D. Geenens, B. Bixio, and C. Thoeye, “Combined ozone-activated sludge treatment of landfill leachate,” *Water Sci. Technol.*, vol. 44, no. 2–3, pp. 359–365, 2001.
- [51] M. Umar, F. Roddick, L. Fan, and H. A. Aziz, “Application of ozone for the removal of bisphenol A from water and wastewater - A review,” *Chemosphere*, vol. 90, no. 8, pp. 2197–2207, 2013.
- [52] T. Kamiya, T. Yamauchi, J. Hirotsuji, and M. Fujita, “Ozone-based decomposition of main endocrine disruption chemicals in sewage effluent,” *Ozone Sci. Eng.*, vol. 27, no. 5, pp. 389–395, 2005.
- [53] H. Schaar, M. Clara, O. Gans, and N. Kreuzinger, “Micropollutant removal during biological wastewater treatment and a subsequent ozonation step,” *Environ. Pollut.*, vol. 158, no. 5, pp. 1399–1404, 2010.
- [54] Umweltbundesamt, “Organische Mikroverunreinigungen in Gewässern - Vierte Reinigungsstufe für weniger Einträge,” *Umweltbundesamt*, p. 26, 2015.
- [55] C. M. Robson and R. G. Rice, “Wastewater Ozonation in the U.S.A. – History and Current Status - 1989,” *Ozone Sci. Eng.*, vol. 13, no. 1, pp. 23–40, Feb. 1991.
- [56] E. C. Wert, F. L. Rosario-Ortiz, D. D. Drury, and S. A. Snyder, “Formation of

- oxidation byproducts from ozonation of wastewater,” *Water Res.*, vol. 41, no. 7, pp. 1481–1490, 2007.
- [57] S. D. Richardson *et al.*, “Identification of new drinking water disinfection by-products from ozone, chlorine dioxide, chloramine, and chlorine,” *Water. Air. Soil Pollut.*, vol. 123, no. 1–4, pp. 95–102, 2000.
- [58] J. Y. Hu, Z. S. Wang, W. J. Ng, and S. L. Ong, “Disinfection by-products in water produced by ozonation and chlorination,” *Environ. Monit. Assess.*, vol. 59, no. 1, pp. 81–93, 1999.
- [59] Rice University, “The electrolysis of water.” [Online]. Available: <https://opentextbc.ca/chemistry/chapter/17-7-electrolysis/>.
- [60] M. Panizza and G. Cerisola, “Direct And Mediated Anodic Oxidation of Organic Pollutants,” *Chem. Rev.*, vol. 109, no. 12, pp. 6541–6569, 2009.
- [61] C. Comninellis and G. Chen, *Electrochemistry for the Environment*. Springer New York, 2010.
- [62] C. Comninellis, “Electrocatalysis in the electrochemical conversion/combustion of organic pollutants for waste water treatment,” *Electrochim. Acta*, vol. 39, no. 11–12, pp. 1857–1862, 1994.
- [63] G. Foti, D. Gandini, C. Comninellis, A. Perret, and W. Haenni, “Oxidation of organics by intermediates of water discharge on IrO₂ and synthetic diamond anodes,” *Electrochem. Solid State Lett.*, vol. 2, no. 5, 1999.
- [64] C. A. Martinez-Huitle and S. Ferro, “Electrochemical oxidation of organic pollutants for the wastewater treatment: direct and indirect processes,” *Chem. Soc. Rev.*, vol. 35, no. 12, pp. 1324–1340, 2006.
- [65] F. Bonfatti, S. Ferro, F. Lavezzo, M. Malacarne, G. Lodi, and A. De Battisti, “Electrochemical Incineration of Glucose as a Model Organic Substrate II . Role of Active Chlorine Mediation,” *J. Electrochem. Soc.*, vol. 147, no. 2, pp. 592–596, 2000.
- [66] S. Stucki, R. Kötz, B. Carcer, and W. Suter, “Electrochemical waste water treatment using high overvoltage anodes Part II: Anode performance and applications,” *J. Appl. Electrochem.*, vol. 21, no. 2, pp. 99–104, 1991.

- [67] Y. Deng and J. D. Englehardt, “Electrochemical oxidation for landfill leachate treatment,” *Waste Manag.*, vol. 27, no. 3, pp. 380–388, 2007.
- [68] A. Anglada, A. Urriaga, and I. Ortiz, “Pilot Scale Performance of the Electro-Oxidation of Landfill Leachate at Boron-Doped Diamond Anodes,” *Environ. Sci. Technol.*, vol. 43, no. 6, pp. 2035–2040, 2009.
- [69] M. J. K. Bashir *et al.*, “Landfill leachate treatment by electrochemical oxidation,” *Waste Manag.*, vol. 29, no. 9, pp. 2534–2541, 2009.
- [70] P. B. Moraes and R. Bertazzoli, “Electrodegradation of landfill leachate in a flow electrochemical reactor,” *Chemosphere*, vol. 58, no. 1, pp. 41–46, 2005.
- [71] A. Cabeza, A. Urriaga, M. J. Rivero, and I. Ortiz, “Ammonium removal from landfill leachate by anodic oxidation,” *J. Hazard. Mater.*, vol. 144, no. 3, pp. 715–719, 2007.
- [72] S. Pei, J. Teng, N. Ren, and S. You, “Low-Temperature Removal of Refractory Organic Pollutants by Electrochemical Oxidation: Role of Interfacial Joule Heating Effect,” *Environ. Sci. Technol.*, vol. 54, no. 7, pp. 4573–4582, 2020.
- [73] M. Panizza, M. Delucchi, and I. Sirés, “Electrochemical process for the treatment of landfill leachate,” *J. Appl. Electrochem.*, vol. 40, no. 10, pp. 1721–1727, 2010.
- [74] M. Panizza and G. Cerisola, “Electrochemical oxidation as a final treatment of synthetic tannery wastewater,” *Environ. Sci. Technol.*, vol. 38, no. 20, pp. 5470–5475, 2004.
- [75] Á. Anglada, A. Urriaga, I. Ortiz, D. Mantzavinos, and E. Diamadopoulos, “Boron-doped diamond anodic treatment of landfill leachate: Evaluation of operating variables and formation of oxidation by-products,” *Water Res.*, vol. 45, no. 2, pp. 828–838, 2011.
- [76] P. Cañizares, R. Paz, C. Sáez, and M. A. Rodrigo, “Costs of the electrochemical oxidation of wastewaters: A comparison with ozonation and Fenton oxidation processes,” *J. Environ. Manage.*, vol. 90, no. 1, pp. 410–420, 2009.
- [77] US Environmental Protection Agency, “Technical fact sheet - Perchlorate,” *Epa 505-F-14-003*, no. January, pp. 1–17, 2014.

- [78] E. T. Urbansky, "Perchlorate as an Environmental Contaminant," *Environ. Sci. Pollut. Res.*, vol. 9, no. 3, pp. 187–192, 2002.
- [79] Public Health Service, "Public health statement Chloroform," *Dep. Heal. Hum. Serv.*, 1997.
- [80] Public Health Service, "Bromoform and Dibromochloromethane," *Dep. Heal. Hum. Serv.*, no. August, pp. 1–2, 2005.
- [81] H. Gallard and U. von Gunten, "Chlorination of Phenols : Kinetics and Formation of Chloroform," vol. 36, no. 5, pp. 884–890, 2002.
- [82] M. J. Frisch *et al.*, "Gaussian 09, revision b. 01, Gaussian," *Inc., Wallingford, CT*, 2010.
- [83] A. D. Becke, "Density-functional exchange-energy approximation with correct asymptotic behavior," *Phys. Rev. A*, vol. 38, no. 6, pp. 3098–3100, Sep. 1988.
- [84] F. Weigend, F. Furche, and R. Ahlrichs, "Gaussian basis sets of quadruple zeta valence quality for atoms H-Kr," *J. Chem. Phys.*, vol. 119, no. 24, pp. 12753–12762, 2003.
- [85] F. Weigend, "Accurate Coulomb-fitting basis sets for H to Rn," *Phys. Chem. Chem. Phys.*, vol. 8, no. 9, pp. 1057–1065, 2006.
- [86] A. V Marenich, C. J. Cramer, and D. G. Truhlar, "Universal Solvation Model Based on Solute Electron Density and on a Continuum Model of the Solvent Defined by the Bulk Dielectric Constant and Atomic Surface Tensions," *J. Phys. Chem. B*, vol. 113, no. 18, pp. 6378–6396, May 2009.
- [87] J. P. Foster and F. Weinhold, "Natural hybrid orbitals," *J. Am. Chem. Soc.*, vol. 102, no. 24, pp. 7211–7218, Nov. 1980.
- [88] Y. Jing and B. P. Chaplin, "Mechanistic Study of the Validity of Using Hydroxyl Radical Probes To Characterize Electrochemical Advanced Oxidation Processes," *Environ. Sci. Technol.*, vol. 51, no. 4, pp. 2355–2365, 2017.
- [89] N. Ambauen, J. Muff, N. L. Mai, C. Hallé, T. T. Trinh, and T. Meyn, "Insights into the kinetics of intermediate formation during electrochemical oxidation of the organic model pollutant salicylic acid in chloride electrolyte," *Water (Switzerland)*, vol. 11, no.

7, 2019.

- [90] N. Ambauen, J. Muff, F. Tscheikner-gratl, T. T. Trinh, C. Hallé, and T. Meyn, “Application of electrochemical oxidation in cold climate regions – Effect of temperature, pH and anode material on the degradation of Bisphenol A and the formation of disinfection by-product,” *J. Environ. Chem. Eng.*, no. June, 2020.
- [91] J. Muff, F. Tscheikner-gratl, T. T. Trinh, and T. Meyn, “Journal Pre-proof,” no. June, 2020.
- [92] A. Y. Bagastyo, J. Radjenovic, Y. Mu, R. A. Rozendal, D. J. Batstone, and K. Rabaey, “Electrochemical oxidation of reverse osmosis concentrate on mixed metal oxide (MMO) titanium coated electrodes,” *Water Res.*, vol. 45, no. 16, pp. 4951–4959, 2011.
- [93] Norwegian Environment Agency, “Grenseverdier for klassifisering av vann, sediment og biota,” p. 24, 2016.
- [94] C. Comninellis and C. Pulgarin, “Anodic oxidation of phenol for waste water treatment,” *J. Appl. Electrochem.*, vol. 21, no. 8, pp. 703–708, 1991.
- [95] Eurostat, “Electricity price statistics,” no. November 2019, pp. 1–12, 2020.
- [96] Olje- og energidepartement, “Kraftproduksjon.” [Online]. Available: <https://energifaktanorge.no/norsk-energiforsyning/kraftforsyningen/>.
- [97] “LENNTECH - Ozone Generators.” [Online]. Available: <https://www.lenntech.com/otozone.htm>.
- [98] “LOITEH - Ozone Generators.” [Online]. Available: <http://www.loiteh.ee/eng/ozone-generators>.
- [99] Á. Anglada, A. M. Urtiaga, and I. Ortiz, “Laboratory and pilot plant scale study on the electrochemical oxidation of landfill leachate,” *J. Hazard. Mater.*, vol. 181, no. 1–3, pp. 729–735, 2010.
- [100] US EPA, “Perchlorate in drinking water.” [Online]. Available: <https://www.epa.gov/dwstandardsregulations/perchlorate-drinking-water-frequent-questions>.
- [101] WHO, “Concise International Chemical Assessment Document (CICAD): a new

chemical safety series in IPCS, internationalizing national reviews,” *Bull. Natl. Inst. Hyg. Sci.*, no. 114, pp. 89–94, 1996.

- [102] United States. Environmental Protection Agency. Office of Water Planning and Standards. Criteria & Standards Division, *Ambient Water Quality Criteria*. Criteria and Standards Division, Office of Water Planning and Standards, U.S. Environmental Protection Agency, 1979, 1979.
- [103] K. E. Dean, R. M. Palachek, J. M. Noel, R. Warbritton, J. Aufderheide, and J. Wireman, “Development of freshwater water-quality criteria for perchlorate,” *Environ. Toxicol. Chem.*, vol. 23, no. 6, pp. 1441–1451, 2004.
- [104] A. Da Pozzo, L. Di Palma, C. Merli, and E. Petrucci, “An experimental comparison of a graphite electrode and a gas diffusion electrode for the cathodic production of hydrogen peroxide,” *J. Appl. Electrochem.*, vol. 35, no. 4, pp. 413–419, 2005.
- [105] M. Sudoh, H. Kitaguchi, and K. Koide, “Electrochemical Production of Hydrogen Peroxide by Reduction of Oxygen,” *J. Chem. Eng. Japan*, vol. 18, no. 5, pp. 409–414, 1985.
- [106] E. Vyhnánková, Z. Kozáková, F. Krčma, and A. Hrdlička, “Influence of electrode material on hydrogen peroxide generation by DC pinhole discharge,” *Open Chem.*, vol. 13, no. 1, pp. 218–223, 2015.
- [107] S. Yang, S. Fernando, T. M. Holsen, and Y. Yang, “Inhibition of Perchlorate Formation during the Electrochemical Oxidation of Perfluoroalkyl Acid in Groundwater,” *Environ. Sci. Technol. Lett.*, vol. 6, no. 12, pp. 775–780, 2019.
- [108] “ElectroCell.” [Online]. Available: <https://www.electrocell.com/>.
- [109] M. Shestakova and M. Sillanpää, “Electrode materials used for electrochemical oxidation of organic compounds in wastewater,” *Rev. Environ. Sci. Biotechnol.*, vol. 16, no. 2, pp. 223–238, 2017.
- [110] P. Mandal, B. K. Dubey, and A. K. Gupta, “Review on landfill leachate treatment by electrochemical oxidation: Drawbacks, challenges and future scope,” *Waste Manag.*, vol. 69, pp. 250–273, 2017.
- [111] M. hui Zhang, H. Dong, L. Zhao, D. xi Wang, and D. Meng, “A review on Fenton

- process for organic wastewater treatment based on optimization perspective,” *Sci. Total Environ.*, vol. 670, pp. 110–121, 2019.
- [112] C. A. Martínez-Huitle and S. Ferro, “Electrochemical oxidation of organic pollutants for the wastewater treatment: Direct and indirect processes,” *Chem. Soc. Rev.*, vol. 35, no. 12, pp. 1324–1340, 2006.
- [113] G. Chen, “Electrochemical technologies in wastewater treatment,” *Sep. Purif. Technol.*, vol. 38, no. 1, pp. 11–41, 2004.
- [114] H. Bhuta, *Advanced Treatment Technology and Strategy for Water and Wastewater Management*. Elsevier Ltd., 2014.
- [115] U. S. Environmental Protection Agency, “Wastewater Technology Fact Sheet Ozone Disinfection,” *United States Environ. Prot. Agency*, pp. 1–7, 1999.
- [116] N. Ambauen, C. Weber, J. Muff, C. Hallé, and T. Meyn, “Electrochemical removal of Bisphenol A from landfill leachate under Nordic climate conditions,” *J. Appl. Electrochem.*, no. 0123456789, 2020.
- [117] N. Ambauen, J. Muff, F. Tscheikner-Gratl, T. T. Trinh, C. Hallé, and T. Meyn, “Application of electrochemical oxidation in cold climate regions – Effect of temperature, pH and anode material on the degradation of Bisphenol A and the formation of disinfection by-products,” *J. Environ. Chem. Eng.*, vol. 8, no. 5, p. 104183, 2020.
- [118] S. Renou, J. G. Givaudan, S. Poulain, F. Dirassouyan, and P. Moulin, “Landfill leachate treatment: review and opportunity,” *J. Hazard. Mater.*, vol. 150, no. 3, pp. 468–493, 2008.

APPENDIX A: SELECTED PAPERS

PAPER I

Insights into the Kinetics of Intermediate Formation during Electrochemical Oxidation of
the Organic Model Pollutant Salicylic Acid in Chloride Electrolyte

Ambauen, N., Trinh, T.T., Mai, N.L., Muff, J., Hallé, C., Meyn, T.

Water 2019, 11, 1322

DOI: 10.3390/w11071322

Article

Insights into the Kinetics of Intermediate Formation during Electrochemical Oxidation of the Organic Model Pollutant Salicylic Acid in Chloride Electrolyte

Noëmi Ambauen ^{1,*}, Jens Muff ², Ngoc Lan Mai ³, Cynthia Hallé ¹, Thuat T. Trinh ¹ and Thomas Meyn ¹

¹ Department of Civil- and Environmental Engineering, Norwegian University of Science and Technology, 7491 Trondheim, Norway

² Department of Chemistry and Bioscience, Aalborg University, 6700 Esbjerg, Denmark

³ Faculty of Applied Sciences, Ton Duc Thang University, Ho Chi Minh City, Vietnam

* Correspondence: noemi.ambauen@ntnu.no; +47-7359-4748

Received: 28 May 2019; Accepted: 21 June 2019; Published: 26 June 2019



Abstract: The present study investigated the kinetics and formation of hydroxylated and chlorinated intermediates during electrochemical oxidation of salicylic acid (SA). A chloride (NaCl) and sulfate (Na₂SO₄) electrolyte were used, along with two different anode materials, boron doped diamond (BDD) and platinum (Pt). Bulk electrolysis of SA confirmed the formation of both hydroxylated and chlorinated intermediates. In line with the density functional theory (DFT) calculations performed in this study, 2,5- and 2,3-dihydroxybenzoic acid, 3- and 5- chlorosalicylic acid and 3,5-dichlorosalicylic acid were the dominating products. In the presence of a chloride electrolyte, the formation of chlorinated intermediates was the predominant oxidation mechanism on both BDD and Pt anodes. In the absence of a chloride electrolyte, hydroxylated intermediates prevailed on the Pt anode and suggested the formation of sulfonated SA intermediates on the BDD anode. Furthermore, direct oxidation at the anode surface only played a subordinate role. First order kinetic models successfully described the degradation of SA and the formation of the observed intermediates. Rate constants provided by the model showed that chlorination of SA can take place at up to more than 60 times faster rates than hydroxylation. In conclusion, the formation of chlorinated intermediates during electrochemical oxidation of the organic model pollutant SA is confirmed and found to be dominant in chloride containing waters.

Keywords: electrochemical oxidation; organic pollutant; salicylic acid; disinfection by-products; boron doped diamond; hydroxyl radicals; chlorinated intermediates; density functional theory

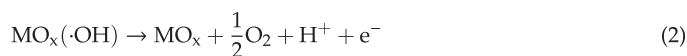
1. Introduction

Mono- and polycyclic aromatic compounds present in wastewaters such as landfill leachate, pose a special challenge when it comes to their removal from the water matrix. Greater parts of them are non-biodegradable, persist in the aquatic environment and demand a dedicated treatment step for their removal. Such persistent organic pollutants can be produced intentionally, such as pesticides, or are unintentionally produced during water disinfection [1]. They may enter the human body through the food chain via bioaccumulation [2]. Many persistent organic pollutants are suspected to be carcinogenic or have other detrimental effects on the aquatic environment [3]. Studies have shown that advanced oxidation processes (AOP) in general [4], and thereof electrochemical oxidation (EO) [5] specifically, are effective treatment processes for the removal of persistent organic pollutants. AOPs mainly focus on the formation of hydroxyl radicals by different means [6,7]. Hydroxyl radicals are

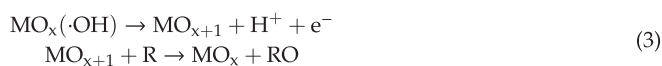
non-selective, highly reactive oxidants and their presence leads to partial degradation or even complete oxidation to CO₂ of organic pollutants. During EO, adsorbed hydroxyl radicals are formed via the electrolytic discharge of water in the electrochemical cell (Equation (1)) [8]:



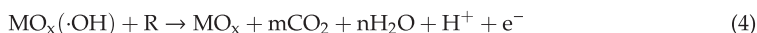
A competing side reaction may occur during the electrolytic discharge of water, the so-called oxygen evolution (Equation (2)) [8]:



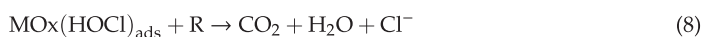
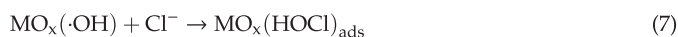
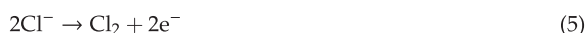
The occurrence of oxygen evolution is subject to the oxygen evolution over-potential of the anode material. In the same way, the transfer of oxygen from the adsorbed hydroxyl radicals to the organic compound (R) depends on the anode material [9]. Commonly, two different electrochemical oxygen transfer reaction (EOTR) mechanisms are distinguished [8]. The first EOTR mechanism takes place at anodes that have a low oxygen evolution over-potential, also known as active anodes (e.g., platinum, Pt) [8]. Hereby, the adsorbed hydroxyl radical reacts with the anode surface, forming higher oxides (MO_{x+1}), which in turn react with the organic pollutant (Equation (3)):



where MO_{x+1}/MO_x is the surface redox couple and also called active oxygen. The second EOTR mechanism takes place at anodes with high oxygen evolution over-potential, also known as non-active anodes (e.g., BDD). Hereby, no formation of higher oxides occurs. Instead, the adsorbed hydroxyl radicals react directly with the organic compound, which at best leads to its complete combustion to CO₂ (Equation (4)):



Depending on the anode material, the active oxygen is called chemisorbed (active anodes) or physisorbed (non-active anodes). In order to be able to conduct EO, the sole presence of an organic pollutant and water molecules is not enough. Electrolytes need to be present, to transfer the charge across the electrochemical cell. Almost all wastewaters contain electrolytes of different natures and thus facilitate the treatment via EO. However, electrolytes do not only transfer charges, but electrochemically active electrolytes may also undergo oxidation at the anode surface. Halide electrolytes will form active halide species under such circumstances, for example NaCl will react to active chlorine. These active species will in turn react with the organic pollutants, resulting in their partial chemical oxidation, a process also known as mediated oxidation (MEO) [10]. Bonfatti et al. [11] proposed the following mechanisms for active chlorine mediated electrochemical oxidation:



Halogenated organic pollutants however are not favored reaction products, since they are generally more toxic than the mother compound and thus disadvantageous for the treatment process [12]. In the same way as the electrolytes, the organic pollutants can also be directly oxidized at the anodes surface, via a direct electron transfer (DET) between the organic pollutant and the anode [13]. DET is restricted

and only occurs within the particular electrochemical window specific to a certain anode material, which in turn is limited by the above-mentioned oxygen evolution over-potential.

In this study, salicylic acid (SA) is used as a model compound for organic pollutants. SA is the main metabolite of acetylsalicylic acid, a commonly known and widely used painkiller. SA has aromatic properties and can be used to represent organic pollutants during electrochemical oxidation. Furthermore, chlorinated SA intermediates have been recently assigned to the group of disinfection by-products (DBP), which are not only of concern due to their cytotoxicity and growth inhibition ability but also because they act as a precursor to form regulated DBPs such as trihalomethanes (THMs). Consequently, this study investigates the degradation of SA in chloride and non-chloride electrolytes and investigates the different oxidation processes and the corresponding formation of intermediates.

Degradation pathways for SA during EO have been reported on previously. Guinea et al. [14] proposed a degradation pathway via hydroxylation of SA, using a BDD anode and cathodic generation of hydrogen peroxide. In the first oxidation step, SA reacted with the hydroxyl radicals originating from the hydrogen peroxide to form three different dihydroxybenzoic acids (dHBAs): 2,3 dihydroxybenzoic acid (23dHBA), 2,5 dihydroxybenzoic acid (25dHBA) and 2,6 dihydroxybenzoic acid (26dHBA). The different dHBAs were next proposed to be further oxidized to lower molecular weight carboxylic acids such as maleic or α -ketoglutaric acid. In a third oxidation step, the low molecular weight carboxylic acid was then degraded to oxalic acid and finally carbon dioxide (CO₂). Others suggested trihydroxybenzoic acids (tHBA), namely 234tHBA, 235tHBA and 246tHBA as possible degradation products of SA [15]. However, chlorinated products of SA formed during EO have not been reported. It is anticipated that chlorine atoms originating from the MEO primarily substitute at the para position of the hydroxyl group of SA, followed by a second substitution at the ortho position [16]. This assumption is endorsed by Broadwater et al. [17], where they identified different chlorinated SA intermediates by the simple chlorination of SA via the addition of NaOCl. Thus, it is expected that we will mainly find 3-chlorosalicylic acid (3CISA) and 5-chlorosalicylic acid (5CISA) and the combined product 3,5-dichlorosalicylic acid (35dCISA). The uncertainty that comes along with the expected chlorinated SA products can be reduced further by the implementation of preliminary density function theory (DFT) computations. These computations will help us to anticipate possible reaction products and thus facilitate the analytical process for their identification. The oxidation pathway of SA via DET is also included in this study as only a few studies investigated the DET of SA. Torriero et al. [18], used cyclic voltammetry (CV) to demonstrate irreversible DET of SA on a glassy carbon (GC) electrode, and Wudarska et al. [19] reported on the electro-reduction behavior of SA and acetylsalicylic acid during CV using a Pt electrode.

The aim of this study is to gain more insight into the degradation of SA during EO with emphasis on the formation of chlorinated SA intermediates. Chlorinated intermediates, unlike their mother compound SA, belong to newly defined DBPs and therefore it is essential to elucidate their formation during EO and fill this gap of knowledge. Hydroxylated intermediates are also investigated, since they originate from the reaction with hydroxyl radicals, which are important for the removal of persistent organic pollutants. Kinetic models for the degradation of SA and the formation of intermediates are developed using DFT and tested through bulk electrolysis in different electrolytes. Model results provided rate constants that are used to assess the importance of different oxidation processes contributing to the degradation of SA. In addition, CV on BDD electrodes for SA are reported and add valuable information on the electroactive behavior of SA, which has been previously reported for different electrode materials and electrochemical reduction by [18,19], respectively.

2. Materials and Methods

Investigation of EOTR and MEO for SA was done by bulk electrolysis. Different mechanisms were identified via the reaction products of the parent compounds. The expected reaction products during bulk electrolysis were anticipated based on DFT computations for both EOTR and MEO. In addition, two different anode materials were tested, BDD and Pt, due to EOTR being highly dependent on the

anode material. MEO is greatly affected by the supporting electrolyte, hence two different electrolytes were compared (NaCl and Na₂SO₄). A kinetic model has been developed in order to predict the degradation of SA and the formation of the reaction products during bulk electrolysis. Furthermore, CV was used to gain information about the electro-activity of SA. Its fate during CV was assessed by using different supporting electrolytes and anode materials. The CV results allow for conclusions to be drawn about the presence or absence of the DET mechanism during bulk electrolysis of SA.

2.1. Cyclic Voltammetry

SA and the two electrolytes (NaCl and Na₂SO₄) were purchased from VWR international AnalaR NORMAPUR. Stock solutions of SA were prepared with demineralized water with a concentration of 1 g/L. The stock solution was kept up to a month and stored in the dark at 4 °C. Electrolyte solutions were prepared with demineralized water. Cyclic voltammetry experiments were carried out with an μ AUTOLABIII/FRA2 (Metrohm) using a 7.07×10^{-6} m² platinum rotating disc electrode (Pt-RDE, Metrohm), a 1.24×10^{-5} m² boron doped diamond rotating disc electrode (BDD-RDE, neoCoat) and a 1.19×10^{-4} m² glassy carbon rod (GC-rod) electrode (Metrohm AG, Hersiau, Switzerland). A Pt wire was used as an auxiliary electrode. The speed of the rotating disc electrode was set to 100 rpm for all experiments. A platinum wire served as a counter electrode and an Ag/AgCl (3M) was used as a reference electrode. All experiments were performed at room temperature (20 °C) using 25 mL electrolyte at a concentration of 0.1 M and a SA concentration of 500 mg/L. The scanning rate was 1 V/s and 5 consecutive scan cycles were run at the time and the potential was swept between −1 and 2 V. CV results were analyzed using NOVA 2.0 software (Metrohm).

2.2. Bulk Electrolysis

The same chemicals as for CV were used and stock solutions were prepared and stored likewise. Bulk electrolysis experiments were carried out, using a micro flow cell (ElectroCell Europe AS, Denmark). Experiments were conducted in galvanostatic mode with an applied current density (j_{app}) of 43 mA/cm². Two different anode materials were used, platinum (Pt) with titanium (Ti), as supporting material and a boron doped diamond (BDD) with niobium (Nb) as supporting material together with a stainless-steel cathode. Both, cathode and anode had an active area of 10 cm². Two polytetrafluoroethylene turbulence-enhancing meshes were placed between the anode and cathode (4 mm inter-electrode cap). The working- and counter-electrode were cooled during the experiment with a tap water stream (ca. 7 °C) from the rear side. The solution (2500 mL) in the tank was magnetically stirred and pumped with a peristaltic pump (Masterflex Cole-Parmer Instrument Co., Vernon Hills, IL, USA) via Teflon tubing to the micro flow cell with a flow rate of 380 mL/min. A cooling coil (stainless steel) immersed into to the solution and connected to a chiller (FP50-ME, Julabo GmbH, Seelbach, Germany) assured a stable temperature (25 °C) during all experiments. The electrolyte concentration used during bulk electrolysis was 0.05 M for both, NaCl and Na₂SO₄. Figure 1 depicts the scheme of the electrolysis set up.

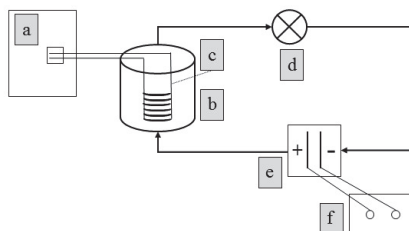


Figure 1. Scheme of electrolysis setup; a: chiller; b: tank; c: cooling coil; d: peristaltic pump; e: electrochemical cell; f: power supply.

The mass transfer coefficient (k_m) was obtained by the diffusion limiting current technique [20] according to Chatzismyeon et al. [21]. Different concentrations (4–24 mM) of potassium ferro cyanide ($K_4[Fe(CN)_6]$) and ferri cyanide ($K_3[Fe(CN)_6]$) in 2:1 ratio were anodically oxidized and polarization curves were generated. The limiting currents were determined by the formula:

$$I_{lim} = (AnFk_m)C_b \quad (9)$$

where I_{lim} : limiting current (A), A : electrode surface (m^2), n : number of exchanged electrons ($n = 1$ for ferro/ferri cyanide couple), F : Faraday constant (C/mol), k_m : mass transfer coefficient (m/s), C_b : bulk concentration of ferro cyanide (mol/m^3). The ratio of I_{lim} to C_b is obtained from the slope when plotting different ferro/ferri cyanide concentration versus the limiting current (plateau) from the polarization curves. The calculated k_m value is inserted into the following Equation (10), describing the initial limiting current density ($j_{lim}(t = 0)$) for the given experimental conditions when BDD anodes are used [22]:

$$j_{lim}(t) = nFk_mCOD(t) \quad (10)$$

where: n : number of electrons exchanged with anode ($n = 4$ when considering chemical oxygen demand (COD)), $COD(t)$: initial bulk COD concentration at time $t = 0$.

2.3. Sample Analysis

Samples obtained from bulk electrolysis were analyzed using an UPLC (Waters, Milford, MA, USA) with XEVO TQ-XS triple quadrupole mass spectrometer (Waters) with a 2.1 mm \times 100 mm high strength silica T3 column (Waters). The UPLC-MS/MS was operated in multiple reaction monitoring mode using electrospray ionization. Water (HPLC grade, VWR) with 2 mM ammonium formate (Sigma-Aldrich, Merck KGaA, Darmstadt, Germany) and 0.1% formic acid (VWR International LLC, Radnor, PA, USA) was used as solvent A and acetonitrile (HPLC grade, VWR) with 2 mM ammonium formate (Sigma-Aldrich) and 0.1% formic acid (VWR) was used as solvent B. For the SA method, a flow of 0.4 mL/min was constantly maintained and deuterated SA (SA-d6, Sigma-Aldrich) was used as an internal standard. Standards for the selection of expected SA products 23dHBA, 25dHBA, 26dHBA, 3CISA, 4CISA, 5CISA and 35dCISA were purchased from Sigma-Aldrich, all analytical grade. Data processing was carried out using the 'Targetlynx' software (Waters).

Active chlorine in bulk electrolysis samples was measured with the DPD (N, N-diethyl-p-phenylenediamine) colorimetric method using DPD powder pillows for 5 mL (Hach, Loveland, CO, USA) and a portable DR300 colorimeter (Hach).

2.4. Density Functional Theory Simulations

DFT simulations were performed to study the relative stability of different products, as well as the electronic property of SA in reaction. All calculations were done with the Gaussian 09 package [23]. Unrestricted spin calculation using Lee-Yang-Parr (B3LYP) [24] functional and def2-TZVPP basis set [25,26] were employed. An implicit solvation model for water was considered using a solvation model based on the quantum mechanical charge density (SMD) [27]. Natural bond theory (NBO) [28] was used to analyze the spin and charge density of the molecules (Figure 2). The default values of Gaussian 09 were used for the convergence of energy and force in the DFT calculations. A similar set up was successfully employed to study to electro-chemical reaction [29].

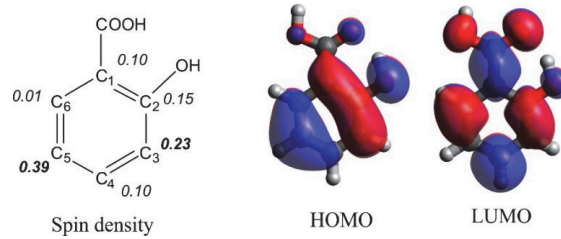


Figure 2. Electronic structure of salicylic acid (SA) radical: spin density calculated by natural bond theory (NBO) method (left) and highest occupied molecular orbital—lowest unoccupied molecular orbital (HOMO-LUMO) (right).

2.5. Kinetic Modelling

A mathematic model predicting the degradation of SA and its intermediates with different electrode materials was developed. A degradation mechanism of SA with NaCl as the supporting electrolyte is proposed in Figure 3. Note that in the case of using Na₂SO₄ as supporting electrolyte, the formation of chlorinated intermediates does not take place.

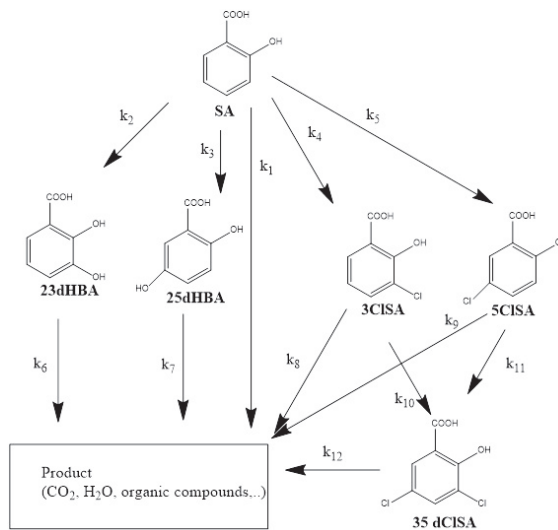


Figure 3. Simplified chemical kinetic model for the degradation of SA.

A first order kinetic equation was chosen to describe each reaction rate (Equation (11)). Calculations were performed in Matlab (version 2017, The MathWorks, Inc., Natick, MA, USA) to find the numerical solution to the set of ordinary differential equations. Reaction rate constants were determined by fitting the experimental data to the model using the least squares method. The fitting quality was estimated by the correlation coefficient R^2 .

$$\begin{aligned}
 \frac{d[\text{SA}]}{dt} &= -(k_1 + k_2 + k_3 + k_4 + k_5)[\text{SA}] \\
 \frac{d[\text{SA}]}{dt} &= -(k_1 + k_2 + k_3 + k_4 + k_5)[\text{SA}] \\
 \frac{d[23\text{dHBA}]}{dt} &= k_2[\text{SA}] - k_6[23\text{dHBA}] \\
 \frac{d[25\text{dHBA}]}{dt} &= k_3[\text{SA}] - k_7[25\text{dHBA}] \\
 \frac{d[3\text{CISA}]}{dt} &= k_4[\text{SA}] - (k_8 + k_{10})[3\text{CISA}] \\
 \frac{d[5\text{CISA}]}{dt} &= k_5[\text{SA}] - (k_9 + k_{11})[5\text{CISA}] \\
 \frac{d[35\text{dCISA}]}{dt} &= k_{10}[3\text{CISA}] + k_{11}[5\text{CISA}] - k_{12}[35\text{dCISA}]
 \end{aligned} \tag{11}$$

3. Results and Discussion

3.1. Prediction of Salicylic Acid Intermediate Formation by DFT Simulations

Considering the formation of hydroxylated and chlorinated products, there are six possibilities to bond to a carbon atom (from C1–C6) of SA (Figure 2). However, due to steric effects, the attacking position at C1 and C2 is very unstable, hence the possibility to bond with OH[−] and Cl[−] at position C3, C4, C5, and C6 was investigated. Table 1 presents the relative stability of the products, the most stable one (relative energy = 0.00 kJ/mol) was chosen as reference. For both the hydroxylated and mono-chlorinated products, the most stable structure is at position C4, while position 4,5 and position 3,5 are the most stable structures for di-chlorinated species. When looking at the experimental data, it shows that the most favorable attacking positions are at C3 and C5 position (discussed in Section 3.2.2 & 3.2.3). Thus, the most favorable intermediates observed during the experiments cannot be fully explained by the relative stability of products based on DFT calculations. It is therefore proposed that the mechanism and kinetics play an important role here. Consequently, further investigations of the electronic structure of the radical SA by DFT and NBO theory were performed. In particular, the spin density (Figure 2) shows that its maximum is at position C3 and C5. The spin density corresponds to the reactivity of the SA radical in the electrochemical oxidation reaction. Simply based on this assessment, it is possible to predict that the attraction of OH[−] and Cl[−] will be favorable at the C3 and C5 position. This is in agreement with the experimental data, where the byproducts for both hydroxylation and chlorination were observed at the C3 and C5 position.

Table 1. Relative energy of hydroxylated and chlorinated products.

Position Hydroxylate Product	Relative Energy (kJ/mol)	Position Mono-Chlorinated Product	Relative Energy (kJ/mol)	Position Di-Chlorinated product	Relative Energy (kJ/mol)
4	0.0	4	0.0	4,5	0.0
6	10.8	5	3.9	3,5	0.1
5	15.7	3	9.7	3,4	4.8
3	18.2	6	29.6	4,6	17.0
n/a	n/a	n/a	n/a	3,6	25.5
n/a	n/a	n/a	n/a	5,6	32.6

3.2. Oxidation of Salicylic Acid and Intermediate Formation

3.2.1. Electro-activity of Salicylic Acid

CV has been used to evaluate the electro-activity of SA. First, a GC rod was used as a baseline for the later comparison with different anode materials. GC is not prone to fouling, unlike the Pt electrode, yet it has an active surface, unlike BDD, meaning that compounds contained in the water matrix have a proper affinity to the anode surface. In a second step, the electro-activity of SA was assessed with a Pt and BDD electrode, which corresponded to the anode materials used for the bulk electrolysis experiments. CV using a GC anode revealed that SA is electro-active, as indicated by the anodic oxidation peak potential E_{pa} observed during the forward scan (Figure 4a).

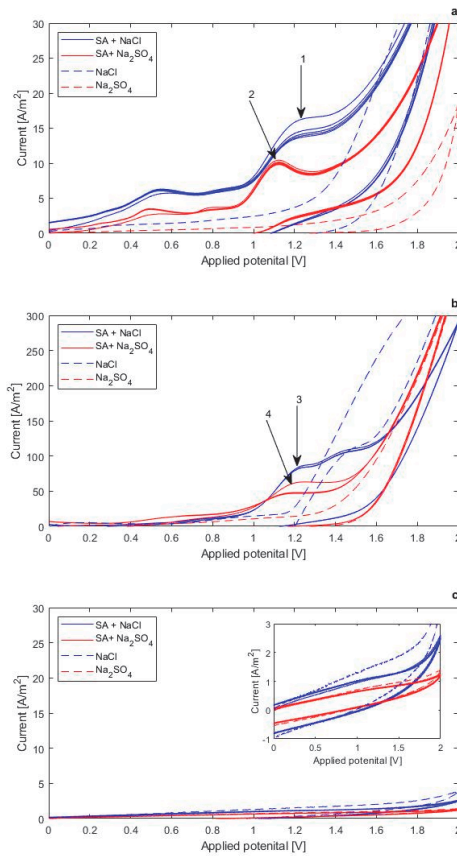


Figure 4. Cyclic voltammetry (CV) for SA in different supporting electrolytes and different anode materials (1V/s, 5 consecutive scan, current normalized for working electrode area). (a) GC, (b) Pt, (c) BDD.

No reversibility of the oxidation peak was observed during a reverse reduction scan of SA. This is in agreement with electrochemical irreversibility being a typical feature for phenolic compounds [30]. The use of two different supporting electrolytes, NaCl and Na₂SO₄, indicates that NaCl leads to a higher anodic peak current i_{pa} (Figure 4a, peak nr. 1) than Na₂SO₄ (Figure 4a, peak nr. 2) for SA. A higher anodic peak current for one supporting electrolyte indicates that the diffusion of the model compound towards the electrode surface is more efficient in NaCl than in Na₂SO₄, which can be associated to the different size of anions (Cl⁻ and SO₄²⁻) [31]. Looking at the E_{pa} for GC and Pt anode, there is a slight shift towards a more positive potential for SA when NaCl is used instead of Na₂SO₄. The exact values for E_{pa} for each electrode material and supporting electrolyte are presented in Table 2.

Table 2. Overview of peak potentials E_{pa} (V) vs. Ag/AgCl (3M) for different anode materials and supporting electrolytes (scan rate: 1 V/s).

Anode	GC		Pt		BDD	
Electrolyte	NaCl	Na ₂ SO ₄	NaCl	Na ₂ SO ₄	NaCl	Na ₂ SO ₄
E_{pa} (V) SA	1.20	1.07	1.22	1.15	n/a	n/a

In addition, SA exhibits a higher i_{pa} and a shift in E_{pa} in the first scan cycle compared to scan cycles 2–5 when using GC (Figure 4a) and Pt (Figure 4b, peak nr. 3 & 4) anodes. A lower E_{pa} in the second and more consecutive scan cycles can be attributed to the formation of a polymeric layer during the EO, which covers the electrode surface [32]. This results in a decreased i_{pa} for the consecutive scan cycles. Only a slight or no decrease of i_{pa} is observed after the second scan cycle which suggests that the polymeric layer is not developing any further. CV of SA on the BDD anode exhibited no oxidation peak E_{pa} (Figure 4c), which shows that SA does not undergo oxidation by DET. This is attributed to the non-active nature of BDD anodes, and results in a low affinity towards compounds contained in the water matrix. This behavior makes BDD anodes less prone to polymeric fouling than the active Pt anodes [8]. Contrary to our findings, Louhichi et al. [33] observed that SA is electro active on BDD electrodes during CV. They further state that a decreasing oxidation peak with increasing cycle numbers suggests a polymeric layer built up on the BDD anode. Furthermore, Montilla et al. [34] observed an anodic oxidation peak of the structurally similar benzoic acid on BDD anodes during CV. Differences in both studies include higher analyte concentrations, a different electrolyte (1M H₂SO₄ or 0.5 M HClO₄) and a considerably lower pH. In addition, the setup used in this study includes an RDE while it was not specified in the above-mentioned studies. Despite the fact that DET of SA on BDD electrodes was not observed in this study, BDD anodes are expected to outperform Pt anodes during bulk electrolysis of SA due to less electrode fouling and the formation of the more freely available physisorbed hydroxyl radicals [8].

CV results could verify the electro-activity of SA on active anodes (GC and Pt). The results confirm that electrons are directly exchanged between SA and these anodes, which contributes to the partial oxidation of SA. Thus, the use of different anode materials and electrolytes emphasized their impact on DET. Recorded anodic peak currents on Pt and GC electrodes showed that NaCl facilitated the transport of SA towards the electrode transport compared to Na₂SO₄.

3.2.2. Formation of Hydroxylated Salicylic Acid Intermediates

Bulk electrolysis was performed to investigate the oxidation of SA via EOTR. The original experimental data can be found in the supporting material (Tables S1–S4). With the NaCl-BDD setting, two hydroxylated products (23dHBA and 25dHBA) could be identified and quantified whereas the third expected hydroxylated product (26HBA) could not be detected at any time. Detected dHBAs were present after 10 min and they remained at a constant concentration throughout the experiment (Figure 5b). A concentration of 1.07×10^{-6} M and 4.85×10^{-6} M for 23dHBA and 25dHBA, respectively suggests a balanced formation and degradation during EO. Guinea et al. [14] also identified 25dHBA to be the most abundant among the three investigated dHBAs. A higher SA concentration (1.20×10^{-3} M) and cathodically generated hydrogen peroxide were used in that study, resulting in a significantly higher amount of each dHBA product. This explains why 26dHBA (limit of quantification (LOQ) of 10 nM) was not found in the present study but was found as a degradation product of SA by Guinea et al. [14].

When the NaCl-Pt setting was used, both, 23dHBA and 25dHBA could be identified and quantified, but 26dHBA could not be detected. In contrast to the BDD anode, the hydroxylated products do not show a constant production rate but do reach a maximum concentration after 60 min with 0.24×10^{-5} M and 0.69×10^{-5} M for 23dHBA and 25dHBA, respectively (Figure 5d). It is also notable that, after reaching a maximum concentration, both hydroxylated products are only eliminated again to a certain extent, similar to the observation on the BDD electrode. The final concentration was 0.13×10^{-5} M for 23dHBA and 0.56×10^{-5} M for 25dHBA. It should be noted that the absolute concentration of dHBAs detected was considerably higher than with the BDD anode, specifically 18% higher for 23dHBA and 13% higher for 25dHBA. This behavior can be attributed to the quasi freely available physisorbed hydroxyl radicals on BDD, which readily react with SA and lead to its complete mineralization (Equation (4)). However, on Pt anodes the hydroxyl radicals are chemisorbed (Equation (3)) and thus exhibit a lower oxidation power, which results in a lower amount of complete mineralized SA and

a higher amount of the intermediate degradation products such as 23dHBA and 25dHBA. Similar findings have been reported by Madsen et al. [35].

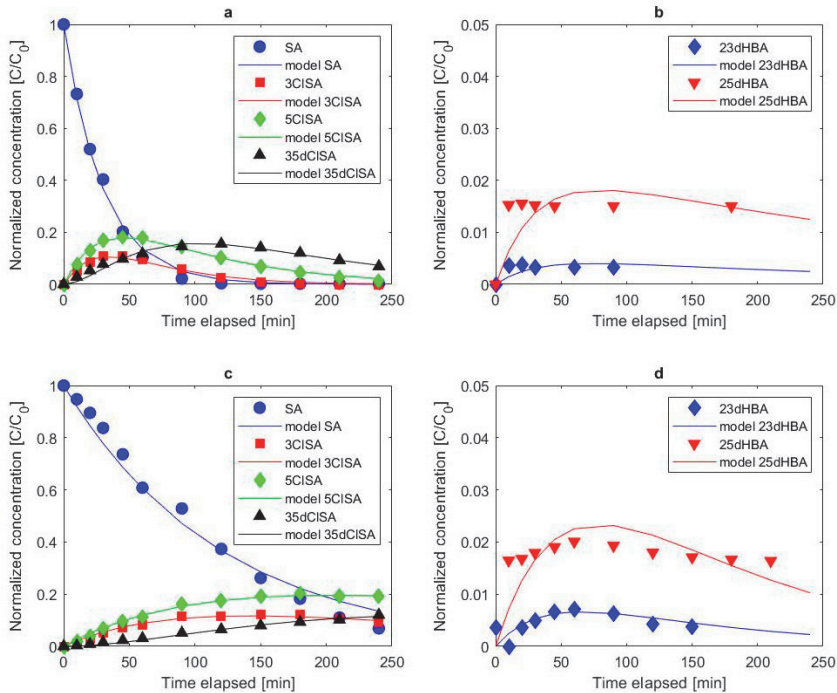


Figure 5. Experimental data and model with chloride (NaCl) as the supporting electrolyte: boron doped diamond (BDD) anode (a) and (b), Pt anode (c) and (d); normalized concentrations with respect to initial SA concentration.

Using the Na₂SO₄-BDD setting, 23dHBA and 25dHBA could also be identified and are depicted in Figure 6a,b, but 26dHBA was not detected. Both hydroxylated compounds were present as when NaCl was used. 23dHBA is present after 10 min at constant concentration of 1.3×10^{-6} M. 25dHBA shows the same pattern as 23dHBA with a concentration of 5.7×10^{-6} M.

With the Na₂SO₄-Pt setting, 23dHBA and 25dHBA could be observed yet 26dHBA could not be detected. However, the hydroxylated products differ in the concentration profile from the results obtained with the other three settings. A clear increase over time of both 23dHBA and 25dHBA is shown in Figure 6d with 3.24×10^{-6} M and 1.24×10^{-5} M as final concentrations for 23dHBA and 25dHBA, respectively.

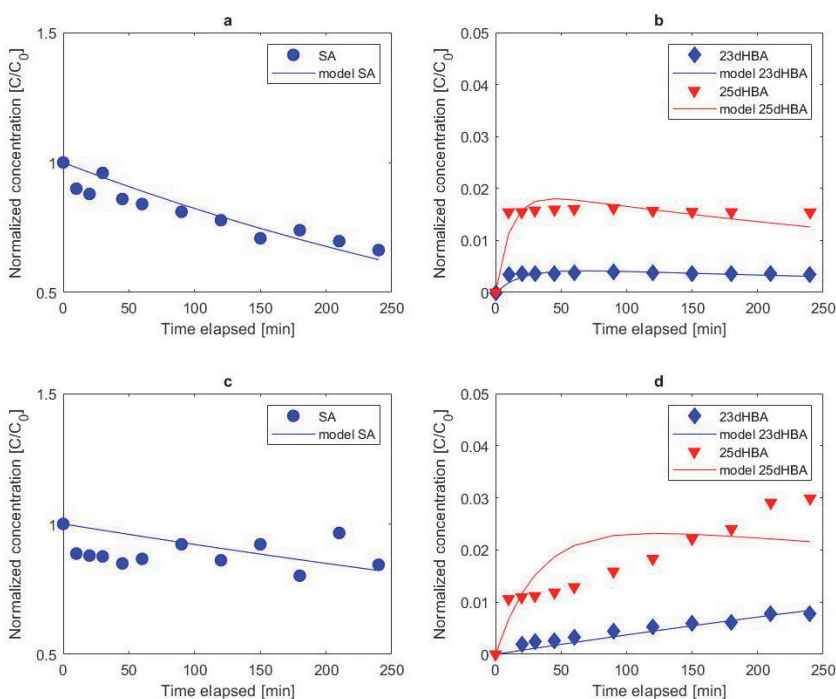


Figure 6. Experimental data and model with sulfate (Na_2SO_4) as the supporting electrolyte: BDD anode (a) and (b), Pt anode (c) and (d); normalized concentrations with respect to initial SA concentration.

3.2.3. Formation of Chlorinated Salicylic Acid

On the BDD anode with NaCl as the supporting electrolyte, the formation of 3CISA, 5CISA and 35dCLSA was observed instantly after the beginning of the experiment (Figure 5a). 3CISA reached the maximum concentration (4.10×10^{-5} M) after 45 min and was further oxidized completely after 180 min. Likewise, 5CISA reached its peak concentration (6.72×10^{-5} M) after 45 min and was almost completely oxidized (4.64×10^{-6} M) by the end of the experiment. 35dCISA reached its peak concentration (5.80×10^{-5} M) after 120 min and exhibited a final concentration of 2.56×10^{-5} M. The observed chlorinated salicylic acid products were formed as expected based on the previous DFT calculations and as suggested by Farinholt et al. [16] and Broadwater et al. [17].

Using a Pt anode showed the same chlorinated product formation i.e., 3CISA, 5CISA and 35dCISA (Figure 5c). All three identified chlorinated products were observed right after the beginning of the experiment. 3CISA reached its peak concentration (4.17×10^{-5} M) after 150 min and decreased thereafter to a final concentration of 3.19×10^{-5} M. The peak concentration of 5CISA (6.90×10^{-5} M) was reached after 180 min and decreased to a final concentration of 6.49×10^{-5} M. For 35dCISA a steady formation and no point of concentration inflection was reached until the end of the experiment where the final concentration amounted to 4.11×10^{-5} M.

Comparing the formation of the chlorinated products on BDD and Pt electrode (Figure 7) it shows that the maximum concentration of 3CISA (BDD: 4.10×10^{-5} M, Pt: 4.18×10^{-5} M) and 5CISA (BDD: 6.77×10^{-5} M, Pt: 6.90×10^{-5} M) are about equal. The LOQ corresponds to 1.50×10^{-7} M for both, 3CISA and 5CISA. For 35dCISA, a peak concentration (5.80×10^{-5} M) was only detected with the BDD electrode (Figure 5a). The experimental time of 240 min was too short to detect a peak concentration of 35dCISA with the Pt electrode and no apparent plateau was reached by the end of the experiment (Figure 5c).

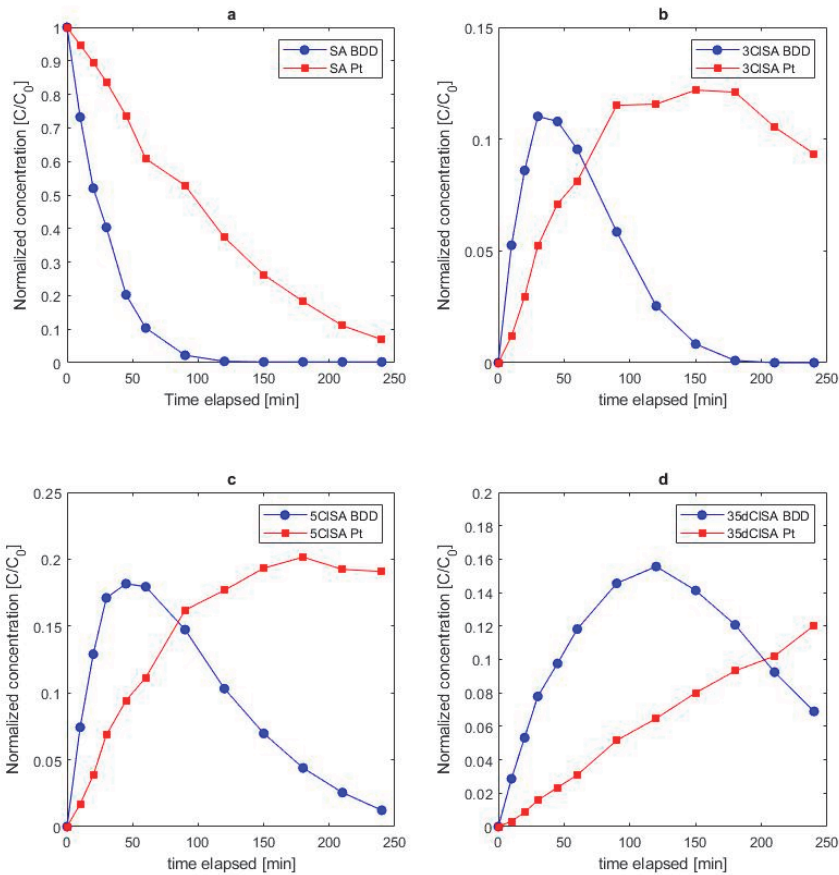


Figure 7. Normalized concentration profiles with respect to initial molar SA concentration $[C_0]$: SA (a) chlorinated degradation products (b–d) on BDD and Pt electrodes.

3.2.4. Influence of Electrolyte Mediated Bulk Oxidation on Intermediate Formation

The two electrolytes form different reactive species that contribute to the MEO of SA. According to the reactivity of the oxidizing species formed, they also have a major impact on the degradation kinetics. The production of free chlorine was lower with the NaCl-Pt than with the NaCl-BDD setting. A final concentration of 9.3 mg Cl_2/L was measured with the Pt anode by the end of the experiment compared to 166 mg Cl_2/L with the BDD anode. This demonstrates that BDD not only favors the production of quasi-free hydroxyl radicals [8], but also favors the production of active chlorine Equations (7) and (8) and the consequent chlorine oxidation of organic compounds, which is the governing oxidation mechanism during EO when using NaCl as a supporting electrolyte. However, the similar production of hydroxylated products of SA on NaCl-BDD, NaCl-Pt and Na_2SO_4 -BDD indicates that the hydroxylation takes part to the same extent regardless of electrolyte and anode material for the three mentioned parameter combinations. These findings show that in all three cases, hydroxylation competes with MEO since the formation of hydroxylated products does not increase. That leads to the further conclusion that despite the hydroxylation of SA there is also an MEO process, which governs the oxidation of SA on Na_2SO_4 -BDD. This assumption is endorsed by the results of Farhat et al. [36] whereby they confirmed the important role of sulfate radicals formed on BDD anodes on the degradation of organic pollutants. Farhat et al. [36] suggested two possible pathways of sulfate radical formation on BDD anode, either via DET of SO_4^{2-} or by the reaction of H_2SO_4 or HSO_4^-

with the anodically generated hydroxyl radicals. Further, they suggest a nonradical activation of persulfate ($S_2O_8^{2-}$) that involves increasing the oxidation rate of organic contaminants. The Na_2SO_4 -Pt parameter setting differs in its result compared to the other three parameter settings with regards to the concentration profile of the two hydroxylated compounds. The maximum concentration of both 23dHBA and 25dHBA differ by more than a factor 2 compared to the obtained concentration with the three other parameter settings. Since hydroxyl radical production is less on Pt than on BDD there is less mediating oxidizing species formed, as confirmed above concerning active chlorine species. Additionally, sulfate active species are not present when the Pt anode is used since the oxidation potential of sulfate (2.01 V vs. standard hydrogen electrode) exceeds the potential window of the Pt anode (depicted in Figure 4b) and oxygen evolution starts before sulfate oxidation. Thus, oxidation of SA at the Pt anode and Na_2SO_4 supporting electrolyte is governed by the higher oxides formed at active electrode surfaces, which are less reactive than the physically adsorbed hydroxyl radicals at the BDD anodes. This is reflected in slower overall degradation kinetics. Thus, the lack of oxidative species other than the higher oxides at the Pt anode surface explains why the partial oxidation of 23dHBA and 25dHBA is governing the process and not complete mineralization.

3.3. Overall Degradation Kinetics of Salicylic Acid

A degradation of 50 mg/L (362'004 nM) SA was followed over time for all four parameter settings and the apparent first order rate constants (k_{SA}) are presented in Table 3. Figure 5a depicts the results using BDD in combination with NaCl as the supporting electrolyte. SA could not be detected after 120 min (LOD of 30 nM). The kinetic behavior observed for SA was in accordance with the theory of the chosen mass transfer limiting conditions on BDD electrodes [22], where the applied current was higher than the limiting current (8 mA/cm²). Oxidation of SA on Pt followed the same pattern as on the BDD anode and is depicted in Figure 5c. However, no complete degradation of SA was achieved during the experimental time whereby 7% of the initial SA concentration was still present at the end of the experiment. When Na_2SO_4 is used as the electrolyte the degradation of SA proceeds at a more moderate rate than with NaCl. For the Na_2SO_4 -BDD setting, 66% of the initial SA concentration could still be observed at the end of the experiment (Figure 6a). The Na_2SO_4 -Pt setting leads to a nearly constant concentration of SA with a final concentration corresponding to 84% of the initial SA concentration (Figure 6c).

The proposed chemical kinetic model (Figure 3) was fitted to the experimental data of SA, hydroxylated and chlorinated products and the corresponding computed results are depicted in Figures 5 and 6. In addition, Table 3 summarizes the rate constants (k) and the fitting quality (R^2) for the four different parameter settings.

The formation of hydroxylated products (k_2 and k_3) of SA are adequately described by the model and exhibit a R^2 between 77% and 88% for all four parameter settings. The only exception is 25dHBA with the Na_2SO_4 -Pt setting and a R^2 of 64%, which means a less adequate fit of the model and the experimental data. This discrepancy can be explained by the scattered experimental data of SA and in consideration of the low amount of 25dHBA that is produced, i.e., less than 3% of SA is degraded to 25dHBA (Figure 6d). Because the kinetic model is assuming first order kinetics and the experimental data of 25dHBA does not exhibit clear first order kinetics, the fitting of the model to the experimental data is less accurate. Looking at the rate constants of the hydroxylated degradation products, it is evident that 25dHBA is formed faster (k_3) than 23dHBA (k_2) for all four parameter settings. These results are supported by the DFT calculation where the relative energy for 23dHBA was calculated to be higher than for 25dHBA, which means that 25dHBA is the more stable product. The degradation of the hydroxylated products to other organic products or complete combustion to CO_2 is expressed through k_6 and k_7 for 23dHBA and 25dHBA, respectively and is generally faster than their formation.

Table 3. Summary rate equations and fitting quality of the kinetic model.

Rate Constants (1/min)	NaCl/BDD	NaCl/Pt	Na ₂ SO ₄ /BDD	Na ₂ SO ₄ /Pt
k ₁	1.28 × 10 ⁻²	2.24 × 10 ⁻³	3.32 × 10 ⁻¹⁴	2.22 × 10 ⁻¹⁴
k ₂	1.75 × 10 ⁻⁴	2.89 × 10 ⁻⁴	2.41 × 10 ⁻⁴	3.87 × 10 ⁻⁵
k ₃	7.62 × 10 ⁻⁴	8.17 × 10 ⁻⁴	1.71 × 10 ⁻³	7.82 × 10 ⁻⁴
k ₄	8.56 × 10 ⁻³	2.27 × 10 ⁻³	n/a	n/a
k ₅	1.10 × 10 ⁻²	2.75 × 10 ⁻³	n/a	n/a
k ₆	3.63 × 10 ⁻³	2.53 × 10 ⁻²	5.07 × 10 ⁻²	3.20 × 10 ⁻¹³
k ₇	2.89 × 10 ⁻³	1.80 × 10 ⁻²	8.70 × 10 ⁻²	3.05 × 10 ⁻²
k ₈	2.22 × 10 ⁻¹⁴	2.22 × 10 ⁻¹⁴	n/a	n/a
k ₉	9.81 × 10 ⁻³	2.22 × 10 ⁻¹⁴	n/a	n/a
k ₁₀	2.59 × 10 ⁻²	5.96 × 10 ⁻³	n/a	n/a
k ₁₁	3.55 × 10 ⁻³	2.53 × 10 ⁻³	n/a	n/a
k ₁₂	9.96 × 10 ⁻³	7.71 × 10 ⁻³	n/a	n/a
k _{SA} , Σ(k ₁ –k ₅)	3.33 × 10 ⁻²	8.37 × 10 ⁻³	1.95 × 10 ⁻³	8.21 × 10 ⁻⁴
Fitting Quality, R² (%)				
SA	98%	96%	95%	92%
23dHBA	77%	88%	87%	88%
25dHBA	78%	80%	88%	64%
3CISA	94%	95%	n/a	n/a
5CISA	96%	97%	n/a	n/a
35dCISA	93%	96%	n/a	n/a

Formation and degradation of chlorinated products of SA are described to an exceeding extent by the suggested kinetic model. R² for both, BDD and Pt anode are between 93% and 97%. The formation of 5CISA proceeds at a faster rate (k₅) than the formation of 3CISA (k₄) on both anode materials. Similar to the hydroxylation of SA, this can also be explained by the preliminary DFT calculations with the predicted relative energy for each compound (Table 1). The relative energy is lower for 5CISA than for 3CISA making 5CISA the more stable product. The decrease of 3CISA and 5CISA consists of the formation of 35dCISA (k₁₀ & k₁₁) and the degradation to other organic products or complete combustion to CO₂ (k₈ & k₉). The sums of k₈ and k₁₀ for 3CISA and k₉ and k₁₀ for 5CISA represent their degradation rate and show that 5CISA is degraded at faster rate than 3CISA on both anode materials. The degradation rate (k₁₂) of 35dCISA is slower than the one of the mono chlorinated SA on both, BDD and Pt anode.

When comparing the rate constants of hydroxylation and chlorination of SA it becomes evident that chlorination takes place at considerably faster rates than hydroxylation. On BDD anodes, the formation of 3CISA is a factor 49 and 11 faster than the formation of 23dHBA and 25dHBA, respectively. Likewise, the formation of 5CISA is a factor 63 and 14 faster than the formation of 23dHBA and 25dHBA, respectively. The same pattern can be observed for when the Pt anode is used yet the hydroxylation and chlorination rates differ less than with the BDD anode. 3CISA is formed by a factor 8 and 3 faster than 23dHBA and 25dHBA, respectively. According to this, the formation of 5CISA is a factor 10 and 3 faster than the formation of 23dHBA and 25dHBA, respectively. In conclusion, chlorination governs the degradation of SA during electrochemical oxidation, no matter the electrode material.

Finally, the kinetic model also provided the apparent rate constant of the SA degradation (k_{SA}), which consists of the sum of k₁ to k₅. Whereby k₁ accounts for the formation of other, not investigated organic products, the oxidation product of SA resulting from DET or other oxidation mechanisms of SA (Figure 3). Further, the degradation of SA to hydroxylated (k₂ and k₃) and chlorinated (k₄ and k₅) products are also accounted for in the apparent rate constant k_{SA}. The proposed kinetic model does not provide an individual rate constant for DET and thus its contribution to the degradation of SA is out of scope of this study. However, when NaCl is used instead of Na₂SO₄, k₁ is more than a factor 1.01 × 10¹¹ higher for both anode materials and thus contributing to a higher degree to k_{SA} as when k₁ is obtained with Na₂SO₄. It indicates that if chlorination is not contributing to k₁ in terms of complete

combustion of SA to CO₂ or by the formation of other, not investigated chlorinated compounds the value of k_1 becomes significantly lower. This suggests that DET of SA, remains a mechanism that contributes to k_1 but plays a minor role in its degradation pathway. By comparing the different values for k_{SA} for the four parameter settings (Table 3) it becomes evident that the degradation of SA is in general faster with NaCl is used than with Na₂SO₄. However, among experiments using the same electrolyte, the use of a BDD anode resulted in a higher k_{SA} than with a Pt anode. On a BDD anode, the k_{SA} is a factor 17 higher for NaCl than for Na₂SO₄, and on a Pt anode the k_{SA} is a factor 10 higher for NaCl than for Na₂SO₄. Regardless of the parameter settings, the proposed kinetic model describes the experimental data of the SA degradation via k_{SA} to an exceeding extent with an R² of 92% or higher.

4. Conclusions

- This study confirms the formation of chlorinated intermediates. Three different chlorinated oxidation products were identified, 3ClSA, 5ClSA and 35dClSA, whereby 5ClSA was more frequently detected than 3ClSA and 35dClSA.
- Hydroxylation of salicylic acid via anodically generated hydroxyl radicals was confirmed via the identification and quantification of 23dHBA and 25dHBA. 25dHBA was more frequently formed than 23dHBA.
- Density functional theory and natural bond theory computations revealed the highest spin density at the C3 and C5 atom of salicylic acid. This explains the formation of the observed chlorinated and hydroxylated intermediates of salicylic acid, and why other intermediates like 26dHBA or 4ClSA were not detected.
- In chloride electrolyte, oxidation via mediating oxidizing species was found to be the governing oxidation process on both tested anode materials, whereas hydroxylation took place but at much lower rates than chlorination.
- Cyclic voltammetry confirmed of direct electron transfer of salicylic acid on Pt anodes, but not on BDD electrodes. The proposed kinetic model adequately describes the degradation of salicylic acid, and the formation of its chlorinated and hydroxylated intermediates and corresponding rate constants could be derived.

Supplementary Materials: The following are available online at <http://www.mdpi.com/2073-4441/11/7/1322/s1>, Tables S1–S4: original experimental data, Table S5: LOQ values of analysed compounds

Author Contributions: N.A., J.M., C.H. and T.M. conceived and designed the experiments. N.A. performed the experiments and analyzed the data. T.T. and N.L.M. performed the DFT and NBT computations. T.T. wrote and validated the kinetic model. N.A. and T.T. wrote the manuscript. J.M., C.H. and T.M. reviewed and edited the manuscript. J.M., C.H. and T.M. supervised the work.

Funding: This work is funded by the Norwegian University of Science and Technology (NTNU) and Søndre Helgeland Miljøverk IKS (SHMIL, Norway).

Acknowledgments: The authors acknowledge the computational resources of the Norwegian Metacentre for Computational Science (NOTUR). A special thank goes to Kåre Andre Kristiansen for his invaluable support in the MS-lab.

Conflicts of Interest: The authors declare no conflict of interest.

References

1. Fuoco, R.; Giannarelli, S. Integrity of aquatic ecosystems: An overview of a message from the South Pole on the level of persistent organic pollutants (POPs). *Microchem. J.* **2019**, *148*, 230–239. [[CrossRef](#)]
2. Li, Z. Health risk characterization of maximum legal exposures for persistent organic pollutant (POP) pesticides in residential soil: An analysis. *J. Environ. Manag.* **2018**, *205*, 163–173. [[CrossRef](#)] [[PubMed](#)]
3. Jones, K.C.; de Voogt, P. Persistent organic pollutants (POPs): State of the science. *Environ. Pollut.* **1999**, *100*, 209–221. [[CrossRef](#)]
4. Wang, F.; Smith, D.W.; El-Din, M.G. Application of advanced oxidation methods for landfill leachate treatment—A review. *J. Environ. Eng. Sci.* **2003**, *2*, 413–427. [[CrossRef](#)]

5. Panizza, M.; Delucchi, M.; Sirés, I. Electrochemical process for the treatment of landfill leachate. *J. Appl. Electrochem.* **2010**, *40*, 1721–1727. [[CrossRef](#)]
6. Andreatti, R.; Caprio, V.; Insola, A.; Marotta, R. Advanced oxidation processes (AOP) for water purification and recovery. *Catal. Today* **1999**, *53*, 51–59. [[CrossRef](#)]
7. Dewil, R.; Mantzavinos, D.; Poullos, I.; Rodrigo, M.A. New perspectives for Advanced Oxidation Processes. *J. Environ. Manag.* **2017**, *195*, 93–99. [[CrossRef](#)]
8. Comninellis, C.; Chen, G. *Electrochemistry for the Environment*; Springer: New York, NY, USA, 2010. [[CrossRef](#)]
9. Foti, G.; Gandini, D.; Comninellis, C.; Perret, A.; Haenni, W. Oxidation of organics by intermediates of water discharge on IrO₂ and synthetic diamond anodes. *Electrochem. Solid State Lett.* **1999**, *2*. [[CrossRef](#)]
10. Martínez-Huitle, C.A.; Ferro, S. Electrochemical oxidation of organic pollutants for the wastewater treatment: Direct and indirect processes. *Chem. Soc. Rev.* **2006**, *35*, 1324–1340. [[CrossRef](#)]
11. Bonfatti, F.; Ferro, S.; Lavezzo, F.; Malacarne, M.; Lodi, G.; de Battisti, A. Electrochemical Incineration of Glucose as a Model Organic Substrate II. Role of Active Chlorine Mediation. *J. Electrochem. Soc.* **2000**, *147*, 592–596. [[CrossRef](#)]
12. Stucki, S.; Kötz, R.; Carcer, B.; Suter, W. Electrochemical waste water treatment using high overvoltage anodes Part II: Anode performance and applications. *J. Appl. Electrochem.* **1991**, *21*, 99–104. [[CrossRef](#)]
13. Iniesta, J.; Michaud, P.; Panizza, M.; Cerisola, G.; Aldaz, A.; Comninellis, C. Electrochemical oxidation of phenol at boron-doped diamond electrode. *Electrochim. Acta* **2001**, *46*, 3573–3578. [[CrossRef](#)]
14. Guinea, E.; Arias, C.; Cabot, P.L.; Garrido, J.A.; Rodríguez, R.M.; Centellas, F.; Brillas, E. Mineralization of salicylic acid in acidic aqueous medium by electrochemical advanced oxidation processes using platinum and boron-doped diamond as anode and cathodically generated hydrogen peroxide. *Water Res.* **2008**, *42*, 499–511. [[CrossRef](#)] [[PubMed](#)]
15. Feng, L.; van Hullebusch, E.D.; Rodrigo, M.A.; Esposito, G.; Oturan, M.A. Removal of residual anti-inflammatory and analgesic pharmaceuticals from aqueous systems by electrochemical advanced oxidation processes, A. review. *Chem. Eng. J.* **2013**, *228*, 944–964. [[CrossRef](#)]
16. Farinholt, L.H.; Stuart, A.P.; Twiss, D. The Halogenation of Salicylic Acid. *J. Am. Chem. Soc.* **1940**, *62*, 1237–1241. [[CrossRef](#)]
17. Broadwater, M.A.; Swanson, T.L.; Sivey, J.D. Emerging investigators series: Comparing the inherent reactivity of often-overlooked aqueous chlorinating and brominating agents toward salicylic acid. *Environ. Sci. Water Res. Technol.* **2018**, *4*, 369–384. [[CrossRef](#)]
18. Torriero, A.A.J.; Luco, J.M.; Sereno, L.; Raba, J. Voltammetric determination of salicylic acid in pharmaceutical formulations of acetylsalicylic acid. *Talanta* **2004**, *62*, 247–254. [[CrossRef](#)]
19. Wudarska, E.; Chrzescijanska, E.; Kusmierk, E. Electroreduction of Salicylic Acid, Acetylsalicylic Acid and Pharmaceutical Products Containing these Compounds. *Port. Electrochim. Acta* **2014**, *32*, 295–302. [[CrossRef](#)]
20. Wragg, A.A.; Tagg, D.J.; Patrick, M.A. Diffusion-controlled current distributions near cell entries and corners. *J. Appl. Electrochem.* **1980**, *10*, 43–47. [[CrossRef](#)]
21. Chatzisympson, E.; Xekoukoulotakis, N.P.; Diamadopoulos, E.; Katsaounis, A.; Mantzavinos, D. Boron-doped diamond anodic treatment of olive mill wastewaters: Statistical analysis, kinetic modeling and biodegradability. *Water Res.* **2009**, *43*, 3999–4009. [[CrossRef](#)]
22. Panizza, M.; Kapalka, A.; Comninellis, C. Oxidation of organic pollutants on BDD anodes using modulated current electrolysis. *Electrochim. Acta* **2008**, *53*, 2289–2295. [[CrossRef](#)]
23. Frisch, D.J.F.M.J.; Trucks, G.W.; Schlegel, H.B.; Scuseria, G.E.; Robb, M.A.; Cheeseman, J.R.; Scalmani, G.; Barone, V.; Mennucci, B.; Petersson, G.A.; et al. Gaussian 09, revision B.01. 2010. Available online: <http://gaussian.com/> (accessed on 13 October 2018).
24. Becke, A.D. Density-functional exchange-energy approximation with correct asymptotic behavior. *Phys. Rev. A* **1988**, *38*, 3098–3100. [[CrossRef](#)]
25. Weigend, F.; Furche, F.; Ahlrichs, R. Gaussian basis sets of quadruple zeta valence quality for atoms H-Kr. *J. Chem. Phys.* **2003**, *119*, 12753–12762. [[CrossRef](#)]
26. Weigend, F. Accurate Coulomb-fitting basis sets for H. to Rn. *Phys. Chem. Chem. Phys.* **2006**, *8*, 1057–1065. [[CrossRef](#)] [[PubMed](#)]
27. Marenich, A.V.; Cramer, C.J.; Truhlar, D.G. Universal Solvation Model Based on Solute Electron Density and on a Continuum Model of the Solvent Defined by the Bulk Dielectric Constant and Atomic Surface Tensions. *J. Phys. Chem. B* **2009**, *113*, 6378–6396. [[CrossRef](#)] [[PubMed](#)]

28. Foster, J.P.; Weinhold, F. Natural hybrid orbitals. *J. Am. Chem. Soc.* **1980**, *102*, 7211–7218. [[CrossRef](#)]
29. Jing, Y.; Chaplin, B.P. Mechanistic Study of the Validity of Using Hydroxyl Radical Probes To Characterize Electrochemical Advanced Oxidation Processes. *Environ. Sci. Technol.* **2017**, *51*, 2355–2365. [[CrossRef](#)]
30. Evans, D.; Hart, J.P.; Rees, G. Voltammetric Behaviour of Salicylic Acid at a Glassy Carbon Electrode and Its Determination in Serum Using Liquid Chromatography With Amperometric Detection. *Analyst* **1991**, *116*, 803–806. [[CrossRef](#)]
31. Dubois, D.; Moninot, G.; Kutner, W.; Jones, M.T.; Kadish, K.M. Electroreduction of Buckminsterfullerene, Electrolyte, and Temperature Effects Aprotic Solvents: Solvent Supporting. *J. Phys. Chem.* **1992**, 7137–7145. [[CrossRef](#)]
32. Lee, J.H.Q.; Koh, Y.R.; Webster, R.D. The electrochemical oxidation of diethylstilbestrol (DES) in acetonitrile. *J. Electroanal. Chem.* **2017**, *799*, 92–101. [[CrossRef](#)]
33. Louhichi, B.; Bensalash, N.; Gadri, A. Electrochemical oxidation of benzoic acid derivatives on boron doped diamond: Voltammetric study and galvanostatic electrolyses. *Chem. Eng. Technol.* **2006**, *29*, 944–950. [[CrossRef](#)]
34. Montilla, F.; Michaud, P.A.; Morallon, E.; Vazquez, J.L.; Comninellis, C.; Morallón, E.; Vázquez, J.L. Electrochemical oxidation of benzoic acid at boron-doped diamond electrodes. *Electrochim. Acta* **2002**, *47*, 3509–3513. [[CrossRef](#)]
35. Madsen, H.T.; Søgaard, E.G.; Muff, J. Chemosphere Study of degradation intermediates formed during electrochemical oxidation of pesticide residue 2,6-dichlorobenzamide (BAM) at boron doped diamond (BDD) and platinum–iridium anodes. *Chemosphere* **2014**, *109*, 84–91. [[CrossRef](#)] [[PubMed](#)]
36. Farhat, A.; Keller, J.; Tait, S.; Radjenovic, J. Removal of Persistent Organic Contaminants by Electrochemically Activated Sulfate. *Environ. Sci. Technol.* **2015**, *49*. [[CrossRef](#)] [[PubMed](#)]



© 2019 by the authors. Licensee MDPI, Basel, Switzerland. This article is an open access article distributed under the terms and conditions of the Creative Commons Attribution (CC BY) license (<http://creativecommons.org/licenses/by/4.0/>).

PAPER II

Application of electrochemical oxidation in cold climate regions – Effect of temperature, pH and anode material on the degradation of Bisphenol and the formation of disinfection by-products

Ambauen, N., Muff, J., Tscheikner-Gratl, F., Trinh, T.T., Hallé, C., Meyn, T.
Journal of Environmental Chemical Engineering 2020, Volume 8, Issue 5, October 2020, 104183
DOI: 10.1016/j.jece.2020.104183



Contents lists available at ScienceDirect

Journal of Environmental Chemical Engineering

journal homepage: www.elsevier.com/locate/jece

Application of electrochemical oxidation in cold climate regions – Effect of temperature, pH and anode material on the degradation of Bisphenol A and the formation of disinfection by-products

Noëmi Ambauen^{a,*}, Jens Muff^{cb}, Franz Tscheikner-Gratl^a, Thuat T. Trinh^a, Cynthia Hallé^a, Thomas Meyn^a

^a Norwegian University of Science and Technology, Department for Civil and Environmental Engineering, Trondheim, Norway

^b Aalborg University, Department of Chemistry and Bioscience, Esbjerg, Denmark

ARTICLE INFO

Editor: Yunho Lee

Keywords:

Bisphenol A
Electrochemical oxidation
Disinfection by-products
Low temperatures

ABSTRACT

This study assessed the feasibility of electrochemical oxidation (EO) for the removal of organic compounds in cold climate regions. A two-level full factorial design was used to test the effect of three factors, temperature (6/20 °C), anode material (Pt/BDD) and pH (7/10) on the degradation of Bisphenol A. Due to the use of a chloride electrolyte, the formation of the disinfection by-products, perchlorate and trichloromethane was assessed too. The 90 % removal of the initial Bisphenol A concentration took up to 71 % (30 min) longer and up to 46 % more power input was required at 6 °C than at 20 °C. At pH 10, degradation and formation kinetics of Bisphenol A and trichloromethane were faster due to the higher oxidation power of OCl^- than HOCl ($\text{pK}_a = 7.5$) and the formation of bisphenolate ions ($\text{pK}_a = 9.6$), which are more prone to electrophilic attack than Bisphenol A. Temperature and anode material were the two factors that significantly affect the trichloromethane formation. Trichloromethane was formed up to 45 % faster at 20 °C than at 6 °C and up to 23 % faster on Pt than on BDD anodes. However, higher trichloromethane concentration were reached on BDD anodes, but were formed at slower rates. The anode material was the only factor, which had a statistically significant influence on the formation of perchlorate. On BDD anode up to 89 % more perchlorate was formed than on Pt anode. The present study shows that the application of EO for organic pollutant removal in regions with low average temperatures is a feasible treatment step although it is associated with higher energy demand and consequently higher costs. The formation of unwanted disinfection by-products in chloride containing waters could not be avoided, but it was shown in this study, that it can be limited by an adequate choice of treatment time, pH and anode material.

1. Introduction

Bisphenol A (BPA) is an important plastic monomer and plasticizer [1,2] and several million tons are produced and consumed annually [3,4]. BPA does not occur naturally in the environment and the large amounts are synthesized to produce polymers present in everyday use items including food and water containers, cans, bottles, sunglasses, electronic equipment and thermal paper [2,5]. BPA is a xenoestrogen and is classified as an endocrine disruptor as it is structurally similar to the hormone estrogen and interacts with the estrogen receptors and thus modulates the endocrine system [6]. BPA was currently (2018) added to the regulation of the European Union (EU) REACH (Registration, Evaluation, Authorization and Restriction of Chemicals) candidate list, classified as a chemical of very high concern [7]. The

responsible European commission furthermore proposed a benchmark value of 0.01 µg/L BPA to be included in the EU directive on the quality of water intended for human consumption [8].

However, BPA is still worldwide detected at different concentrations in water and effluents [9]. Thus, the removal of BPA from wastewaters and landfill leachate (LL) is a pervasive topic and has been successfully addressed in the past by the use of different advanced oxidation processes (AOP). All AOP have in common, that they produce the highly reactive hydroxyl radicals, which non-selectively react with organic pollutants contained in the water matrix, leading to their partial or complete oxidation [10]. The different AOP produce hydroxyl radicals via different mechanisms, e.g. regular and enhanced Fenton oxidation as well as ozonation (e.g. [11,12]). Different studies reported complete removal of BPA from wastewater and LL by electrochemical oxidation

* Corresponding author.

E-mail address: noemi.ambauen@ntnu.no (N. Ambauen).

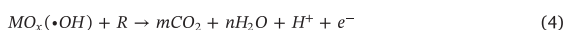
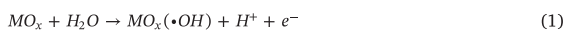
<https://doi.org/10.1016/j.jece.2020.104183>

Received 3 February 2020; Received in revised form 9 June 2020; Accepted 13 June 2020

Available online 15 June 2020

2213-3437/© 2020 Elsevier Ltd. All rights reserved.

(EO) [13–15]. Adsorbed hydroxyl radicals are produced during EO via the electrolytic discharge of water (Eq. (1)) [16].



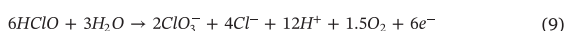
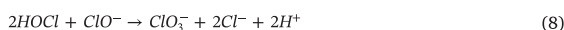
$\bullet OH$: hydroxyl radical, $MO_x(\bullet OH)$: adsorbed hydroxyl radical, MO_{x+1} : higher oxide, R: organic pollutant, RO: oxidized organic pollutant

The further transfer of the oxygen from the hydroxyl radicals to the organic pollutants depends on the anode material. Hereby it is distinguished between active and non-active materials [16]. Active anodes such as platinum (Pt) form higher oxides at their surface via the reaction with the adsorbed hydroxyl radical, which then reacts with the organic pollutant (Eqs. (2) & (3)). Non-active anodes, e.g. boron doped diamond (BDD), don't form higher oxides, instead the adsorbed hydroxyl radical reacts directly with the organic pollutant (Eq. (4)) [16]. Both, active and non-active materials have been tested during EO of BPA such as Pt, glassy carbon (GC) or BDD [17]. It was found that the use of BDD anodes is most effective to mineralize BPA compared to Pt anodes, where the formation of intermediate products prevailed over complete mineralization [17,18]. However, BDD anodes do not only favor the mineralization of BPA, but also the formation of undesirable halogenated organic by-products such as trichloromethane ($CHCl_3$) [19], a compound belonging to the group of trihalomethanes (THMs). THM formation has been confirmed by simple chlorination experiments of BPA with sodium hypochlorite [20]. Also, the formation of the persistent perchlorate ion (ClO_4^-) is favored on BDD anodes [21], which has a detrimental effect to the aquatic environment [22]. Since 2011, the US EPA regulates perchlorate under the safe drinking water act, but as per today, they did not establish a maximum contamination goal yet [23]. However, a maximum contaminant level goal of 56 ppb of ClO_4^- is suggested in public water supplies [24]. Two states in the USA set a limit for perchlorate in drinking water to 2 ppb (Massachusetts) and 6 ppb (California). The WHO defined a limit of 0.7 mg/L for chlorate (ClO_3^-), a precursor ion of perchlorate, which was recently deemed too high by the council of the EU. They proposed to lower the chlorate limit to 0.25 mg/L [8]. Despite the formation of by-products, EO is considered to be an efficient and suitable process, when it comes to the removal of BPA and other organic pollutants [25–27]. and other organic pollutants [16,28] from aqueous solutions. The major advantage of EO compared to other AOPs is that no residual sludge is produced that would require further treatment or disposal [29].

Most of the studies investigating the effect of temperature on the electrochemical removal of BPA or organic pollutants were carried out at room temperature or above [30]. An increase of temperature from 25 °C to 40 °C resulted in an apparent increased oxidation rate of the organic load of 44 % from 2.7 to $3.9 \times 10^{-4} s^{-1}$ respectively. Turro et al. [31] found that the total carbon removal during EO of LL at 30 °C was negligible, but increased to 15 % after increasing the treatment temperature to 60 °C, while COD removal performed equally at all tested temperatures and did not seem to be affected by an increased temperature. Furthermore, Panizza et al. [32] stated an enhanced oxidation reaction of organics by free chlorine species, when temperature was increased from 25 °C to 50 °C during anodic oxidation of LL. However, Darsinou et al. [33] found that an increase from 30 °C to 70 °C lead to a six-fold higher reaction rate of BPA during sono-activated persulfate oxidation. Unfortunately, little is known about the performance of EO for the organic pollutant removal at temperatures lower than room temperature. Anglada et al. [34] reported a decreasing mass transfer coefficient with decreasing temperature from 40 °C to 10 °C during EO of LL.

Only few studies exist that investigated the effect of cold temperatures on water and wastewater treatment. Kettunen et al. [35]

compared an anaerobic LL treatment at 11 and 24 °C and observed a hydraulic retention time (HRT) of 1.5–2 days and 65 % COD removal and a HRT of 10 h and 75 % COD removal respectively. Smith et al. [36] reported a stable COD removal during psychrophilic anaerobic wastewater treatment and concluded a promising potential for its application in cold climate regions. Apart from those findings, it is obvious that more knowledge is needed in order to estimate their applicability for climate regions where cold temperatures prevail. Hence, this study investigates EO process for the removal of organic pollutants from aqueous solutions at low temperatures (6 °C). BPA was chosen as the organic model pollutant as it is well studied and abundant in wastewaters. Additionally, this study also investigates the formation of the unwanted chlorination by-products ClO_4^- and $CHCl_3$. Eqs. (5)–(10) depict the generation of $HClO/ClO^-$ and the formation of ClO_4^- in the electrolytic cell [37]:



Cl^- : chloride ion; Cl_2 : gaseous chlorine, $HClO/ClO^-$: free chlorine; ClO_3^- : chlorate; ClO_4^- : perchlorate

Several studies show the formation of $CHCl_3$ as a result of free chlorine reacting with chlorinated BPA congeners [19,38,39]. Gallard et al. [40] found that $CHCl_3$ is formed from mono-, di-, tri- and tetra-chlorinated phenols, which are incorporated by up to 12 % to $CHCl_3$ under their given experimental conditions. These aforementioned chlorinated phenols are reported metabolites from BPA chlorination, either formed during direct chlorination [41] or indirect chlorination during EO [19]. This study does not investigate the reaction pathway from BPA to $CHCl_3$ yet it is plausible to assume $CHCl_3$ formation takes place in the above-described way.

This study is part of a larger project, that investigates the landfill leachate treatment by EO in Northern Norway, which lays in the sub-arctic climate zone. A particle separation step (coagulation / sedimentation) is already implemented on site, which will provide the feedwater to a potential EO treatment. The effluent after coagulation (coagulant: $FeCl_3$) has an alkaline pH (≈ 10) which is beneficial for the particle formation [42]. The solution pH affects the dissociation of active chlorine (Eq. (7)) as well as the dissociation of the organic pollutant BPA, which has a pK_a of 9.6 [43]. Thus, besides the influence of temperature and anode material, this study also investigates the pH as an important parameter of the EO of BPA and the formation of chlorinated by-products. The influence of the applied current was not investigated since many other studies have studied addressed its influence on the degradation of organic pollutants [44–47]. However, it was addressed in a subsequent study (under review) under more applied conditions, since energy costs strongly depend on the applied current. This study is intended to get a conclusion on whether EO is a suitable treatment step to remove organic pollutants in cold climate regions.

2. Material and methods

2.1. Chemicals

Bisphenol A for bulk electrolysis was purchased from Sigma-Aldrich (Merck, Germany) with a purity grade ≥ 99 %. Stock solution (0.5 M) of BPA was prepared with acetonitrile and stored up to a month. Working solutions (2.5 L) were prepared by adding 25 μL of the stock solution to obtain the desired BPA concentration of 5.0 mM. Sodium

chloride (NaCl) and sodium sulfate (Na_2SO_4) were both purchased from VWR (Avantor, USA) with ISO standard purity grade. The electrolytes were added daily to the working solution to obtain a concentration of 0.0033 M NaCl and 0.0003 M Na_2SO_4 . Deuterated Bisphenol A (d16) was used as internal standard for BPA and was purchased from Dr. Eherstorfer (LGC, UK) with certified reference material standard. A certified reference standard calibration mix of THMs (trichloromethane, bromodichloromethane, dichlorobromomethane, tribromomethane) was purchased from Sigma Aldrich. Dichloromethane was used as an internal standard for the THMs and purchased from Sigma Aldrich with certified reference material standard. Solvents used for UPC² analysis, water and methanol were purchased from VWR and were both HPLC grade ($\geq 99.5\%$) ammonium acetate (7.5 M) was purchased from Sigma Aldrich. Isopropanol HPLC grade ($\geq 99.5\%$) for the reconstitution of BPA was purchased from VWR.

2.2. Electrochemical experiments

Bulk electrolysis was conducted with an electrolytical cell (ElectroCell Europe AS, Denmark) with either an Nb/BDD or Ti/Pt anode and a stainless-steel cathode. Both, anode and cathode are plate electrodes with an active area of 10 cm^2 and an interelectrode gap of 4 mm and a PTFE turbulence enhancing mesh in between. The electrodes are cooled with tap water (ca. 7°C) from the rear end. The electrolytical cell is connected via Teflon tubing to the solution tank (5 L glass beaker) and the solution is pumped with a peristaltic pump (Masterflex Cole-Parmer Instrument Co., USA). All experiments were carried out under galvanostatic conditions with an applied current (j_{app}) of 42.7 mA/cm^2 (limiting current density) and a flow rate of 384 mL/min . The pH of the solution was adjusted to either 7 or 10 by adding either H_2SO_4 (0.1 M) or NaOH (0.1 M). The working solution was kept at constant temperature by a cooling coil (stainless steel) connected to a chiller (FP50-ME, Julabo GmbH, Germany) and regulated with a proportional-integral-derivative controller. Temperature was set at 20°C or at 6°C . Fig. 1 depicts the set-up that was used in the present study.

2.3. Analytical methods

BPA was quantified by UPC² (Waters, USA) with XEVO TQ-S triple quadrupole mass spectrometer (Waters) with an Aquity UPC² BEH $1.7\text{ }\mu\text{m}$ column (Waters). Measurements were conducted in multiple reaction monitoring mode using electrospray ionization. The mobile phases were compressed CO_2 (solvent A), methanol containing 10 mM ammonium acetate (solvent B) and 100 % methanol as makeup solvent. A flow rate of 2.5 mL/min and a makeup flow rate of 0.8 mL/min were applied. The automated backpressure was set to 1500 psi. The initial solvent gradient was 95 % A and 5 % B, hold for 0.3 min, increased to 70 % A and 30 % B from 0.3 to 1.3 min and hold for 0.4 min, then decreased to 95 % A and 5 % B from 1.7 min to 1.8 min and hold for 0.7 min. BPA samples were dried under vacuum (SpeedVac, Thermo Fischer Scientific, USA) at 45°C and reconstituted in isopropanol prior

to analysis. Masslynx (Waters) and Targetlynx (Waters) where the software used for measurements and data analysis respectively.

THMs was quantified using a headspace injector (Tekmar HT3, Teledyne Technologies, USA) coupled to a GC-MS (GC/MS Triple quad 7000, Agilent, USA). The method used was adapted from Perkin Elmer [48]. The samples or standards (10 mL) were placed in 20 mL headspace vials together with $20\text{ }\mu\text{L}$ of internal standard (dichloromethane), and sealed with a crimp cap. A trap column (Purge/Trap K Vocarb[®] 3000, Supelco, USA) and a DB-624 UI GC column (Agilent) with a length of 30 m, 0.25 mm diameter and $1.40\text{ }\mu\text{m}$ film thickness was used for the headspace GC analysis. The oven program for the GC started at 35°C hold for 3 min followed by a ramp of 30°C/min up to 125°C , hold for 1 min, followed by a second ramp of 50°C/min up to 250°C and a final hold of 4 min. Concentrations were determined by a linear calibration curve that included 6 calibration points (3 ppb–100 ppb). Masshunter (Agilent) was the software used for measurements and Masshunter Quant (Agilent) software was used to integrate concentration peaks, to determine the calibration curve and for further data analysis.

Free chlorine was measured with a portable colorimeter (DR 300, Hach, USA) using the *N,N*-diethyl-*p*-phenylenediamine (DPD) method. The limit of detection is 0.1 mg/L .

Chloride and perchlorate were measured using an ion chromatography 940 Professional IC Vario (Metrohm, Switzerland) together with an 858 Professional Sample Processor (Metrohm) and a 10 mL 800 Dosino (Metrohm). A high-performance separation column Metrosep A Supp5 (Metrohm) was used with polyvinyl alcohol with quaternary ammonium groups as column substrate and column dimensions of $250 \times 4.0\text{ mm}$ and $5\text{ }\mu\text{m}$ particle size. Sodium bicarbonate Na_2CO_3 3.2 mM and sodium carbonate NaHCO_3 1 mM (Sigma Aldrich) with 20 % acetone with HPLC grade (VWR Chemicals) was used as eluent. The suppressor solution was 0.1 M sulfuric acid (Merck, USA) and 0.1 M oxalic acid (Sigma Aldrich) in ultra-pure water. The flow rate was set to 0.7 mL/min and the thermostat to 40°C . MagIC Net 3.2 software (Metrohm) was used for measurements and sample analysis.

2.4. Factorial design

The experiments followed a full factorial design with 3 factors (A, B, C) at two levels (Table 1). This results in a 2^3 factorial design with 8 treatment combinations and seven degrees of freedom. A linear regression model (Eq. (11)) was used to estimate the intercept (b_0), the model constants (b_{1-7}), where Y is the response and factors A to C assumed to be independent variables [49]. The regression model also accounts for the product terms of the independent variables to model a possible interaction between two or three factors.

$$Y = b_0 + b_1 A + b_2 B + b_3 C + b_4 AB + b_5 AC + b_6 BC + b_7 ABC \quad (11)$$

Since the full factorial has replicates ($r = 2$), the model has 8 degrees of freedom ($(r-1)2^k$).

The experiments were completely randomized and Analysis of variance (ANOVA) was done using Minitab. The null hypothesis (H_0) stated that no effect is significant ($\text{Effect}_j = 0$) and alternative hypothesis (H_1) assumed at least one effect is significant ($\text{Effect}_j \neq 0$). A significance level of 5 % ($\alpha = 0.05$) was chosen.

3. Kinetic modelling

Reaction rate constants (k) of the BPA degradation were obtained by a first order kinetic model (Eqs. (13)–(17)). The model is based on the mass action law by Guldberg and Waage [50], stating that the chemical reaction rates (R) are proportional to the masses of the reactants, which mathematically results in Eq. (12) [51]:

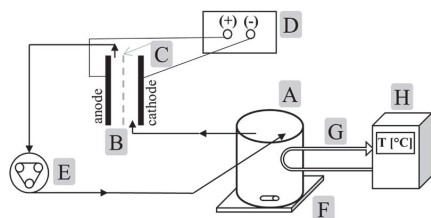


Fig. 1. Experimental set-up used; A: Tank, B: electrolytical cell, C: turbulence enhancing mesh, D: potentiostat, E: peristaltic pump, F: magnetic stirrer plate, G: cooling coil, H: chiller.

Table 1
Overview of factorial design.

Factor	Low level value (-)	High level value (+)
A: Temperature [°C]	6	20
B: Anode material	Pt	BDD
C: pH	7	10

$$R_A = -\frac{dC_A}{dt} = k^*(C_A)^{p^*}(C_B)^{q^*}(C_C)^r \quad (12)$$

R_A : reaction rate C: concentration of reactants, k: reaction rate constant, t: time, A-C: stoichiometric constants, p-r: reaction order

The formation of CHCl_3 involves the reaction between HClO/ClO^- and unknown, not measured intermediate products of BPA. The percentage of the formed HClO/ClO^- that is incorporated into CHCl_3 is very small, i.e. the concentrations measured of CHCl_3 and HClO/ClO^- differed by a factor of 10^3 [M]. For modelling purposes, it was therefore assumed that the HClO/ClO^- concentration remains constant. The model for BPA degradation and the formation of BPA is given in Eqs. (13) & (14):

$$\frac{d[\text{BPA}]}{dt} = -(k_{\text{BPA}} + k_{\text{CHCl}_3})^*[\text{BPA}] \quad (13)$$

$$\frac{d[\text{CHCl}_3]}{dt} = k_{\text{CHCl}_3}^*(1 - [\text{BPA}] - [\text{CHCl}_3]) - k_{(\text{deg})\text{CHCl}_3}^*[\text{CHCl}_3] \quad (14)$$

BPA: Bisphenol A; CHCl_3 : Trichloromethane

The conversion of Cl^- and the formation of HClO/ClO^- and ClO_4^- were modelled with Eq. (15)–(17). The oxidation pathway of chloride (Eqs. (5)–(10)) is underlying the model for the formation of free chlorine and perchlorate.

$$\frac{d[\text{Cl}^-]}{dt} = -(k_{\text{Cl}^-} + k_{\text{HClO}/\text{ClO}^-})^*[\text{Cl}^-] \quad (15)$$

$$\frac{d[\text{HClO}/\text{ClO}^-]}{dt} = k_{\text{HClO}/\text{ClO}^-}^*[\text{Cl}^-] - k_{(\text{deg})\text{HClO}/\text{ClO}^-}^*[\text{HClO}/\text{ClO}^-] \quad (16)$$

$$\frac{d[\text{ClO}_4^-]}{dt} = k_{\text{ClO}_4^-}^*[\text{HClO}/\text{ClO}^-] - k_{(\text{deg})\text{ClO}_4^-}^*[\text{ClO}_4^-] \quad (17)$$

Cl^- : Chloride; HClO/ClO^- : free chlorine; ClO_4^- : perchlorate

A nonlinear regression was performed to fit the model to the experimental data using the least square method (RStudio, USA) and the rate constants as the fitting parameters. The mean squared error (MSE) was chosen as the parameter to measure the goodness of fit of the nonlinear regression model to the experimental data [52].

4. Results & discussion

4.1. Factorial effects on Bisphenol A degradation

The statistical approach of a full factorial design was chosen to evaluate the effects and interaction effects of the three factors (A, B and C) presented in Table 1 on the EO of BPA. The response (Y_1 – Y_3) was measured using the corresponding normalized first order apparent rate constant of the BPA degradation (k_{BPA}) of each individual experiment (Table 2), which were calculated using the kinetic model (Eqs. (13) & (14)). The obtained values for each factor level combination are summarized in Table 2.

An experiment had a duration of 4 h and in all cases the concentration of BPA was below the method detection limit of 5.0 nM at the end of the experiment (SI:1, SI:6). The Pareto plot (SI:2) showed that one-way, two-way and three-way interactions all have a significant effect on the BPA degradation since the effects are all larger than the reference line. The value of the reference line was obtained from Student's t-distribution and corresponded to $t_{\alpha/2,df} = 2.31$ for the chosen significance level α of 5 % and 7 degrees of freedom (df). From

the Pareto plot, it can be further seen that the pH (factor C) has the largest effect on the BPA degradation followed by temperature (factor A), and the anode material (factor B). The interaction factor AB of temperature and anode material has the largest effect among the two-way interaction effects. This means that the performance of the anode material also depends on the applied temperature, whereby the performance is measured as the degradation rate of BPA (k_{BPA}). For instance, on BDD electrodes k_{BPA} is faster than on Pt electrodes, yet the BPA degradation on BDD electrodes decreases when 6 °C instead of 20 °C are applied, thus k_{BPA} also depends on the applied temperature. The interaction effect of BC, anode material and pH as well as AC, temperature and pH, almost exhibit the same effect magnitude. ABC, the three-way interaction effect of temperature, anode material and pH exhibits the least effect on the BPA degradation. Since all main effects and higher order interaction effects were found to be significant, they all have to be included in the linear regression model. The relationship between the response Y_1 (k_{BPA}) and the 3 factors, temperature (A), anode material (B) and pH (C) is thus given in the following linear regression equation:

$$k_{\text{BPA}} = 0.0338 - 0.0061 A - 0.0093 B + 0.0018 C - 0.0031 AB + 0.0010 AC - 0.0001 BC + 0.0006 ABC \quad (18)$$

The goodness of fit for the linear regression model was examined by using the residual plots (SI:3). The normal probability plot showed that the residuals are normally distributed, and no outliers were detected. Evaluation of the residual versus fit plot, shows that the residuals have a constant variance and the residual versus order plot showed no correlation among the residuals. These findings allow to conclude that the estimated coefficients (b_0 – b_7) can be determined with the least square regression model represented in Eq. (18), with a coefficient of determination R_{adj}^2 of 96.11 %. The adjusted R^2 was chosen to describe the fit of the model because it adjusts the model for the numbers of predictors in the model and thus avoids that the model fit increases by simply adding more predictors to the model. Finally, this leads to the conclusion that the null hypothesis (H_0), which stated that no effect significantly affects the BPA degradation (k_{BPA}), is rejected with the probability of less than 5 % of a wrongful rejection (Type 1 error). Consequently, the alternative hypothesis H_1 is accepted, which stated that at least one effect is significant.

Fig. 2 depicts the interval plots of the 3 response variables, k_{BPA} , k_{CHCl_3} and $k_{\text{ClO}_4^-}$. The x-axis shows the three different factors, which are grouped such that the mean response for every factor combination is depicted as well as the standard error of the mean, when duplicate measurements were made. It can be seen from Fig. 2a, that the best performance in terms of BPA degradation was found with the factor combination 20 °C/BDD/pH10 (green upwards pointing triangle, run 3 and 13). The average k_{BPA} of both replicates corresponds to 0.1845 [1/min], which is a factor 3.6 faster than for the lowest k_{BPA} obtained (0.0506 [1/min]) at 6 °C/BDD/pH7 (red, downwards pointing triangle, run 1 and 6) (Fig. 2a). A pH of 10 and warmer temperatures of 20 °C are thus favorable over 6 °C and pH 7. However, the anode material for both, the slowest and fastest BPA degradation was BDD. This observation is against the initial assumption that chemisorbed hydroxyl radicals formed on Pt anodes, which are less freely available and which therefore result in less oxidative power than the physisorbed hydroxyl radicals formed on BDD anodes [16]. In addition, bulk homogeneous chemical reactions, such as reactions with free chlorine typically are more influenced by changes in temperature than surface electrochemical reactions. Therefore, it was anticipated that Pt, which is assumed more dependent on free chlorine mediated oxidation to be more influenced by the change in temperature than BDD. Consequently, it was expected that Pt anodes would be involved in the factor level combination that leads to the least favorable degradation kinetics of BPA. This observation allows concluding that the anode material for the slowest scenario factor combination is outcompeted by the other two tested factors (temperature and pH) in terms of effect on the

Table 2Experimental design matrix of all factor (X_i) level combinations and observed response factors (Y_i).

Run order	A Temperature	B Anode material	C pH	Y_1 k_{BPA} 10^{-3} [1/min]	Y_2 k_{HClO_3} 10^{-3} [1/min]	Y_3 $k_{ClO_4^-}$ 10^{-3} [1/min]
1	-	+	-	55.4	0.15	13.5
2	-	-	-	48.2	0.59	0.6
3	+	+	+	175.0	0.62	N/A
4	-	-	+	71.2	0.70	1.0
5	+	+	-	76.6	0.55	N/A
6	-	+	-	45.7	0.20	N/A
7	-	-	-	60.2	0.30	N/A
8	-	-	+	62.1	0.56	N/A
9	+	-	+	80.4	0.91	N/A
10	-	+	+	95.0	0.44	18.2
11	+	+	-	85.8	0.71	17.0
12	+	-	-	50.5	0.77	0.7
13	+	+	+	193.9	0.76	18.8
14	+	-	-	53.1	0.91	N/A
15	-	+	+	75.9	0.33	N/A
16	+	-	+	82.2	0.72	0.8

degradation kinetic (k_{BPA}). However, for the remaining factor combinations, the mean k_{BPA} was always higher when a BDD anode was used instead of the Pt anode (Fig. 2a), which supports the initial assumption of BDD anodes contributing to a faster k_{BPA} .

BPA has a dissociation constant of $pK_a = 9.6$, hence at pH 10, the BPA is present in the form of bisphenolate anion [43] and the free chlorine is present as a 100 % ClO^- . On the other hand, at pH 7, BPA is present in its protonated form and free chlorine is prevailing in the form of $HClO$ (77.2 %) yet ClO^- is still present (22.8 %). As it was hypothesized based on the results from Deborde et al. [53], ClO^- shows to be the stronger oxidant for BPA than $HClO$. These findings are also confirmed by Li et al. [19] where they state that in alkaline solution (pH 11) the ClO^- exhibited higher reactivity with the phenolic group of BPA than $HClO$ in acidic conditions (pH 3), which the authors attributed to the negative electron activity of the phenolic group. However, Gallard et al. [38] observed the maximum apparent first order rate constant of BPA chlorination between pH 8 and 9 with a decrease after pH 9 and attributed it to the low reactivity of ClO^- . They furthermore state that the increase of the apparent rate constant with increasing the pH up to pH 9 is solely due to the ionized form of BPA and its reaction with $HClO$. Furthermore, Cominellis et al. [54] observed a higher electrochemical oxidation index (EOI) in alkaline media (pH 12–13) for phenol and attributed this to the fact that the deprotonated form of phenol (phenolate ion) is more reactive towards the electrophilic attack of hydroxyl radicals on the aromatic ring. The EOI is the average current efficiency and a measure of the efficiency of the EO on phenol or any other organic compound [54]. In conclusion, a high pH is favoring faster degradation kinetics of BPA by means of intermediate oxidation via the more reactive ClO^- free chlorine species and by facilitating the electrophilic attack of the deprotonated BPA.

Looking at the effect of the temperature, the hypothesis that the degradation kinetics of BPA is slower at 6 °C than at 20 °C could be

confirmed. These findings were anticipated based on Arrhenius's law, which describes the temperature dependence of chemical reaction rates (k), whereby lower temperatures result in lower reaction rates. Nonetheless, even at 6 °C the removal of BPA below LOD (5.0 nM) was still reached in less than 60 min with a total experimental time of 4 h. An average treatment time for 90 % removal of 29 min was observed, varying from 12 – 42 min (71 %) for 20 °C/BDD/pH10 and 6 °C/Pt/pH7 respectively. This suggests, that even at low temperature of 6 °C the EO of BPA is still a suitable process for the removal of the model organic compound BPA. Thus, the applicability of EO in climate regions where cold temperatures prevail is feasible in terms of degradation goals. However, one has to keep in mind that the treatment time will have to be longer at lower temperatures as Fig. 3a depicts when looking at the time where complete degradation of BPA was achieved. As a consequence, the energy consumption and thus the costs of the treatment will be higher for EO treatment at lower temperatures, posing a disadvantage of the EO process in cold climate regions. Specific energy consumption (E_{sp}) to remove the initial BPA concentration to 90 % showed that the average E_{sp} at 20 °C is 21 % lower than at 6 °C with 2302 kW h/kgO₂ and 2920 kW h/kgO₂ respectively, given in equivalent oxygen consumption for full BPA mineralization. E_{sp} was calculated according to Eq. (19) [55] and based on the calculated theoretical oxygen demand for BPA, which equals 2.52 mgO₂/mg BPA [16].

$$E_{sp} = \frac{E_{cell} * I * \Delta t}{V * \Delta COD} \quad (19)$$

When looking at the extreme cases for both 20 and 6 °C the E_{sp} difference is 46 % with 1788 kW h/kgO₂ (20 °C/BDD/pH10) and 3291 kW h/kgO₂ (6 °C/BDD/pH7) respectively. On the other hand, the electrodes in this study were cooled and the solution temperature was willingly kept stable at 6 °C, but under more applied conditions the solution temperature would most likely rise due to heat production within the

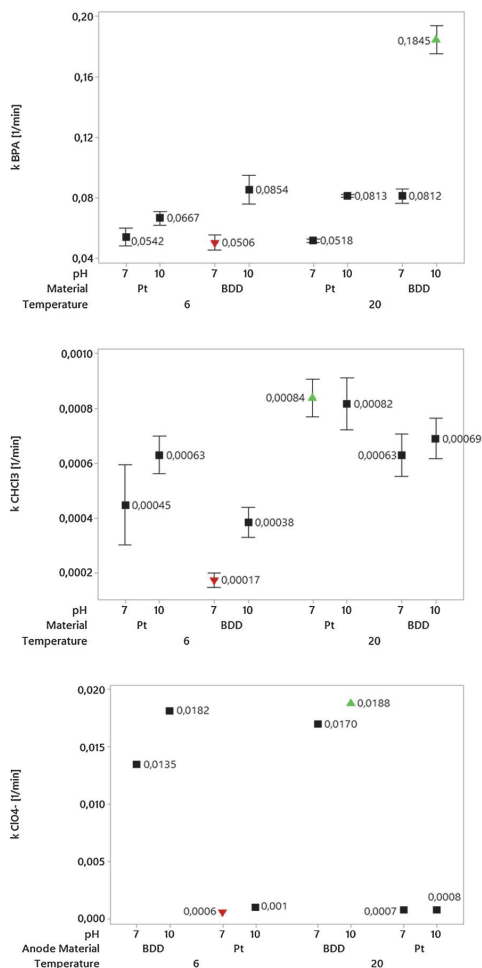


Fig. 2. Interval plots with 1 standard error for response factors for a) BPA, b) CHCl_3 and c) ClO_4^- .

electrolytical cell, which in turn would warm up the recirculated aqueous solution and thus accelerate the degradation kinetics. No reported case of a multiple single passes pilot plant could be found in literature, but it is assumed that the solution temperature would increase less compared to a batch mode. It is therefore of interest to further investigate the role of cold temperatures on the performance of EO under more applied conditions.

4.2. Formation of hazardous disinfection by-products

4.2.1. Trichloromethane

To statistically evaluate the influence of the factors and factor interaction given in Table 1 on the production of CHCl_3 , the same statistical assumptions as for BPA degradation were made. As the response factor (Y_2), the first order kinetic rate constant of CHCl_3 formation, k_{CHCl_3} [1/min] was chosen. k_{CHCl_3} was obtained by solving the differential equation system given in Eqs. (13) & (14) and by nonlinear fitting of the model to the data by means of the least square method. In addition, a time lag was built into the model due to the lack of measurements and thus missing information of BPA intermediates, which

are precursors of CHCl_3 . The time lag was specifically adjusted for every experiment such that the standard error between the data and model was minimized. Fig. 4a depicts a typical lag for the formation of CHCl_3 for 20 °C/BDD/pH7.

CHCl_3 was formed during all experiments, i.e. for each factor combination, but differed in the formation rate and thus in the maximum observed concentrations and the final concentrations (SI:5, SI:7). BPA was in all cases not detectible anymore after 60 min, but CHCl_3 production continued over the experimental time of 4 h. This indicates that CHCl_3 is formed from intermediate BPA products, which were not measured in this study. The concentration of CHCl_3 was normalized by the corresponding initial BPA concentration. The Pareto plot (SI:2) for the effects and interaction effects shows that only factor A (temperature) and factor B (anode material) are significantly affecting the response factor k_{CHCl_3} . Factor C (pH) and all factor combinations have no significant effect on k_{CHCl_3} . The corresponding linear regression model, which describes the response factor k_{CHCl_3} , is given in Eq. (20):

$$k_{\text{CHCl}_3} = 0.000265 + 0.000024A - 0.000107B \quad (20)$$

The goodness of fit of the linear regression model was again measured by looking at the residual plots (SI:3). It was confirmed that the parameters (b_0 - b_2) of the significant factors can be estimated by the least square regression model presented in Eq. (20) with a coefficient of determination R^2_{adj} of 72.18 %.

The temperature had the largest effect on the formation of CHCl_3 . At 6 °C the average k_{CHCl_3} was 0.00041 [1/min] compared to 0.00074 [1/min] at 20 °C, meaning that the reaction kinetics were on average 45 % faster at higher temperature. For the extreme events (20 °C/Pt/pH7) and (6 °C/BDD/pH7) k_{CHCl_3} even differs by 79 % (Fig. 3b). This observation comes to no surprise as the CHCl_3 formation depends on the degradation of BPA, which was highly affected by temperature and consequently temperature affects the CHCl_3 formation in the same way.

The anode material is the second factor (B), which significantly affects k_{CHCl_3} during the EO of BPA. This can be seen in Fig. 3b, which depicts the fastest and slowest formation of CHCl_3 along with the data from the respective other anode material. On average, CHCl_3 formations were 21 % faster on Pt than on BDD anodes. Interestingly, peak concentrations during the 4 h experiments were on average higher on BDD anodes than on Pt anodes, with 16.2 and 12.5 $\mu\text{g/L}$ respectively (SI:4). Thus, a CHCl_3 concentration plateau or subsequent degradation was reached faster, when a Pt anode was used, while a higher concentration was reached at slower rates on BDD. Even though k_{CHCl_3} was faster on Pt anode, Pt remains the favorable choice of anode material due to a lower final CHCl_3 concentration regarding the hazardous impact of CHCl_3 on the aquatic environment. Jasper et al. [56] report results contrary to this study, stating that peak CHCl_3 concentrations were reached faster on the non-active BDD than on the active $\text{TiO}_2/\text{IrO}_2$ anode. They attributed their findings to the fast mineralization of CHCl_3 precursors on the BDD anode. They further observed a complete degradation of CHCl_3 during the course of the experiments (12 h), which was not observed in this study due to the shorter duration of experiments (4 h).

In this study, the effect of the pH on the formation of CHCl_3 was not found to be statistically significant but other studies state the opposite. Deborde et al. [53] observed that the reaction rate of BPA with HClO/ClO^- to form disinfection by-products such as CHCl_3 or chloramines is higher at a $\text{pH} \geq 8$ than at $\text{pH} \leq 7$ with 10^2 [M/s] and $10^{1.75}$ [M/s] respectively and corresponds to a difference of a factor 1.78. In this study, the mean k_{CHCl_3} value for experiments at pH 10 is 0.00063 [1/min] and 0.00052 [1/min] for experiments at pH 7, which differs by a factor 1.2, whereby the mean value is based on all experiments at different anode materials and temperatures, which may explain the observed difference. Even though the pH does not significantly affect the formation of CHCl_3 , the reason for a faster k_{CHCl_3} at pH 10 than at pH 7 is similar to the one for BPA. ClO^- , which is the prevailing form of free chlorine at pH 10 is considered more reactive towards phenolic

compounds than HClO, prevailing at pH 7 [53]. This means that not only is the degradation of BPA faster at pH 10 but consequently also the formation of CHCl_3 , which is a product of BPA intermediates and free chlorine. Additionally, the fact that BPA is more prone to electrophilic attack when present in its deprotonated form at higher pH is also contributing to a faster k_{CHCl_3} and enhances the effect of ClO_2^- .

When comparing the degradation of BPA and the formation of CHCl_3 it has to be kept in mind that BPA is depleted within 60 min to below the detection limit in most of the factor combinations. Consequently, the EO of BPA under applied conditions would not continue beyond this time. Thus, the formation of CHCl_3 would stop before higher concentration can develop. The maximum observed CHCl_3 concentration during the experimental time of 4 h was 19.7 ppb ($20^\circ\text{C}/\text{BDD}/\text{pH}10$). US EPA proposes a relevant standard for THMs in drinking water of 100 ppb [57]. In the case of this study, no bromated THMs were observed because no bromide was added to the aqueous solution. CHCl_3 was below the proposed standard of 100 ppb at all times.

4.2.2. Perchlorate formation

The statistical analysis of the effects of the factors and factor interactions given in Table 1 were done by means of a full factorial design but without replicates since the analytical measurement of ClO_4^- was very time consuming ($> 1\text{ h/sample}$) and thus a replicate analysis was economically not feasible. Besides no replicates, the analysis was the same as for the replicated experiments but Lenth's method was used to calculate the unstandardized effects as the standardized effects cannot be calculated when no replicates are used [58]. The 3-way interaction effect (ABC) was excluded from the analysis since otherwise the degree of freedom for error equals zero due to the lack of replicated experiments. The first order kinetic rate constant $k_{\text{ClO}_4^-}$ [1/min] for ClO_4^- formation was chosen as response factor (Y_3). $k_{\text{ClO}_4^-}$ was estimated by solving the differential equation system (Eqs. (15)–(17)) whereby concentrations were normalized by the initial chloride ion (Cl^-) concentration (SI:8). Fig. 4b shows the model output for the formation of ClO_4^- for the parameter settings $20^\circ\text{C}/\text{BDD}/\text{pH}7$. The model fit for HClO is lower compared to the fit for Cl^- and ClO_4^- due to the lack of measurement of products other than ClO_4^- that are formed from HClO. A poorer fit is reflected in a higher standard error (SE) which is 0.003 for HClO and 0.0003 for both Cl^- and ClO_4^- . The Pareto plot (SI:2) clearly shows that among all the tested factors and factor interactions only factor B (anode material) has a significant effect on $k_{\text{ClO}_4^-}$. The linear regression for the response factor $k_{\text{ClO}_4^-}$ is described in Eq. (21):

$$k_{\text{ClO}_4^-} = 0.00883 + 0.00806 B \quad (21)$$

The goodness of fit of the linear regression model was again estimated with the residual plots (SI:3) of $k_{\text{ClO}_4^-}$. The parameters (b0-b1) can be estimated by the least square regression model presented in Eq. (20) with a coefficient of determination R_{adj}^2 of 96.3 %.

Perchlorate was detected ($\text{LOD} = 0.094\text{ mg/L}$) during all experiments whether a BDD or Pt anode was used. Other studies confirm that ClO_4^- is formed during EO where Cl^- or ClO_3^- is involved as an electrolyte [59,60]. On BDD anode, $k_{\text{ClO}_4^-}$ was 95.4 % faster than on Pt, with a respective average $k_{\text{ClO}_4^-}$ of 0.0169 [1/min] and 0.0008 [1/min]. The data underlying the fastest and slowest $k_{\text{ClO}_4^-}$ is depicted in Fig. 3c, together with the experiments on the respective other anode material and illustrates the influence of the anode material on the ClO_4^- formation. The maximum ClO_4^- concentration on BDD anode was 90.4 mg/L and 10.4 mg/L on Pt, resulting in a difference of 89 %. Bergmann et al. [21] observed similar results using rotating disc electrodes whereby they observed 98 % more ClO_4^- and a final concentrations of 123 ppm and 2.35 ppb for BDD and Pt respectively. Polcaro et al. [59] could only find traces of ClO_4^- when an active anode (Ti/RuO₂) was used, but found considerable amount of ClO_4^- when they used a BDD anode. Azizi et al. [60] proposed a reaction mechanism for the formation of ClO_4^- from ClO_3^- on BDD anodes. They suggest that on

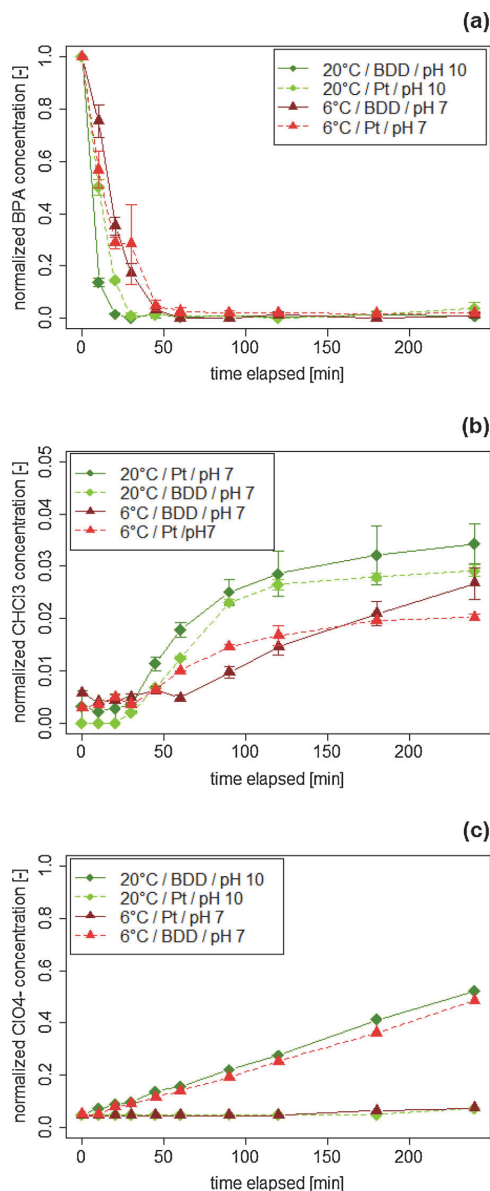


Fig. 3. Degradation of BPA (a); formation of CHCl_3 (b); formation of ClO_4^- (c) for the factor level combinations resulting in the fastest (dark green diamond, solid line) and slowest (dark red triangle, solid line) reaction rates. Corresponding data on the other anode material is also depicted for the fastest (light green diamond, dashed line) and for the slowest (light red triangle, dashed line) kinetics for comparison reason. (For interpretation of the references to colour in this figure legend, the reader is referred to the web version of this article).

BDD anodes, ClO_4^- can be formed by oxidation of ClO_3^- via the formation of ClO_3^{\cdot} from direct electron transfer at the anode surface followed by the reaction with hydroxyl radicals ($\cdot\text{OH}$) to form ClO_4^- . Jung et al. [61] confirmed the formation of ClO_4^- during electrolysis using a Ti/Pt anode. They found concentrations of ClO_4^- up to 4 mg/L with an

initial Cl^- concentration of 30 mg/L and a corresponding electrolysis time of 40 min. Their results are comparable to the ones in this study with a final ClO_4^- concentration of 10.4 mg/L on Pt anode, an initial Cl^- concentration of 45 mg/L and an electrolysis time of 240 min. Jung et al. and Azizi et al. [60,61] propose the same reaction mechanisms for the formation of ClO_4^- from ClO_3^- . However, due to the active nature of Pt anodes, the ClO_3^- and the $\cdot\text{OH}$ are chemisorbed on the anode surface, which in theory makes them less freely available [16] and thus lower oxidation rates of ClO_3^- to ClO_4^- are expected with the Pt anode. The findings of this study are in agreement with literature and confirm that the use of BDD anodes leads to the production of fairly high concentrations of the unwanted disinfection by-product ClO_4^- . In fact, all the measured ClO_4^- concentrations in this study are well above the suggested maximum contaminant level (US EPA) of 56 ppb for drinking water. One has to keep in mind that EO of BPA in this study is intended to remove organic pollutants from wastewater and not drinking water and thus, as the effluent is usually discharged to a water body, remaining ClO_4^- would be diluted many times. This suggests that even though ClO_4^- is formed, it can be limited and controlled by the right choice of electrodes and treatment time. Hence, EO for chloride containing wastewaters can still be a feasible treatment to remove organic pollutants like BPA.

5. Conclusions

- All 3 tested factors, temperature, anode material and pH as well as their higher order interactions have a statistically significant effect on the degradation of Bisphenol A during electrochemical oxidation.
- The pH was found to have the highest effect on the electrochemical removal of Bisphenol A, whereby a pH 10 is favorable over pH 7. This is attributed to the higher oxidation power of hypochlorite (ClO^-) species prevailing at pH 10 and the fact that deprotonated Bisphenol A at pH 10 is more prone to electrophilic attack on the aromatic ring than the protonated form at pH 7.
- Decreasing the temperature of the solution to 6 °C to mimic cold climate temperatures showed that Bisphenol A was still removed below the detection limit (5.0 nM) within the experimental time of 4 h. However, a considerable difference of power input of on average of 20 % was observed between 6 °C and 20 °C for 90 % Bisphenol A removal, which needs to be considered from an economical point of view.
- Further studies are suggested to evaluate the cold temperature impact on electrochemical oxidation of Bisphenol A under more applied conditions due to heat development within the electrolytical cell that may lessen the adverse impact of cold temperatures. It is further suggested to compare batch mode and single pass mode with regard to heat development in the cell and the solution.
- Temperature and anode material significantly affect Trichloromethane formation. Up to 45 % faster Trichloromethane formation rates were observed at 20 °C compared to 6 °C. Higher trichloromethane concentrations were measured when BDD anodes were used but formation rates were on average 23 % faster on Pt anodes.
- In all experiments, the final concentration of Trichloromethane stayed below 100 ppb, the standard proposed by US EPA for THMs in drinking water.
- Cold temperatures do not significantly influence the production of perchlorate and neither does the pH. Only the anode material, Pt or BDD, has a significant influence on the production of perchlorate, with Pt being the more favorable material in terms of less perchlorate production.
- Perchlorate was observed at the end of every experiment at a higher concentration than the suggested limit of US EPA of 56 ppb for drinking water with up to 90.4 ppm on BDD and up to 10.4 ppm on Pt anodes. However, the treated water is subject to dilution after discharge to the water body, which will most likely decrease the

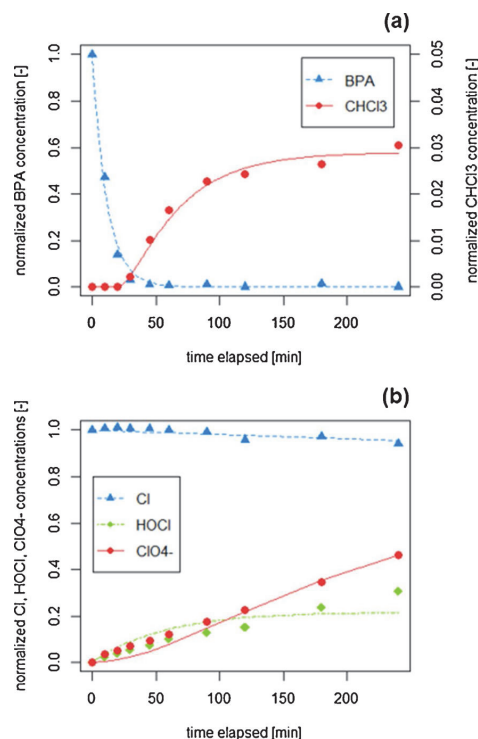


Fig. 4. Kinetic model output for 20 °C/BDD/pH7 (experiment 11); model: line, data points: experimental data; a) BPA and CHCl_3 with a delay for CHCl_3 ; b) Cl^- , HOCl and ClO_4^- .

perchlorate concentration below the limit of 56 ppb.

- The present study shows that the application of EO for organic pollutant removal in regions with low average temperatures is a feasible treatment step but the choice of electrode material, solution pH and treatment time needs to be carefully considered.

CRedit authorship contribution statement

Noëmi Ambauen: Writing - original draft, Writing - review & editing, Project administration, Investigation, Conceptualization, Methodology, Visualization. **Jens Muff:** Supervision, Writing - review & editing. **Franz Tscheikner-Gratl:** Data curation, Software, Formal analysis, Writing - review & editing, Methodology. **Thuat T. Trinh:** Software, Formal analysis. **Cynthia Hallé:** Supervision, Writing - review & editing, Methodology. **Thomas Meyn:** Supervision, Conceptualization, Methodology, Project administration, Funding acquisition.

Declaration of Competing Interest

The authors declare that they have no known competing financial interests or personal relationships that could have appeared to influence the work reported in this paper.

Acknowledgements

This work was supported by the Norwegian University of Science and Technology, Trondheim, Norway; and the Søndre Helgeland Miljøverk IKS, Åremma, Norway. The authors like to thank Trine

Hårberg Ness, Kåre Andre Kristiansen, Zdenka Bartosova and Susana Villa Gonzalez for their invaluable support in the laboratory.

Appendix A. Supplementary data

Supplementary material related to this article can be found in the online version, at doi:<https://doi.org/10.1016/j.jece.2020.104183>.

References

- [1] L.N. Vandenberg, R. Hauser, M. Marcus, N. Olea, W.V. Welshons, Human exposure to bisphenol A (BPA) $\&$, *Reprod. Toxicol.* 24 (2007) 139–177, <https://doi.org/10.1016/j.reprotox.2007.07.010>.
- [2] T. Deblonde, C. Cossu-Leguille, P. Hartemann, International Journal of Hygiene and emerging pollutants in wastewater : a review of the literature, *Int. J. Hyg. Environ. Health* 214 (2015) 442–448, <https://doi.org/10.1016/j.ijheh.2011.08.002>.
- [3] B.S. Rubin, A. Bisphenol, An endocrine disruptor with widespread exposure and multiple effects, *J. Steroid Biochem. Mol. Biol.* 127 (2011) 27–34, <https://doi.org/10.1016/j.jsbmb.2011.05.002>.
- [4] (EFSA) European Food Safety Authority, Scientific Opinion on the risks to public health related to the presence of bisphenol A (BPA) in foodstuffs : Executive summary 1 EFSA Panel on Food Contact Materials, Enzymes, Flavourings and Processing Aids 13 (2015), <https://doi.org/10.2903/j.efsa.2015.3978>.
- [5] M.K. Björnström, J. de Boer, A. Ballesteros-Gomez, Chemosphere Bisphenol A and replacements in thermal paper : A review 182 (2017), <https://doi.org/10.1016/j.chemosphere.2017.05.070>.
- [6] J.C. Gould, L.S. Leonard, S.C. Maness, B.L. Wagner, K. Conner, T. Zacharewski, S. Safe, D.P. McDonnell, K.W. Gaido, Bisphenol A interacts with the estrogen receptor h in a distinct manner from estradiol, *Mol. Cell. Endocrinol.* 142 (1998) 203–214.
- [7] ECHA European chemicals agency, Inclusion of substances of very high concern in the Candidate List for eventual inclusion in Annex XIV (Decision of the European Chemicals Agency) 1 (2018) 1–6.
- [8] Council of the European Union, Proposal for a DIRECTIVE OF THE EUROPEAN PARLIAMENT AND OF THE COUNCIL on the Quality of Water Intended for Human Consumption (recast), (2018) 2018.
- [9] J. Michałowicz, Bisphenol A - Sources, toxicity and biotransformation, *Environ. Toxicol. Pharmacol.* 37 (2014) 738–758, <https://doi.org/10.1016/j.etap.2014.02.003>.
- [10] R. Andreozzi, V. Caprio, A. Insola, R. Marotta, Advanced oxidation processes (AOP) for water purification and recovery, *Catal.* Today 53 (1999) 51–59, [https://doi.org/10.1016/S0920-5861\(99\)00102-9](https://doi.org/10.1016/S0920-5861(99)00102-9).
- [11] B. Acedo, F.J. Beltr, F.J. Rivas, Mineralization of Bisphenol a by Advanced, (2009), pp. 589–594, <https://doi.org/10.1002/jctb.2085>.
- [12] M. Umar, F. Roddick, L. Fan, H. Abdul, Chemosphere Application of ozone for the removal of bisphenol A from water and wastewater – a review, *Chemosphere*. 90 (2013) 2197–2207, <https://doi.org/10.1016/j.chemosphere.2012.09.090>.
- [13] N. Oturan, E.D. Van Hullebusch, H. Zhang, L. Mazza, H. Budzinski, K. Le Menach, M.A. Oturan, Occurrence and removal of organic micropollutants in landfill leachates treated by electrochemical advanced oxidation processes, *Environ. Sci. Technol.* 49 (2015) 12187–12196, <https://doi.org/10.1021/acs.est.5b02809>.
- [14] T. Li, X. Li, J. Chen, G. Zhang, H. Wang, Treatment of Landfill Leachate by Electrochemical Oxidation and Anaerobic Process, 79 (n.d.), doi:10.2175/106143006X115435.
- [15] S. Fudala-Ksiażek, M. Sobaszek, A. Luczkiewicz, A. Pieczynska, A. Ofiarska, A. Fiszka-Borzyżkowska, M. Sawczak, M. Fieck, R. Bogdanowicz, E.M. Siedlecka, Influence of the boron doping level on the electrochemical oxidation of raw landfill leachates: advanced pre-treatment prior to the biological nitrogen removal, *Chem. Eng. J.* 334 (2018) 1074–1084, <https://doi.org/10.1016/j.cej.2017.09.196>.
- [16] C. Cominellis, G. Chen, *Electrochemistry for the Environment*, Springer-Verlag, New York, 2010, <https://doi.org/10.1007/978-0-387-68318-8>.
- [17] M. Murugananthan, S. Yoshihara, T. Rakuma, T. Shirakashi, Mineralization of bisphenol A (BPA) by anodic oxidation with boron-doped diamond (BDD) electrode, *J. Hazard. Mater.* 154 (2008) 213–220, <https://doi.org/10.1016/J.JHAZMAT.2007.10.011>.
- [18] Y. Cui, X. Li, G. Chen, Electrochemical degradation of bisphenol A on different anodes, *Water Res.* 43 (2009) 1968–1976, <https://doi.org/10.1016/J.WATRES.2009.01.026>.
- [19] H. Li, Y. Long, X. Zhu, Y. Tian, J. Ye, Influencing factors and chlorinated byproducts in electrochemical oxidation of bisphenol A with boron-doped diamond anodes, *Electrochim. Acta* 246 (2017) 1121–1130, <https://doi.org/10.1016/j.electacta.2017.06.163>.
- [20] G.V. Korshin, J. Kim, L. Gan, Comparative study of reactions of endocrine disruptors bisphenol A and diethylstilbestrol in electrochemical treatment and chlorination, *Water Res.* 40 (2006) 1070–1078, <https://doi.org/10.1016/j.watres.2006.01.003>.
- [21] M.E.H. Bergmann, J. Rollin, T. Iourchouk, The occurrence of perchlorate during drinking water electrolysis using BDD anodes, *Electrochim. Acta* 54 (2009) 2102–2107, <https://doi.org/10.1016/j.electacta.2008.09.040>.
- [22] J.W. Park, J. Rinchard, F. Liu, T.A. Anderson, R.J. Kendall, C.W. Theodorakis, The thyroid endocrine disruptor perchlorate affects reproduction, growth, and survival of mosquitofish, *Ecotoxicol. Environ. Saf.* 63 (2006) 343–352, <https://doi.org/10.1016/j.ecoenv.2005.04.002>.
- [23] US EPA, Perchlorate in drinking water, (n.d.), <https://www.epa.gov/>
- [24] dwstandardsregulations/perchlorate-drinking-water-frequent-questions.
- [25] US EPA, ENVIRONMENTAL PROTECTION AGENCY - National Primary Drinking Water Regulations: Proposed Perchlorate Rule, Pre-publication Version, (2019) https://www.epa.gov/sites/production/files/2019-05/documents/prepub_final_version_npdrw_proposed_perchlorate_rule-508.pdf.
- [26] A. Boscolo Boschetto, F. Gottardi, L. Milan, P. Pannocchia, V. Tartari, M. Tavan, R. Amadelli, A. De Battisti, A. Barbieri, D. Patracchini, G. Battaglin, Electrochemical treatment of bisphenol-A containing wastewaters, *J. Appl. Electrochem.* 24 (1994) 1052–1058, <https://doi.org/10.1007/BF00241198>.
- [27] H. Kuramitz, M. Matsushita, S. Tanaka, Electrochemical removal of bisphenol A based on the anodic polymerization using a column type carbon fiber electrode, *Water Res.* 38 (2004) 2331–2338, <https://doi.org/10.1016/j.watres.2004.02.023>.
- [28] Z.H. Mussa, F.F. Al-Qaim, M.R. Othman, M.P. Abdullah, Removal of simvastatin from aqueous solution by electrochemical process using graphite-PVC as anode: a case study of evaluation the toxicity, kinetics and chlorinated by-products, *J. Environ. Chem. Eng.* 4 (2016) 3338–3347, <https://doi.org/10.1016/j.jece.2016.07.006>.
- [29] C.A. Martínez-Huitle, S. Ferro, Electrochemical oxidation of organic pollutants for the wastewater treatment: direct and indirect processes, *Chem. Soc. Rev.* 35 (2006) 1324–1340, <https://doi.org/10.1039/B517632H>.
- [30] P. Mandal, B.K. Dubej, A.K. Gupta, Review on landfill leachate treatment by electrochemical oxidation: drawbacks, challenges and future scope, *Waste Manag.* 69 (2017) 250–273, <https://doi.org/10.1016/j.wasman.2017.08.034>.
- [31] G.F. Pereira, R.C. Rocha-Filho, N. Bocchi, S.R. Biaggio, Electrochemical degradation of bisphenol A using a flow reactor with a boron-doped diamond anode, *Chem. Eng. J.* 198–199 (2012) 282–288, <https://doi.org/10.1016/j.cej.2012.05.057>.
- [32] E. Turro, A. Giannis, R. Cossu, E. Gidaralos, D. Mantzavinos, A. Katsounis, Reprint of: electrochemical oxidation of stabilized landfill leachate on DSA electrodes, *J. Hazard. Mater.* 207–208 (2012) 73–78, <https://doi.org/10.1016/j.jhazmat.2012.01.083>.
- [33] M. Panizza, M. Delucchi, I. Sirés, Electrochemical process for the treatment of landfill leachate, *J. Appl. Electrochem.* 40 (2010) 1721–1727, <https://doi.org/10.1007/s10800-010-0109-7>.
- [34] B. Darsinou, Z. Frontists, M. Antonopoulou, I. Konstantinou, D. Mantzavinos, Sono-activated persulfate oxidation of bisphenol A: kinetics, pathways and the controversial role of temperature, *Chem. Eng. J.* 280 (2015) 623–633, <https://doi.org/10.1016/j.cej.2015.06.061>.
- [35] Á. Anglada, A.M. Urtiaga, I. Ortiz, Laboratory and pilot plant scale study on the electrochemical oxidation of landfill leachate, *J. Hazard. Mater.* 181 (2010) 729–735, <https://doi.org/10.1016/j.jhazmat.2010.05.073>.
- [36] R.H. Kettunen, T.H. Hoiljoki, J.A. Rintala, Anaerobic and sequential anaerobic-aerobic treatments of municipal landfill leachate at low temperatures, *Bioresour. Technol.* 58 (1996) 31–40, [https://doi.org/10.1016/S0960-8524\(96\)00102-2](https://doi.org/10.1016/S0960-8524(96)00102-2).
- [37] A.L. Smith, S.J. Skerlos, L. Raskin, Psychrophilic anaerobic membrane bioreactor treatment of domestic wastewater, *Water Res.* 47 (2013) 1655–1665, <https://doi.org/10.1016/j.watres.2012.12.028>.
- [38] A. Kapalka, L. Joss, Á. Anglada, C. Cominellis, K.M. Udert, Direct and mediated electrochemical oxidation of ammonia on boron-doped diamond electrode, *Electrochim. Commun.* 12 (2010) 1714–1717, <https://doi.org/10.1016/J.ELECOM.2010.10.004>.
- [39] H. Gallard, A. Leclercq, J.-P. Croué, Chlorination of bisphenol A: kinetics and by-products formation, *Chemosphere*. 56 (2004) 465–473, <https://doi.org/10.1016/J.CHEMOSPHERE.2004.03.001>.
- [40] P.J. Vikesland, E.M. Fiss, K.R. Wigginton, K. Mcneil, W.A. Arnold, Halogenation of Bisphenol-A, Triclosan, and Phenols in Chlorinated Waters Containing Iodide, (2013), <https://doi.org/10.1021/es304927j>.
- [41] H. Gallard, U. von Gunten, Chlorination of phenols : kinetics and formation of chloroform, *Environ. Sci. Technol.* 36 (2002) 884–890, <https://doi.org/10.1021/es010076a>.
- [42] T. Yamamoto, A. Yasuhara, Chlorination of bisphenol A in aqueous media: formation of chlorinated bisphenol A congeners and degradation to chlorinated phenolic compounds, *Chemosphere*. 46 (2002) 1215–1223, [https://doi.org/10.1016/S0045-6535\(01\)00198-9](https://doi.org/10.1016/S0045-6535(01)00198-9).
- [43] J.C. Crittenden, R.R. Trussell, D.W. Hand, K.J. Howe, G. Tchobanoglous, *MWH's Water Treatment: Principles and Design*, John Wiley & Sons, 2012.
- [44] J. Bohdziewicz, G. Kamin, Kinetics and equilibrium of the sorption of bisphenol A by carbon nanotubes from wastewater : ska, *Water Sci. Technol.* (2013) 1306–1314, <https://doi.org/10.2166/wst.2013.373>.
- [45] M. Panizza, A. Barbucci, R. Ricotti, G. Cerisola, Electrochemical degradation of methylene blue, *Sep. Purif. Technol.* 54 (2007) 382–387, <https://doi.org/10.1016/j.seppur.2006.10.010>.
- [46] M. Murugananthan, S. Yoshihara, T. Rakuma, N. Uehara, T. Shirakashi, Electrochemical degradation of 17 β -estradiol (E2) at boron-doped diamond (Si/BDD) thin film electrode, *Electrochim. Acta* 52 (2007) 3242–3249, <https://doi.org/10.1016/j.electacta.2006.09.073>.
- [47] M.A. Quiroz, J.L. Sánchez-Salas, S. Reyna, E.R. Bandala, J.M. Peralta-Hernández, C.A. Martínez-Huitle, Degradation of 1-hydroxy-2,4-dinitrobenzene from aqueous solutions by electrochemical oxidation: role of anodic material, *J. Hazard. Mater.* 268 (2014) 6–13, <https://doi.org/10.1016/j.jhazmat.2013.12.050>.
- [48] G.F. Pereira, R.C. Rocha-Filho, N. Bocchi, S.R. Biaggio, Electrochemical degradation of bisphenol A using a flow reactor with a boron-doped diamond anode, *Chem. Eng. J.* 198–199 (2012) 282–288, <https://doi.org/10.1016/j.cej.2012.05.057>.
- [49] Anand Patankar, Qualitative and Quantitative Determination of Trihalomethanes (THMs) in Drinking Water using Selected Ion and Full Ion (SIFI™), n.d. https://www.perkinelmer.com/CMSResources/Images/20130104_4-Qualitative and Quantitative Determination of Trihalomethanes.pdf.

- [49] R. Walpole, R. Myers, S. Myers, K. Ye, *Probability & Statistics for Engineers and Scientists*, 8th ed, Pearson Education, 2010, <https://doi.org/10.2307/3315054>.
- [50] P. Érdi, J. Tóth, *Mathematical Models of Chemical Reactions - Theory and Applications of Deterministic and Stochastic Models*, Manchester University Press, 1989.
- [51] I.A. Gargurevich, Chemical reaction thermodynamics and reaction rate theory, *J. Chem. Eng. Process Technol.* 07 (2016), <https://doi.org/10.4172/2157-7048.1000287>.
- [52] N.D. Bennett, B.F.W. Croke, G. Guariso, J.H.A. Guillaume, S.H. Hamilton, A.J. Jakeman, S. Marsili-libelli, L.T.H. Newham, J.P. Norton, C. Perrin, S.A. Pierce, B. Robson, R. Seppelt, A.A. Voinov, B.D. Fath, *Environmental Modelling & Software* Characterising performance of environmental models q, *Environ. Model. Softw.* 40 (2013) 1–20, <https://doi.org/10.1016/j.envsoft.2012.09.011>.
- [53] M. Deborde, U. von Gunten, Reactions of chlorine with inorganic and organic compounds during water treatment-Kinetics and mechanisms: a critical review, *Water Res.* 42 (2008) 13–51, <https://doi.org/10.1016/j.watres.2007.07.025>.
- [54] C. Comminellis, C. Pulgarin, *Anodic oxidation of phenol for waste water treatment*, *J. Appl. Electrochem.* 21 (1991) 703–708.
- [55] J. Zou, X. Peng, M. Li, Y. Xiong, B. Wang, F. Dong, B. Wang, *Electrochemical oxidation of COD from real textile wastewaters: kinetic study and energy consumption*, *Chemosphere.* 171 (2017) 332–338, <https://doi.org/10.1016/j.chemosphere.2016.12.065>.
- [56] J.T. Jasper, Y. Yang, M.R. Hoffmann, *Toxic byproduct formation during electrochemical treatment of latrine wastewater*, *Environ. Sci. Technol.* 51 (2017) 7111–7119, <https://doi.org/10.1021/acs.est.7b01002>.
- [57] US EPA, *EPA Drinking Water Guidance on Disinfection By-Products Advice Note No. 4. Version 2. Disinfection By-Products in Drinking Water*, (n.d.) 1–27.
- [58] R.V. Lenth, Lenth's method for the analysis of unreplicated experiments, *Environ. Stat. Qual. Reliab.* (2008) 4–6, <https://doi.org/10.1002/9781118445112.stat04086>.
- [59] A.M. Polcaro, A. Vacca, M. Mascia, F. Ferrara, *Product and by-product formation in electrolysis of dilute chloride solutions*, *J. Appl. Electrochem.* (2008) 979–984, <https://doi.org/10.1007/s10800-008-9509-3>.
- [60] O. Azizi, D. Hubler, G. Schrader, J. Farrell, B.P. Chaplin, *Mechanism of perchlorate formation on boron-doped diamond film anodes*, *Environ. Sci. Technol.* 45 (2011) 10582–10590, <https://doi.org/10.1021/es202534w>.
- [61] Y. Jung, K. Woon, B. Soo, J. Kang, *An investigation of the formation of chlorate and perchlorate during electrolysis using Pt / Ti electrodes : the effects of pH and reactive oxygen species and the results of kinetic studies*, *Water Res.* 44 (2010) 5345–5355, <https://doi.org/10.1016/j.watres.2010.06.029>.

PAPER III

Electrochemical removal of Bisphenol A from Landfill Leachate under Nordic Climate
Conditions

Ambauen, N., Weber, C.T., Muff, J., Hallé, C., Meyn, T.
Journal of Applied Electrochemistry 2020
DOI :10.1007/s10800-020-01476-3.



Electrochemical removal of Bisphenol A from landfill leachate under Nordic climate conditions

Noëmi Ambauen¹ · Clara Weber¹ · Jens Muff² · Cynthia Hallé¹ · Thomas Meyn¹

Received: 2 May 2020 / Accepted: 1 September 2020
© The Author(s) 2020

Abstract

This study investigated the applicability of electrochemical oxidation for landfill leachate treatment in climate areas, where cold temperatures prevail (like Northern Norway). Experiments were completed with pre-treated (coagulation/flocculation and separation) landfill leachate at 6 and 20 °C in order to assess the temperature influence on the degradation of the organic pollutant Bisphenol A and the fate of the ordinary wastewater parameters COD and nitrate. Furthermore, two different anode materials (Ti/Pt and Nb/BDD) and three different current densities (10, 43 and 86 mA cm⁻²) were compared. Additionally, the formation of the two groups of disinfection by-products, trihalomethanes and perchlorate, was monitored. A 99% removal of Bisphenol A was confirmed at 6 °C on both tested anode materials, but a current density of at least 43 mA cm⁻² must be applied. Removal rates were on average 38% slower at 6 °C than at 20 °C. For comparison, Bisphenol A removal in clean electrolyte disclosed faster degradation rates (between 50 and 68%) due to absent landfill leachate matrix effects. The energy consumption for 99% Bisphenol A removal was 0.28 to 1.30 kWh m⁻³, and was on average 14% higher at 6 °C compared to 20 °C. Trihalomethanes were mainly formed on Pt anodes in the ppb range, while perchlorate was primarily formed at BDD anodes in the ppm range. Formation of disinfection by-products increased with increased applied current and temperature. Electrochemical oxidation was found to be a suitable treatment process for landfill leachate in cold climate areas by successfully meeting treatment goals.

✉ Noëmi Ambauen
noemi.ambauen@ntnu.no

Clara Weber
claratw@ntnu.no

Jens Muff
jm@bio.aau.dk

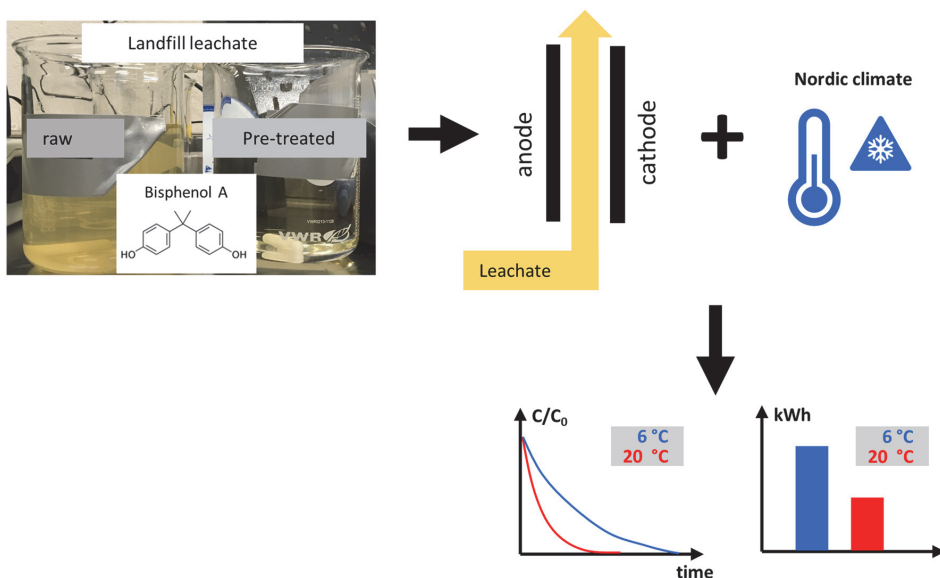
Cynthia Hallé
cynthia.halle@ntnu.no

Thomas Meyn
thomas.meyn@ntnu.no

¹ Department of Civil- and Environmental Engineering, Norwegian University of Science and Technology, S.P. Andersens Veg 5, Trondheim, Norway

² Department of Chemistry and Bioscience, Aalborg University, Niels Bohrs Vej 8, Esbjerg, Denmark

Graphic abstract



Keywords Bisphenol A · Applied current · Temperature · Energy consumption · Disinfection by-products · Organic pollutants

1 Introduction

Several advanced oxidation processes (AOPs) have been assessed for their suitability to treat different kind of wastewaters. Among AOPs, electrochemical oxidation (EO) has gained great attention because large amounts of water can be treated, no residual waste is produced, and no addition of chemicals is needed [1]. Several studies investigated the performance of EO to remove common wastewater parameters from landfill leachate (LL). For instance, Panizza et al. [2] successfully removed chemical oxygen demand (COD) from LL to below the disposal limit (160 mg L^{-1}) and de Oliveira et al. [3] reported a COD removal of 90% or higher. Satisfactory removal of ammonium nitrogen ($\text{NH}_3\text{-N}$) from LL of up to 100% by EO has been reported by Li et al. [4]. A substantial advantage of using EO to treat LL and other wastewaters is that also refractory organic compounds can be removed due to the production of the highly reactive hydroxyl radicals [5]. Hereby, it has to be distinguished between active and non-active anode material, which either form chemisorbed or physisorbed hydroxyl radicals [6, 7]. Oxidation of refractory organic compounds can also take place via indirect oxidation [8]. The most prominent indirect oxidation pathway is via the oxidation of Cl^- ions to

active chlorine (HOCl and OCl^- , depending on pH), which further react with organic pollutants leading to their partial oxidation [9]. Oxidation via hydroxyl radicals or mediating oxidizing species, allows for the removal of e.g. pharmaceuticals and personal care products (PPCPs) [10] or fulvic- and humic like substances [11]. Other recalcitrant compounds being leached from everyday items such as Bisphenol A (BPA) [12] can also be removed successfully by EO [13]. Oturan et al. [14] specifically studied the degradation of polycyclic aromatic hydrocarbons (PAHs), volatile organic carbons (VOCs) and polychlorinated biphenyls (PCBs) contained in LL and observed an electrochemical removal of those compounds between 80 and 100%.

The above-mentioned studies were all completed either at room temperature or in climate areas, where fairly warm temperatures dominate. In general, wastewater treatment systems typically work more efficiently in moderate to warm temperatures because growth rates are higher, chemical reactions are faster, treatment times are shorter and consequently energy costs are lower [15]. A few studies can be found on psychrophilic biological wastewater treatment. Smith et al. [16] reported a stable COD removal during psychrophilic anaerobic wastewater treatment, indicating a promising potential for its application in cold climate regions.

Kettunen et al. [17] compared anaerobic and sequential anaerobic treatment of LL at 11 and 24 °C. They reported that at 11 °C and a hydraulic retention time (HRT) of 1.5 to 2 days, a COD removal of 65% was achieved while at 24 °C and an HRT of 10 h 75% of the COD was removed. These findings suggest a clear adverse impact of cold temperatures on the wastewater treatment efficiency. However, no studies exist up to date that assess the performance of chemical wastewater treatment like EO in cold climate regions, a knowledge gap addressed in this article. This is also very relevant with regard to an increased focus on the technology in arctic regions. The LL for this study is collected on a site close to the city of Mosjøen, Norway, which lays in the sub-arctic climate zone with an average yearly air temperature of 3.6 °C. The yearly average LL temperature is 6 °C, which is higher than the average air temperature due to the isolating properties of the soil. A preliminary study [18] showed that BPA can be successfully removed from a model electrolyte solution at 6 °C by EO experiments.

The aim of this study was to assess the impact of the Nordic climate on the performance of EO treatment for LL and evaluate its feasibility for application at low temperatures. Due to LL treatment regulations, an important focus was the removal of specific organic pollutants such as BPA. BPA is abundantly present in the collected leachate from the landfill in Mosjøen and is listed on the Norwegian list of priority substance and must be removed below detection limit ($0.11 \mu\text{g L}^{-1}$ or 5 nM) after treatment. EO performance at the yearly average temperature of the LL (6 °C) was compared to room temperature (20 °C) and two different anode materials (active: Ti/Pt and non-active: Nb/BDD) as well as three different applied currents (10, 43 and 86 mA cm^{-2}) were evaluated. Additionally, the formation of trihalomethanes (THMs) and perchlorate were studied as known disinfection by-products (DBPs) during EO of chloride containing waters and are of major concern [19, 20]. A full factorial design approach with replicates was chosen to conduct the study.

2 Methods

2.1 Landfill leachate characteristics

LL for this study was pretreated on-site with coagulation/flocculation using FeCl_3 as a coagulant, followed by a lamella clarifier. The pH was adjusted with NaOH to about pH 10 in order to have optimum conditions for particle and heavy metal removal during coagulation/flocculation. The supernatant of the lamella clarifier was used to perform the experiments carried out in this study. The LL was spiked with additional BPA before experiments to obtain an initial concentration of $5.0 \mu\text{M}$. 100-fold higher concentration for

the experiments was chosen for a better monitoring of the degradation over time due to the detection limit of the analytical method. Furthermore, due to batch variations, the original BPA concentration varied a lot, spiking of BPA allowed to obtain equal initial concentrations. No household waste is disposed in the SHMIL landfill. Solely special industrial waste like gypsum and asbestos waste, sand from sand traps, slag, sludge from oil separators and hazardous waste such as caustic, toxic and highly flammable waste are disposed on site. Consequently, the leachate composition is based on the disposed waste. Its characteristics are summarized in Table 1.

2.2 Experimental set-up

The experimental set-up (Fig. 1) consisted of an electrochemical flow cell (ElectroCell Europe AS, Denmark), a 5 L solution tank, a chiller (FP50-ME, Julabo GmbH, Germany) and a peristaltic pump (Masterflex Cole-Parmer Instrument Co., USA). Anode material was either Nb/BDD or Ti/Pt and cathode was stainless steel. The square shaped active electrode area is 10 cm^2 with an interelectrode gap of 4 mm (Fig. 1). A turbulence enhancing mesh was installed between anode and cathode. Both electrodes were cooled with tap water from their rear side. The LL was pumped via Teflon tubing from the tank through the electrochemical flow cell and back. LL in the tank was continuously stirred by means of a magnetic stirrer and its temperature was kept stable with the connected chiller. The experiments were carried out under galvanostatic conditions, i.e. with a constant applied current, a duration of 240 min and volume of 2.5 L.

2.3 Experimental design

The experiments were carried out following a full factorial design. An overview of the factors and factors level is given in Table 2.

A total of 24 experiments have been conducted, including replicates. Several response factors (Y_i) have been chosen and are described by their corresponding linear regression

Table 1 Overview of landfill leachate characteristics

Parameter	Unit	LL (pre-treated)
pH	–	9.9
COD	$\text{mgO}_2 \text{ L}^{-1}$	99.5
BOD ₅	$\text{mgO}_2 \text{ L}^{-1}$	< 10
TOC	mg L^{-1}	39.5
sum PAH	$\mu\text{g L}^{-1}$	0.32
BTEX	$\mu\text{g L}^{-1}$	2.99
Bisphenol A	$\mu\text{g L}^{-1}$	11
Ammonium (NH_4^+)	mg L^{-1}	72.8

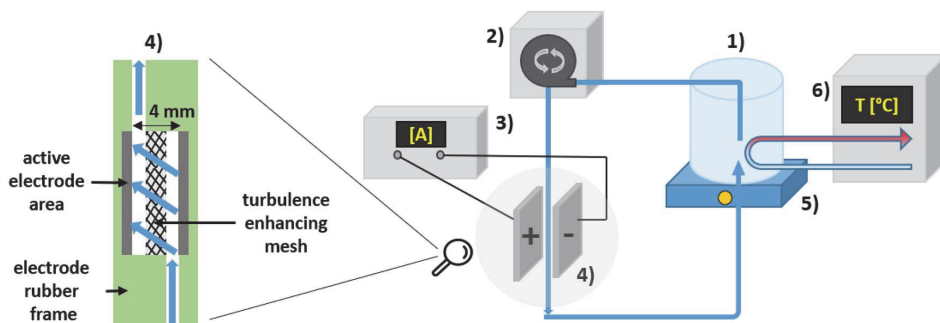


Fig. 1 Experimental set-up; 1: solution tank, 2: peristaltic pump, 3: potentiostat, 4: electrochemical flow cell, 5: magnetic stirrer, 6: chiller with cooling coil

Table 2 Overview of factors and factor levels implemented in the full factorial design

Factor	Level of factor		
Temperature (°C)	6	20	
Anode material	Pt	BDD	
Applied current (mA cm ⁻²)	10	43	86

model (Eq. 1). The statistical software Minitab (Minitab Inc., USA) was used for statistical analysis and estimation of the model parameters (b_0 – b_7). Experiments also followed a random order generated by Minitab.

$$Y = b_0 + b_1A + b_2B + b_3C + b_4AB + b_5AC + b_6BC + b_7ABC \quad (1)$$

Y: response variable; b_0 : constant (intercept); b_1 – b_7 : coefficients; A–ABC: main- and interaction effects.

The null hypothesis (H_0) assumed that no factor is significantly affecting the response variable ($\text{Effect}_j = 0$), while the alternative hypothesis (H_1) assumed that at least one factor significantly affected the response ($\text{Effect}_j \neq 0$). A significance level of 5% ($\alpha = 0.05$) was chosen.

2.4 Chemicals

Bisphenol A was used to spike the LL was purchased from Sigma-Aldrich (Merck, USA) and had a purity grade of 99%. BPA stock solution was prepared in 100% acetonitrile (VWR, Avantor, USA). Deuterated (d16) Bisphenol A (analytical grade) was used as internal standard for BPA and purchased from Sigma-Aldrich. THMs standard mix (analytical grade) and the corresponding internal standard dichloromethane (analytical grade) were purchased from Sigma-Aldrich. Orthophosphoric acid (85%), used to preserve TOC samples was purchased from VWR. Sodium thiosulfate was used to quench the samples and was purchased

from Sigma-Aldrich. Solvents used for liquid chromatography, methanol, acetonitrile, as well as ammonium acetate were purchased from VWR (HPLC purity grade). Chemicals and solvents used for ion chromatography, sodium bicarbonate, sodium carbonate, acetone, oxalic acid and sulfuric acid were purchased from Sigma-Aldrich (analytical grade). Deionized water was provided in the local laboratory by an Elga PURELAB® Ultra, Type 1+ device.

2.5 Analytical methods

Cuvette tests from Hach (Hach Co., USA) were used to measure ammonium NH_4^+ (LCK 303, 2–47 mgNH₄-N L⁻¹), nitrate NO_3^- (LCK 339, 0.23–13.5 mgNO₃-N L⁻¹) and chemical oxygen demand COD (LCK 314, 15–150 mgO₂ L⁻¹). The cuvette tests were analyzed with a Hach DR3900 laboratory spectrophotometer for water analysis. Free chlorine (HClO/ClO⁻) was measured with a Hach Pocket Colorimeter™ II, using the N,N-diethyl-p-phenylenediamine (DPD) method with a LOQ of 0.1 mgCl₂ L⁻¹.

Total organic carbon (TOC) was measured with the TOC analyzer Apollo 9000 (Tekmar, Teledyne Technologies, USA). Prior to measurement, samples were diluted 10 times and preserved by adding an adequate amount of concentrated phosphoric acid to obtain a final sample pH between 2–3. Measurement procedure followed the Norwegian standard NS EN 1484 [21] and has an LOQ of 0.5 mgC L⁻¹.

Perchlorate measurements were conducted with an ion chromatography 940 Professional IC Vario (Metrohm, Switzerland) along with a 858 Professional Sample Processor (Metrohm). A high-performance Metrosep A Supp5 (Metrohm) separation column was used with dimensions 250 × 4.0 mm and a 5 μm particle size. A flow rate of 0.7 mL min⁻¹ was applied and a LOQ of 0.32 mg L⁻¹ was determined. The software MagIC Net 3.2 (Metrohm) was used to measure the samples and results were analyzed using Excel (Microsoft, USA).

Quantification of Bisphenol A (BPA) was done by a UPC² (Waters, USA) with XEVO TQ-S triple quadrupole mass spectrometer (Waters) with an Aquity UPC² BEH 1.7 μm column (Waters). Compressed CO₂ (solvent A) and methanol with 10 mM ammonium acetate (solvent B) were used as liquid phases and 100% methanol for the make-up flow. The respective flow rate and make-up flow rate were set to 2.5 mL min⁻¹ and 0.8 mL min⁻¹ and an automated backpressure of 1500 psi was applied. The LOQ was determined to 5.0 nM BPA. Masslynx (Waters) and Targetlynx (Waters) were the softwares used for measurement and data analysis respectively. Samples were dried using a SpeedVac vacuum concentrator SPD-300DDA (Thermo Fischer Scientific, USA) and reconstituted in analytical grade 2-isopropanol (VWR) prior to measurement.

THMs were quantified with a headspace injector (Tekmar HT3, Teledyne Technologies, USA) coupled to a GC-MS (GC/MS Triple quad 7000, Agilent, USA). Quenched samples (10 mL) were placed in 20 mL crimp cap sealed head space vials. Headspace analysis was done using a trap column (Purge/Trap K Vocab® 3000, Supelco, USA) and a DB-624 UI GC column (Agilent) with a length of 30 m, 0.25 mm diameter and 1.40 μm film thickness. The LOQ for trichloromethane (CHCl₃), bromodichloromethane (CHCl₂Br), chlorodibromomethane (CHClBr₂) and tribromomethane (CHBr₃) are 3 ppb, 6 ppb, 6 ppb and 6 ppb respectively. Samples were measured using Masshunter software (Agilent) and Masshunter Quant software (Agilent) was used for sample analysis and quantification.

3 Results and discussion

3.1 Experimental reproducibility

The experimental design was carried out with replicates. Table 3 summarizes the averaged response parameters (SI:1) together with their coefficient of variation (CV), which is the ratio of the standard deviation and the mean of the two replicate experiments. The CV is unitless and allows therefore to compare the dispersion of the two replicated values also in between two different factors. A high CV value indicates higher dispersion. As can be seen in Table 3, the CVs vary greatly between the different factors for the same experimental conditions. This observation may be explained by the different measurement methods for the corresponding response factor (BPA, COD, NO₃⁻ and THMs), which are afflicted with different measurement uncertainties. In addition, the different measurement methods were carried out by different personnel, another source contributing to the observed inter-factor CV variation. CV also shows variability for the same response factor but different experimental conditions.

3.2 Removal of Bisphenol A

The degradation of BPA over time at different applied currents and temperatures is shown in Fig. 2. No complete removal could be achieved at 10 mA cm⁻², but higher removal of BPA was reached at BDD anodes (Fig. 2b, d) than at Pt anodes (Fig. 2a, c), while the applied temperature only played a secondary role. At higher applied currents, 43 and 86 mA cm⁻² (Fig. 2), complete BPA removal was achieved for all experimental conditions. At

Table 3 Average response factor of each replicated experiment, grouped after experimental factorial combination

Temp (°C)	j_{app} (mA cm ⁻²)	Anode (-)	BPA (min ⁻¹)	CV _{BPA} (%)	COD (%)	CV _{COD} (%)	NO ₃ ⁻ (%)	CV _{NO3} (%)	Σ THM (ppb)	CV _{THM} (%)
6	10	Pt	0.002	85.8	0.3	0.6	15.9	15.5	6.8	64.0
6	10	BDD	0.007	10.4	10.4	24.6	72.7	5.9	10.0	1.6
6	43	Pt	0.023	10.1	10.1	55.4	41.1	35.0	72.8	33.0
6	43	BDD	0.044	3.9	8.9	34.4	40.3	8.9	27.6	1.7
6	86	Pt	0.118	9.9	16.2	0.4	85.0	4.0	200.8	6.9
6	86	BDD	0.070	7.5	9.9	3.8	34.3	10.4	27.0	2.1
20	10	Pt	0.003	18.2	1.6	74.7	14.4	13.6	8.1	25.6
20	10	BDD	0.006	6.6	12.5	3.0	82.0	7.8	5.1	9.9
20	43	Pt	0.036	7.9	15.7	14.9	68.4	17.4	88.0	10.5
20	43	BDD	0.093	0.4	13.7	9.3	69.8	3.5	23.9	4.2
20	86	Pt	0.164	1.7	23.5	8.0	99.6	10.5	143.3	21.0
20	86	BDD	0.220	21.6	16.9	3.6	55.2	5.3	30.1	21.1

Corresponding coefficient of variation is given to the right

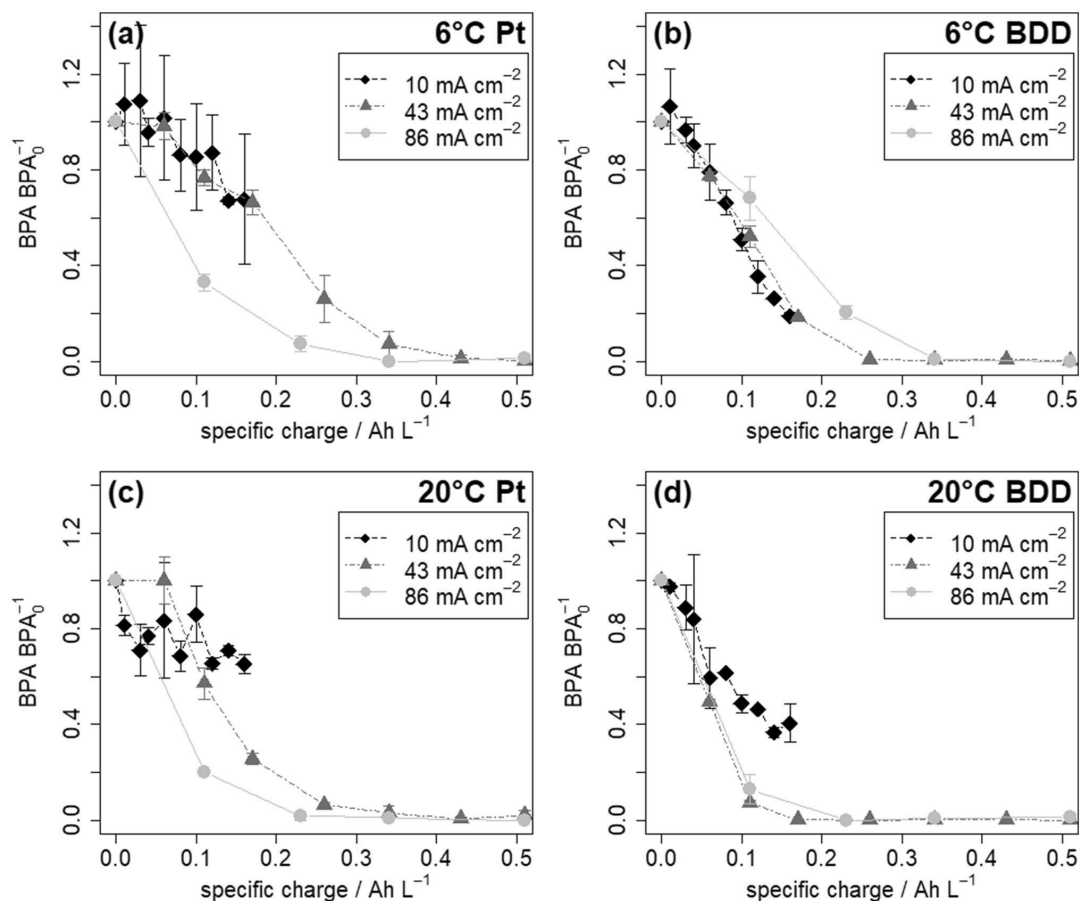


Fig. 2 Degradation of BPA in LL vs specific charge (Ah L^{-1}) until complete removal or maximal experimental time was reached: **a** Pt and 6°C , **b** BDD and 6°C , **c** Pt and 20°C , **d** BDD and 20°C ; Error bars indicate the standard deviation of the two replicate experiments

Pt anode (Fig. 2a, c), complete BPA removal was reached at 86 mA cm^{-1} after less specific charged passed than at an applied current of 43 mA cm^{-1} . A higher applied temperature did not change the specific charged passed at 86 mA cm^{-1} for complete BPA removal but lead to a lower specific charge passed at 43 mA cm^{-1} to completely remove BPA. On BDD anode (Fig. 2b, d) at 6°C a higher specific charged passed at 86 mA cm^{-1} than at 43 mA cm^{-1} until complete removal of BPA. This behaviour was also observed at BDD anode and 20°C but the difference in the specific charge passed between 43 and 86 mA cm^{-1} for complete BPA removal is marginal compared to 6°C . This may be attributed to the higher applied current that not only favours BPA degradation, but also unwanted side reactions, which are more expressed for

BDD and can be confirmed by a lower charge efficiency constant (Fig. 3b), as discussed below.

These above made observations are supported by the statistical analysis of variance. Current density, temperature and the interaction between those two and the interaction between temperature and anode material were identified as significant effects (SI:2). The corresponding regression equation is given in SI:4 with an adjusted coefficient of determination (R^2_{adj}) corresponding to 88.9%. These observations are confirmed when looking at the reaction rate constants (k_{BPA}), graphically summarized (Fig. 3a, c) and their exact numbers can be found in Table 3. The reaction rates were calculated using a first order kinetic model fitted to the experimental data over time. The difference for k_{BPA} for the two different anode materials at 10 mA cm^{-2} corresponds to

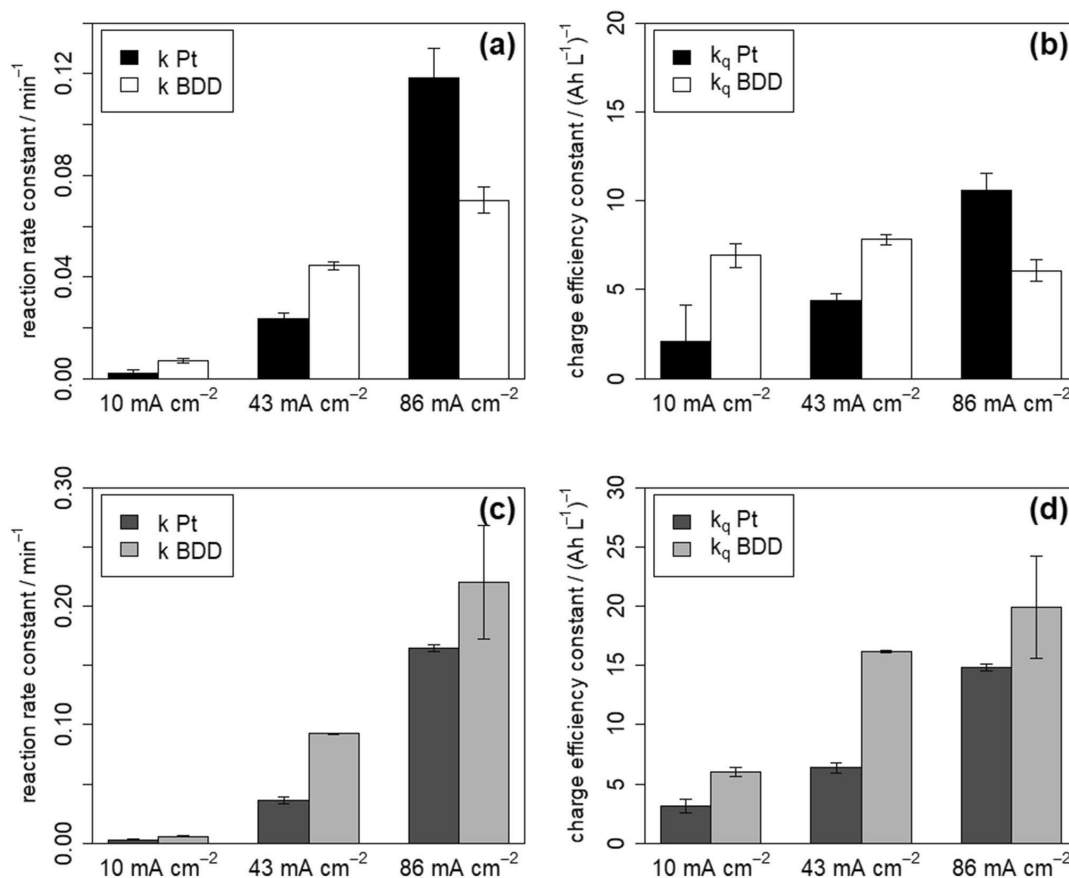


Fig. 3 Comparison of reaction rates and current efficiencies for BPA: **a** reaction rate constants (k) at 6 °C, **b** charge efficiency constant (k_q) at 6 °C, **c** reaction rate constants at 20 °C, **d** charge efficiency constant at 20 °C

72% and 55% at 6 and 20 °C respectively. At the same current, the temperature difference only altered k_{BPA} by 25% and 20% for Pt and BDD anode respectively. This clearly shows that the temperature influence was considerably smaller than the influence of anode material, when the lowest current was applied (10 mA cm^{-2}). The influence of the different applied temperatures was bigger at 43 mA cm^{-2} where k_{BPA} differed by 35% and 52% on Pt and BDD anode respectively. The effect of the anode material was in the same range for 10 and 43 mA cm^{-2} and caused a difference of k_{BPA} of 47% and 61% at 6 and 20 °C respectively. It is visible that the cold temperature plays a more important role by causing a larger difference in k_{BPA} at a higher applied current (43 mA cm^{-2}) than at 10 mA cm^{-2} , where the anode material had a higher impact. Still, the anode material causes a larger difference of k_{BPA} than the temperature, also at 43 mA cm^{-2} . At the

highest applied current (86 mA cm^{-2}), the influence of temperature on k_{BPA} was lower on Pt anode than on BDD anodes and caused differences of k_{BPA} of 28% and 68% respectively. The anode material caused a variation of k_{BPA} at 86 mA cm^{-2} of 68% and 25% for 6 and 20 °C respectively.

From the results above it can be concluded that 6 °C lead in general to a slower k_{BPA} than 20 °C. An exception to this statement is the parameter combination BDD and 10 mA cm^{-2} , where 6 °C resulted in a factor 1.3 (20%) faster k_{BPA} than 20 °C. According to literature [22, 23] and the Arrhenius's law that predicts slower kinetics at lower temperatures, it was expected a priori that the parameter combination 6 °C, Pt anode and 10 mA cm^{-2} would lead to the slowest BPA degradation. On the other side, the fastest BPA degradation was expected at 20 °C, BDD anode and 86 mA cm^{-2} . Both presumptions were confirmed with

respective reaction rate constants, which differ by 99%. It can further be concluded that BDD anode resulted generally in faster k_{BPA} than Pt anodes. Again, there is one exception to this statement where the opposite was observed. At 6 °C and 86 mA cm⁻², a factor 1.7 (68%) faster k_{BPA} was observed at Pt than on BDD anode (Fig. 3a) %. Lastly, when comparing the different k_{BPA} among the different current densities (Fig. 3a, c) it is evident that an increasing applied current results in increasing k_{BPA} , which applies for both anode materials and both temperatures, with no exception. A linear correlation between an increasing k_{BPA} and the increasing applied current density could be found for BDD but not for Pt anode (SI: 8).

The reaction rate constants (k_{BPA}) give valuable insights into the rate of degradation, but they do not account for the current efficiency during EO of BPA. In order to consider the relative current efficiency, the charge efficiency constant (k_q) for BPA was calculated, adapted from Muff et al. [24] (Eq. 2):

$$\frac{d[BPA]}{dQ} = -k_q * [BPA] \quad (2)$$

Q: specific charge (Ah L⁻¹), k_q : charge efficiency constant [(Ah L⁻¹)⁻¹], [BPA]: BPA concentration, normalized.

Figure 3 depicts the calculated k_{BPA} and k_q for BPA. At 6 °C. An increase of k_{BPA} is observed with increasing applied current, valid for both, Pt and BDD anode (Fig. 3a). On Pt anodes 6 °C, k_q increases with an increasing applied current similarly to k_{BPA} (Fig. 3b). However, the relative difference between the different applied currents is smaller for the charge efficiency constant than for the reaction rate constants. The ratio of the charge efficiency constant is 2.1:2.4 and 11.9:5.1 for the reaction rate constant for the three different applied currents and increasing order. On the other hand, no increase of k_q for BDD anode at 6 °C is observed. In fact, k_q remains in the same range for all three different applied current and is slightly smaller at 86 mA cm⁻² than at 10 mA cm⁻² (Fig. 3b). This shows that the current efficiency is not lost at higher applied current, which is important in order maintain a fast and efficient process. The same pattern can be observed for the reaction rate constant at 20 °C (Fig. 3c). An increase of k_q on Pt anode with increasing applied current is observed, with a ratio (2.0: 2.3) similar to the one at 6 °C (Fig. 3d). Contrary to the observation at 6 °C, an increase of k_q can be observed on BDD anode at 20 °C (Fig. 3d). Muff et al. [24] observed that k_q increased when the oxidation rate (k) of their model organic compound (naphthalene) decreased. They attributed this behaviour to the suppression of the water oxidation side reaction, which is known to be more expressed at higher applied currents. This trend can be seen in the present study only for BDD anodes at 6 °C. The best current efficiency at 6 °C was

obtained at 43 mA cm⁻² for BDD anode and at 86 mA cm⁻² for Pt anode. At 20 °C, the best current efficiency was at 86 mA cm⁻² for both, Pt and BDD anode.

A preliminary study by Ambauen et al. [18] explored the degradation of 5.0 µM BPA at 43 mA cm⁻² and pH 10 in clean electrolyte solution, containing NaCl and Na₂SO₄. Concentrations of NaCl and Na₂SO₄ were the same as found on average in the LL, 0.0033 and 0.0003 M respectively. All the other experimental settings, pumping rate, experimental time and solution pH were the same as in the present study. Figure 2b depicts the degradation in the LL matrix for the same experimental conditions as in the preliminary study. Table 4 summarizes the corresponding first order BPA reaction rate constants and their differences between the distinct solutions. Reaction rates for BPA in clear electrolyte solution (Table 4) were adapted from Ambauen et al. [18]. It is evident that BPA degradation followed the same pattern in both solutions. However, the matrix effect causes a reduction of BPA degradation rates of at least 50%. Although the differences reductions are in the same range of magnitude, an increase is observed with decreasing temperature and when switching from BDD to Pt anode. An initial delay is observed on Pt anode (Fig. 2b) in the LL, whereas in the clean electrolyte BPA degradation started immediately. In clean electrolyte, active chlorine is formed at slower rates on Pt anodes than on BDD anodes [25]. The LL contains inorganic anions like Cl⁻ and bicarbonate, which can act as hydroxyl radical scavengers. In turn, those scavenging reactions decelerate the EO of organic pollutants such as BPA. Cl⁻ and the hypochlorite ion (OCl⁻), the form of active chlorine present at pH 10, react with hydroxyl radicals and thus act as scavengers (Eq. 4a, 4b) [26]:



Bicarbonate (HOC₃⁻) and carbonate (CO₃²⁻) ions are contained in most aqueous solutions [27]. At pH 10, these anions are present to 30% as CO₃²⁻ and to 70% as HCO₃⁻. Equation (5a) and (5b) depict the reactions for bicarbonate and carbonate ions with hydroxyl radicals [28].

Table 4 comparison first order BPA degradation rates (min⁻¹) in different solutions for 43 mA cm⁻², pH 10 and 240 min treatment time

	Clean electrolyte k (min ⁻¹)	Landfill leachate k (min ⁻¹)	Reduction Δk (%)
6 °C/Pt	0.072	0.023	68
6 °C/BDD	0.097	0.044	55
20 °C/Pt	0.087	0.036	59
20 °C/BDD	0.187	0.093	50



This circumstance combined with other occurring competing reactions caused by the LL matrix content constituents can explain the initial observed delay of BPA degradation on Pt anodes. The complex LL matrix slows down the degradation of BPA and consequently longer treatment times are required and are accompanied by higher costs.

In conclusion, these results show that it is possible to efficiently degrade the organic pollutant BPA to below detection limit under cold operating temperatures that are dominating in subarctic climate regions. The removal of the initial BPA concentration of $11 \mu\text{g L}^{-1}$ to below detection limit furthermore upgrades the effluent from class 3 (no chronic long term toxic effects) to class 2 (no toxic effects) according to the Norwegian guidelines for water classification [29]. However, the applied current densities must be reasonably high, i.e. at least 43 mA cm^{-2} , in this study, in order to achieve complete BPA degradation within 4 h treatment time. Additionally, when choosing BDD over Pt as anode material, BPA degradation is in general promoted faster.

3.3 Removal of COD

While the TOC content remained relatively stable, a decrease of COD could be observed, indicating that most of the organic content of the LL was oxidized, but not mineralized (SI: 6). The applied current was the most significant factor influencing the COD degradation (Fig. 4). By increasing the current density from 10 to 86 mA cm^{-2} , COD removal at 20°C increased from 2 to 23% and 13 to 17% for Pt and BDD anode respectively. At 6°C , COD removal was around 10% for BDD for all applied current densities. After

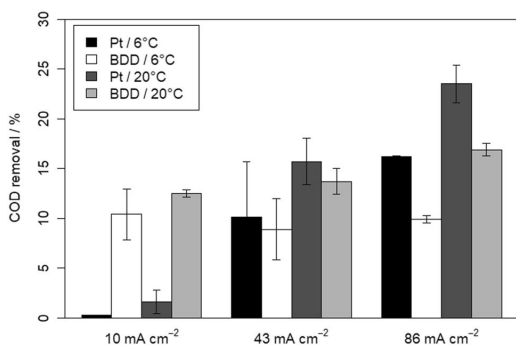


Fig. 4 COD degradation at different applied currents

a slight increase of COD at the start, the COD was reduced by 16% at 6°C on Pt anode.

Under similar conditions, the COD removal was in general higher on Pt anodes compared to BDD, except for 10 mA cm^{-2} . This is supported by the statistical analysis, that finds a significant interaction effect between the anode material and the applied current (SI: 2).

Zhou et al. [30] observed an increase in COD removal from reverse osmosis concentrate with increasing applied current, but stated that COD removal was always highest at non-active BDD compared to the active Ti/IrO₂-RuO₂ anode, no matter the applied current. Contrary to this, de Moura et al. [30] found a higher COD removal percentage at Ti/Pt than at BDD anode for real waste water samples with an initial concentrations of 341 mg L^{-1} COD and 208 mg L^{-1} Cl⁻ (0.0036 M). After 2 h of treatment at 25°C , they observed a COD removal of 25.2 and 1.0% for Pt and BDD anode respectively. They further observed an increase in COD removal by doubling the applied current from 25.2% to 30.5% at Pt anode and from 1.0% to 4.5% on BDD anode. This study observed the same as Zhou et al. [30] for 10 mA cm^{-2} but this behavior changes for 43 and 86 mA cm^{-2} where the observations are similar to the ones from de Moura et al. [31]. A possible explanation for this change in behavior might be the increasing current efficiency (CE) with decreasing applied current on BDD (Fig. 5). CE was calculated according to Eq. 6 [7]:

$$CE_{\text{COD}} = FV \frac{(COD_t - COD_{t+\Delta t})}{8I\Delta t} \quad (6)$$

F: Faraday constant (As mol^{-1}); V: volume (L); COD ($\text{molO}_2 \text{ L}^{-1}$); I: current (A); t, t + Δt : time (s).

This leads to a reduced side reactions such as oxygen evolution [7] and thus COD is removed more efficiently at lower currents. The current efficiencies at Pt anodes are

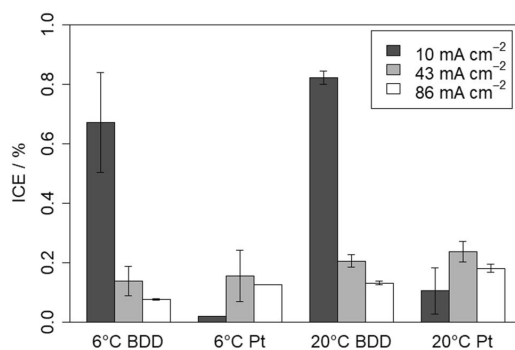
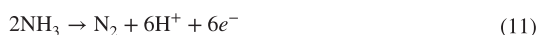
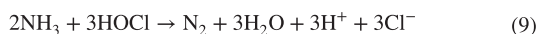
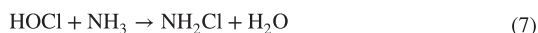


Fig. 5 ICE [%] for COD removal at different temperatures and anode materials

lowest at 10 mA cm^{-2} and highest at 43 mA cm^{-2} . Furthermore, current efficiencies at 43 and 86 mA cm^{-2} are always better at Pt than BDD anodes which is reflected in higher COD removal (Fig. 4) for those higher applied currents.

3.4 Ammonium removal and nitrate formation

The pH of the LL after pre-treatment was 9.9, which means that active chlorine species are present to 99.54% as OCl^- and to 0.46% as HOCl . At pH 9.9, 30.1% of the ammonium is present as NH_4^+ and the remaining 69.9% are present in form of NH_3 (aq). A blank test with no applied current (data not shown) revealed that no NH_3 is lost into the gas phase during the experimental time of 4 h. During the EO of NH_3 via indirect oxidation by HOCl [32] (Eq. 7) or OCl^- [33] (Eq. 8) monochloramines (NH_2Cl) can be formed. Their formation is assumed to have caused a large variance during NH_4^+ measurements [34], which lead to discarding the measurements. Apart from chloramines, NH_3 and NH_4^+ can also be oxidized to elementary N_2 or to NO_3^- respectively via indirect oxidation by HOCl (Eqs. 9, 10) [35]. As most of the ammonium is present as NH_3 and most of active chlorine as OCl^- due to the high LL pH, the indirect oxidation to N_2 or NO_3^- are assumed to take place but they only account for a marginal part. In addition, direct electron transfer at the BDD anode surface can lead to the oxidation of NH_3 to N_2 at high pH (Eq. 11) and 1.6 V vs. MSE (2.2 V vs. SHE) [32]. On Pt anode, direct oxidation of NH_3 to N_2 cannot take place due to the low oxygen evolution overpotential that starts at 1.9 V compared to BDD anode where oxygen evolution first starts at 2.6 V vs. SHE [7]. This suggests that the pathway proposed in Eq. 11 most likely took place on BDD anode. However, only the formation of NO_3^- could be measured in this study (Fig. 6) confirming only the pathway suggested in Eq. (10).



HOCl : active chlorine; NH_3 : ammonia; NH_2Cl : chloramine; NH_4^+ : ammonium; NO_3^- : nitrate.

Figure 6 shows that an increased current did increase the formation of NO_3^- on Pt anode at both, 6 and 20°C . In contrary, NO_3^- formation decreased with increasing current on BDD anodes at both temperatures (additional data are given in SI: 7). This behaviour may be explained by the fact, that with an increasing current, the direct oxidation of NH_3 to N_2 governs NH_3 oxidation on BDD anodes, while indirect oxidation via active chlorine becomes inferior. No direct NH_3 oxidation takes place on Pt anodes but indirect oxidation of NH_4^+ via HOCl to NO_3^- is promoted by increasing the applied current [36]. This leads consequently to higher formation of NO_3^- with an increased applied current. Cabeza et al. [37] observed an increase of NH_4^+ removal from LL with an increasing applied current. This is because NH_4^+ oxidation is attributed to mainly occur via indirect oxidation by active chlorine generated via chloride oxidation in the electrolytic cell [38].

3.5 Formation of disinfection by-products

Formation of THMs was observed during all experiments (Fig. 7a–c), and statistical analysis of the total measured THM concentration for each experiment indicates that the applied current and the anode material, as well as their interaction effect, are significantly influencing their production. At 10 mA cm^{-2} , the anode material has only a minor influence CHCl_3 formation shows to be slightly higher at BDD anodes while formation of CHCl_2Br , CHClBr_3 and CHBr_3 seems to be favored at Pt anode. Increasing the current to 43 or 86 mA cm^{-2} increased the THMs formation proportionally. THM production is favored at Pt anode and differs by a factor 1.8 (6°C and 43 mA cm^{-2}) to 8.3 (6°C and 86 mA cm^{-2}), whereby it is always less at BDD anodes for the same experimental settings. Jasper et al. [19] also observed a much lower THMs production on the non-active BDD anode compared to an active $\text{TiO}_2/\text{IrO}_2$ during EO of latrine wastewater. They attributed this observation to the fact that organic THMs precursors are much more rapidly mineralized to CO_2 on BDD than on Pt anodes and

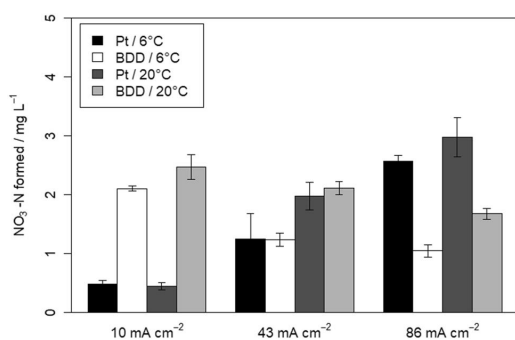


Fig. 6 Formation of nitrate (NO_3^-) at different applied currents

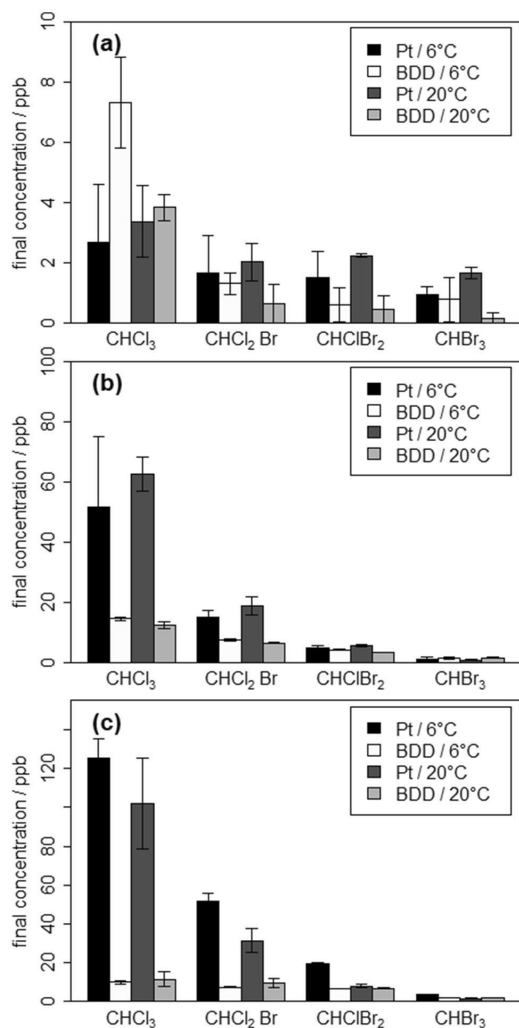


Fig. 7 Formation of THMs at three different applied currents

therefore less THMs are observed on BDD anodes. This is also in line with state-of-the-art literature that non-active anodes generally lead to faster mineralization of organic compounds than active anodes [7]. CHCl₃ and CHCl₂Br are formed in a greater amount than CHBr₃ and CHClBr₂, which is explained by the different initial Cl⁻ and Br⁻ concentrations of the LL, 157.0 and 2.1 mg L⁻¹ respectively. Temperature had no statistical influence on the THMs formation. For 43 mA cm⁻², 20 °C leads to a factor 1.8 higher THMs concentrations than 6 °C, but for 86 mA cm⁻² the opposite is observed (factor 1.9). Thus, it can be concluded that low temperature is of little importance for THM formation,

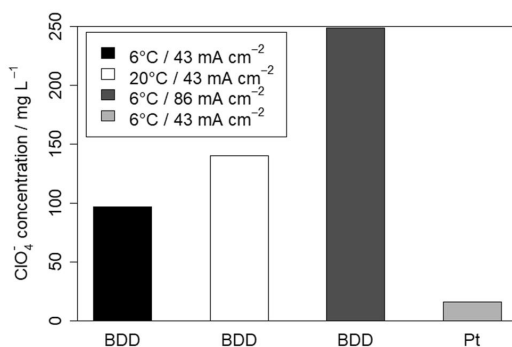


Fig. 8 Perchlorate Production at different temperatures, applied current and anode material (current is given per cm² of active electrode area)

while the anode material must be carefully considered, and an appropriate applied current must be chosen in order to minimize their formation.

Based on the formation of THMs, BDD is the better choice. However, other studies showed that an extensive amount of perchlorate can be formed on BDD anodes during EO of chloride containing waters [39]. In the present study final concentrations of perchlorate (ClO₄⁻) were measured to proof its presence or absence during EO. Figure 8 shows the measured final ClO₄⁻ concentrations after an experimental time of 240 min. On BDD anode, 96 mg L⁻¹ of ClO₄⁻ were produced, which corresponds to an 83% higher concentration than on the Pt electrode, where 16.1 mg L⁻¹ have been found with otherwise similar experimental conditions. Furthermore, ClO₄⁻ increased when either the temperature (140.2 mg L⁻¹) or the applied current (248.8 mg L⁻¹) were increased. Compared to 6 °C and BDD anode, increasing the current caused the biggest difference in ClO₄⁻ production of 158%. At an applied current of 10 mA cm⁻² no ClO₄⁻ was detected for any temperature or anode material and is therefore not shown in Fig. 8. The observed formation of ClO₄⁻ in line with literature [19], where perchlorate was only discovered at the non-active BDD anode and THMs only at the active TiO₂/IrO₂ anode during EO of latrine wastewater. The fact that this study observed a small amount of perchlorate on Pt anode may be explained by the difference in the used active anode material and slightly different experimental conditions such as a higher applied current.

While THMs are volatile compounds that may disappear other time from the water phase, ClO₄⁻ may be of higher concern since it remains in the aqueous solution. In addition, THMs are formed in the ppb range on Pt anodes while ClO₄⁻ was formed in the ppm range on BDD anodes. Toxicity tests (96 h, flow through) for fish (rainbow trout) show

that the concentration which is lethal for 50% of the population (LC_{50}) corresponds to 36 mg L^{-1} for chloroform [40] and 2 mg L^{-1} for perchlorate [41]. Maximum perchlorate concentration reached on BDD anode was 237 mg L^{-1} and 16 mg L^{-1} on Pt anode. The maximum chloroform concentration reached on BDD anode was $15 \text{ } \mu\text{g L}^{-1}$ and $136 \text{ } \mu\text{g L}^{-1}$ on Pt anode. This means that the perchlorate LC_{50} for fish was exceeded on both anode materials but to a much higher extent on the BDD anode. The LC_{50} for chloroform was not exceeded at neither anode material. In that regard, final perchlorate concentrations in this study cause higher toxicity than chloroform. This leads to the conclusion that Pt anode would be the favourable material with respect to DBP formation.

3.6 Energy consumption

The amount of energy, which was necessary for 99% removal of BPA and 1 kg of COD respectively, was estimated for the different experimental conditions (Fig. 9). The energy consumption was found to be on average 6% less on BDD anodes than on Pt when the same temperature and current

were applied, since degradation of BPA was generally faster on BDD electrodes (Fig. 9a).

However, the applied current does affect the energy consumption to a greater extent. The average difference of energy consumption between 6 and $20 \text{ } ^\circ\text{C}$ corresponds to 12% (0.1 kWh m^{-3}). A bigger difference of the average energy consumption corresponding to 74% (0.9 kWh m^{-3}) was observed between 43 and 86 mA cm^{-2} . It should be noted that no results are shown for a current density of 10 mA cm^{-2} in Fig. 9a, since BPA removal was not sufficient under these conditions. In other words, increasing the current from 43 to 86 mA cm^{-2} means increasing the average energy consumption by 74% but reducing the treatment time by 48%. Additionally, a LL temperature of 6 instead of $20 \text{ } ^\circ\text{C}$ increases the energy consumption on average by 12% and the treatment times by 25%. Even though a high current would reduce the treatment time and higher energy consumption could be justified by low energy prices in Norway, it has to be kept in mind that a higher applied current also leads to the formation of more unwanted DBPs and thus the lower current seems to be the favorable choice. On the other hand, due to low energy prices in Norway ($0.11 \text{ } \text{€ kWh}^{-1}$) and the rather moderate difference in energy consumption between 6 and $20 \text{ } ^\circ\text{C}$, the EO of cold LL to remove organic pollutants like BPA is absolutely feasible. Almost 100% of the energy in Norway is produced by hydropower plants which also makes a higher energy consumption ecologically more reasonable. Furthermore, heat development in the electrolytical cell as well as the installed on-site pre-treatment would likely increase the LL temperature under more applied conditions, thus reducing the energy consumption during EO.

The COD removal within 240 min was linearly extrapolated to obtain the theoretical energy demand to remove 1 kg COD. Similar to BPA, an increasing energy consumption with increasing applied current of 7% and 65% for an increase from 10 to 43 mA cm^{-2} and from 43 to 86 mA cm^{-2} respectively was observed. As an exception to this observation, the removal of COD on Pt anode and $6 \text{ } ^\circ\text{C}$, as can be seen in Fig. 9b, has a higher energy demand at 10 mA cm^{-2} than at 43 or 86 mA cm^{-2} . Only 0.3% of the initial COD concentration ($99.6 \text{ mg O}_2 \text{ L}^{-1}$) were removed during 240 min for the given experimental conditions, resulting in an extraordinary long treatment time and subsequently in a higher energy consumption. Correspondingly, treatment times were shorter at the higher applied current, i.e. 92% and 25% for an increase from 10 to 43 mA cm^{-2} and from 43 to 86 mA cm^{-2} respectively. It can further be seen (Fig. 9b) that the energy consumption for COD removal is higher at 6 than at $20 \text{ } ^\circ\text{C}$ for the otherwise same conditions, on average 55%. The rationale for and against a higher current or temperature is the same as for BPA, stated above.

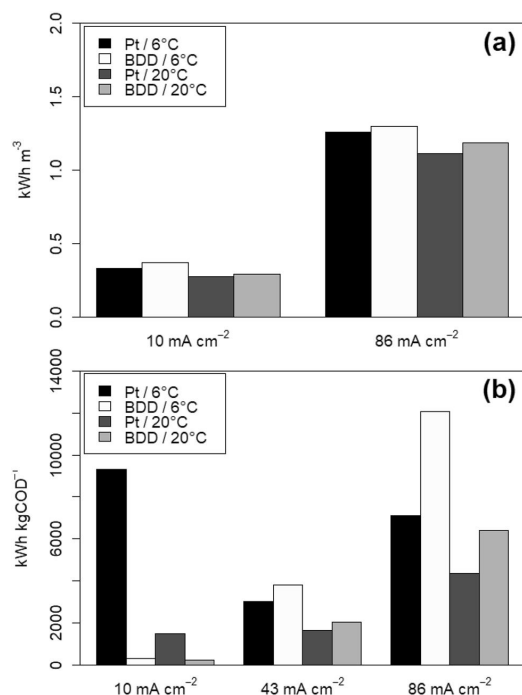


Fig. 9 a Energy consumption (kWh m^{-3}) for 99% BPA removal; b estimated energy consumption for 1 kg COD removal

4 Conclusions

The 99% removal of the organic pollutant Bisphenol A was achieved within the experimental time of 240 min on both tested anode materials (Pt and BDD) and at both tested temperatures (6 and 20 °C). However, a current of at least 43 mA cm⁻² must be applied. Corresponding treatment times differed on average by 25% (24 min) and the equivalent energy consumption by 12% (0.1 kWh m⁻³) between 6 °C and 20 °C. The best current efficiency was achieved at 86 mA cm⁻² except for 6 °C and BDD where 43 mA cm⁻² showed to be the most efficient current. The higher energy costs to maintain the most efficient current can be justified by low energy prices in Norway and thus making the process feasible for application.

Similar to Bisphenol A, a higher COD removal (6%) was reached on average at 20 °C than at 6 °C for all experimental conditions and was higher on Pt than on BDD anodes except for 10 mA cm⁻². No complete COD removal was reached within the experimental time whereby maximum COD removal was 23%.

The formation of trihalomethanes was observed during all experiments. On average, up to 76% (60 µg L⁻¹) more trihalomethanes were formed on Pt than on BDD anode and their formation increased with an increasing applied current. The temperature did not show a significant influence on the formation of the trihalomethanes. Contrary to the trihalomethanes, perchlorate formation mostly took place on BDD anodes with a maximum concentration of 260 mg L⁻¹ while it was almost negligible on Pt anodes with a maximum observed concentration of 16 mg L⁻¹. The formation of perchlorate was generally a factor 1000 higher than the formation of trihalomethanes, attaching more importance to the Pt anode that minimizes perchlorate production.

The findings of this study show that the electrochemical removal of organic pollutants (Bisphenol A) is possible from the leachate at cold temperatures without more extensive pre-treatment like TOC, COD or NH₄⁺ removal. Nonetheless, further studies are suggested with a large-scale pilot plant to investigate the heat development within the electrolytical cells since this could be a beneficial aspect with regard to the removal kinetics in cold climates.

Author contributions Conceptualization: NA, CH, TM; Methodology: NA, CW, CH, TM; Formal analysis and Investigation: NA, CW; Visualization: NA, CW; Writing—original draft: NA; Writing—review and editing: NA, JM, TM; Funding acquisition: TM; Resources: TM; Supervision: JM, CH, TM.

Funding Open Access funding provided by NTNU Norwegian University of Science and Technology (incl St. Olavs Hospital - Trondheim University Hospital). This study was financially supported by the Norwegian University of Science and Technology and the Søndre Helgelands Miljøverk IKS, Norway.

Compliance with ethical standards

Conflict of interest The authors declare no conflict and no competing interests.

Open Access This article is licensed under a Creative Commons Attribution 4.0 International License, which permits use, sharing, adaptation, distribution and reproduction in any medium or format, as long as you give appropriate credit to the original author(s) and the source, provide a link to the Creative Commons licence, and indicate if changes were made. The images or other third party material in this article are included in the article's Creative Commons licence, unless indicated otherwise in a credit line to the material. If material is not included in the article's Creative Commons licence and your intended use is not permitted by statutory regulation or exceeds the permitted use, you will need to obtain permission directly from the copyright holder. To view a copy of this licence, visit <http://creativecommons.org/licenses/by/4.0/>.

References

- Sirés I, Brillas E, Oturan MA et al (2014) Electrochemical advanced oxidation processes: today and tomorrow. A review. *Environ Sci Pollut Res* 21:8336–8367. <https://doi.org/10.1007/s11356-014-2783-1>
- Panizza M, Delucchi M, Sirés I (2010) Electrochemical process for the treatment of landfill leachate. *J Appl Electrochem* 40:1721–1727. <https://doi.org/10.1007/s10800-010-0109-7>
- de Oliveira MS, da Silva LF, Barbosa AD et al (2019) Landfill leachate treatment by combining coagulation and advanced electrochemical oxidation techniques. *ChemElectroChem* 6:1427–1433. <https://doi.org/10.1002/celec.201801677>
- Li J, Yang ZH, Xu HY et al (2016) Electrochemical treatment of mature landfill leachate using Ti/RuO₂-IrO₂ and Al electrode: optimization and mechanism. *RSC Adv* 6:47509–47519. <https://doi.org/10.1039/c6ra05080h>
- Comninellis C (1994) Electrocatalysis in the electrochemical conversion/combustion of organic pollutants for waste water treatment. *Electrochim Acta* 39:1857–1862
- Wang JL, Xu LJ (2012) Advanced oxidation processes for wastewater treatment: formation of hydroxyl radical and application. *Crit Rev Environ Sci Technol* 42:251–325. <https://doi.org/10.1080/10643389.2010.507698>
- Comninellis C, Chen G (2010) *Electrochemistry for the environment*. Springer, New York
- Martinez-Huitle CA, Ferro S (2006) Electrochemical oxidation of organic pollutants for the wastewater treatment: direct and indirect processes. *Chem Soc Rev* 35:1324–1340. <https://doi.org/10.1039/B517632H>
- Martínez-Huitle CA, Panizza M (2018) Electrochemical oxidation of organic pollutants for wastewater treatment. *Curr Opin Electrochem* 11:62–71. <https://doi.org/10.1016/j.coelec.2018.07.010>
- Wang J, Wang S (2016) Removal of pharmaceuticals and personal care products (PPCPs) from wastewater: a review. *J Environ Manage* 182:620–640. <https://doi.org/10.1016/j.jenvman.2016.07.049>
- Xiao S, Peng J, Song Y et al (2013) Degradation of biologically treated landfill leachate by using electrochemical process combined with UV irradiation. *Sep Purif Technol* 117:24–29. <https://doi.org/10.1016/j.seppur.2013.04.024>
- Deblonde T, Cossu-Leguille C, Hartemann P (2011) Emerging pollutants in wastewater: a review of the literature. *Int J Hydrogen Environ Health* 214:442–448. <https://doi.org/10.1016/j.ijh.2011.08.002>

13. Jo EY, Lee TK, Kim Y, Park CG (2016) Effect of anions on the removal of bisphenol A in wastewater by electro-oxidation process. *Desalin Water Treat* 57:29500–29508. <https://doi.org/10.1080/19443994.2016.1197156>
14. Oturan N, Van Hullebusch ED, Zhang H et al (2015) Occurrence and removal of organic micropollutants in landfill leachates treated by electrochemical advanced oxidation processes. *Environ Sci Technol* 49:12187–12196. <https://doi.org/10.1021/acs.est.5b02809>
15. Lettinga G, Rebac S, Zeeman G (2001) Challenge of psychrophilic anaerobic wastewater treatment. *Trends Biotechnol* 19:363–370. [https://doi.org/10.1016/S0167-7799\(01\)01701-2](https://doi.org/10.1016/S0167-7799(01)01701-2)
16. Smith AL, Skerlos SJ, Raskin L (2013) Psychrophilic anaerobic membrane bioreactor treatment of domestic wastewater. *Water Res* 47:1655–1665. <https://doi.org/10.1016/j.watres.2012.12.028>
17. Kettunen RH, Hoilijoki TH, Rintala JA (1996) Anaerobic and sequential anaerobic-aerobic treatments of municipal landfill leachate at low temperatures. *Bioresour Technol* 58:31–40. [https://doi.org/10.1016/S0960-8524\(96\)00102-2](https://doi.org/10.1016/S0960-8524(96)00102-2)
18. Ambauen N, Muff J, Tscheikner-Gratl F et al (2020) Application of electrochemical oxidation in cold climate regions—effect of temperature, pH and anode material on the degradation of Bisphenol A and the formation of disinfection by-products. *J Environ Chem Eng* 8:104183. <https://doi.org/10.1016/j.jece.2020.104183>
19. Jasper JT, Yang Y, Hoffmann MR (2017) Toxic byproduct formation during electrochemical treatment of latrine wastewater. *Environ Sci Technol* 51:7111–7119. <https://doi.org/10.1021/acs.est.7b01002>
20. Díaz V, Ibáñez R, Gómez P et al (2011) Kinetics of electro-oxidation of ammonia-N, nitrites and COD from a recirculating aquaculture saline water system using BDD anodes. *Water Res* 45:125–134. <https://doi.org/10.1016/j.watres.2010.08.020>
21. Standard Norge NS-EN 1484 (1997) Water analysis—guidelines for the determination of total organic carbon (TOC) and dissolved organic carbon (DOC)
22. Panizza M, Cerisola G (2004) Influence of anode material on the electrochemical oxidation of 2-naphthol part 2. *Bulk Electrolysis Exp* 49:3221–3226. <https://doi.org/10.1016/j.electacta.2004.02.036>
23. Cañizares P, Domínguez JA, Rodrigo MA et al (1999) Effect of the current intensity in the electrochemical oxidation of aqueous phenol wastes at an activated carbon and steel anode. *Ind Eng Chem Res* 38(10):3779–3785. <https://doi.org/10.1021/ie9901574>
24. Muff J, Sogaard EG (2010) Electrochemical degradation of PAH compounds in process water: a kinetic study on model solutions and a proof of concept study on runoff water from harbour sediment purification. *Water Sci Technol* 61:2043–2051. <https://doi.org/10.2166/wst.2010.129>
25. Ambauen N et al (2019) Insights into the kinetics of intermediate formation during electrochemical oxidation of the organic model pollutant salicylic acid in chloride electrolyte. *Water* 11:1322. <https://doi.org/10.3390/w11071322>
26. Fang J, Fu Y, Shang C (2014) The roles of reactive species in micropollutant degradation in the UV/free chlorine system. *Environ Sci Technol* 48:1859–1868. <https://doi.org/10.1021/es4036094>
27. Liao CH, Kang SF, Wu FA (2001) Hydroxyl radical scavenging role of chloride and bicarbonate ions in the H₂O₂/UV process. *Chemosphere* 44:1193–1200. [https://doi.org/10.1016/S0045-6535\(00\)00278-2](https://doi.org/10.1016/S0045-6535(00)00278-2)
28. El Hachemi ME, Naffrechoux E, Suptil J, Hausler R (2013) Bicarbonate effect in the ozone-UV process in the presence of nitrate. *Ozone Sci Eng* 35:302–307. <https://doi.org/10.1080/01919512.2013.794650>
29. Norwegian Environment Agency (2016) Grenseverdier for klassifisering av vann, sediment og biota. 24
30. Zhou M, Liu L, Jiao Y et al (2011) Treatment of high-salinity reverse osmosis concentrate by electrochemical oxidation on BDD and DSA electrodes. *Desalination* 277:201–206. <https://doi.org/10.1016/j.desal.2011.04.030>
31. de Moura DC, do Nascimento Brito C, Quiroz MA et al (2015) Cl-mediated electrochemical oxidation for treating an effluent using platinum and diamond anodes. *J Water Process Eng* 8:e31–e36. <https://doi.org/10.1016/j.jwpe.2014.11.005>
32. Kapalka A, Joss L, Anglada A et al (2010) Direct and mediated electrochemical oxidation of ammonia on boron-doped diamond electrode. *Electrochem Commun* 12:1714–1717. <https://doi.org/10.1016/j.elecom.2010.10.004>
33. Qiang Z, Adams CD (2004) Determination of monochloramine formation rate constants with stopped-flow spectrophotometry. *Environ Sci Technol* 38:1435–1444. <https://doi.org/10.1021/es0347484>
34. (1984) International Standard ISO 7510/1 Water quality—Determination of ammonium—Part 1: manual spectrometric method
35. Li L, Liu Y (2009) Ammonia removal in electrochemical oxidation: mechanism and pseudo-kinetics. *J Hazard Mater* 161:1010–1016. <https://doi.org/10.1016/j.jhazmat.2008.04.047>
36. Panizza M, Cerisola G (2006) Olive mill wastewater treatment by anodic oxidation with parallel plate electrodes. *Water Res*. <https://doi.org/10.1016/j.watres.2006.01.020>
37. Cabeza A, Urriaga A, Rivero MJ, Ortiz I (2007) Ammonium removal from landfill leachate by anodic oxidation. *J Hazard Mater* 144:715–719. <https://doi.org/10.1016/j.jhazmat.2007.01.106>
38. Chiang LC, Chang JE, Wen TC (1995) Indirect oxidation effect in electrochemical oxidation treatment of landfill leachate. *Water Res* 29:671–678. [https://doi.org/10.1016/0043-1354\(94\)00146-X](https://doi.org/10.1016/0043-1354(94)00146-X)
39. Tian Y, Zhu X, Ye J et al (2017) Influencing factors and chlorinated byproducts in electrochemical oxidation of bisphenol A with boron-doped diamond anodes. *Electrochim Acta* 246:1121–1130. <https://doi.org/10.1016/j.electacta.2017.06.163>
40. United States. Environmental Protection Agency. Office of Water Planning and Standards. Criteria and Standards Division (1979) Ambient Water Quality Criteria. Criteria and Standards Division, Office of Water Planning and Standards, U.S. Environmental Protection Agency
41. Dean KE, Palachek RM, Noel JM et al (2004) Development of freshwater water-quality criteria for perchlorate. *Environ Toxicol Chem* 23:1441–1451. <https://doi.org/10.1897/02-648>

Publisher's Note Springer Nature remains neutral with regard to jurisdictional claims in published maps and institutional affiliations.

APPENDIX B: ADDITIONAL DATA

Table 9: List of parameters that have to annually monitored in landfill leachate in Norway, from [7]

Parameter	Sigevann Kvartalsvis 1			Sigevannssediment 1 gang per år1	
	Kort-navn	Enhet	Best. gren- se2	Enhet	Best. gren- se2
ÅRLIG PROGRAM					
Surhetsgrad	pH				
Temperatur		°C			
Ledningsevne		mS/m	1		
Suspendert stoff	SS	mg/l			
Tørstoff innhold	TS			%w	
Korngradering					
Sporingsstoff (se omtale i kapittel 4.2.1)					
Kjemisk oksygenforbruk	KOF	mg/l	10		
Biokjemisk oksygenforbruk	BOF	mg/l	10		
Total organisk karbon	TOC	mg/l	10	mg/kg TS	1
Total nitrogen	N-tot	mg/l	0,1		
Ammonium nitrogen	NH3 / NH4+	mg/l	0,1		
Total fosfor	P-tot	mg/l	0,05		
Jern	Fe	mg/l	1	mg/kg TS	1
Mangan	Mn	mg/l	0,1	mg/kg TS	0,1
Sink	Zn	µg/l	3	mg/kg TS	3
Kobber	Cu	µg/l	1,5	mg/kg TS	1,5
Bly	Pb	µg/l	1	mg/kg TS	1
Kadmium	Cd	µg/l	0,1	mg/kg TS	0,1
Nikkel	Ni	µg/l	5	mg/kg TS	5
Krom	Cr	µg/l	1	mg/kg TS	1
Arsen	As	µg/l	2	mg/kg TS	2
Kvikksølv	Hg	µg/l	0,01	mg/kg TS	0,01
Fenoler		µg/l	0,5	mg/kg TS	0,5
Oljeforbindelser	Upolare HC	µg/l	100	mg/kg TS	100
Polysykliske aromatiske hydrokarboner	PAH16	µg/l	0,2	mg/kg TS	0,01
Monosykliske aromater	BTEX	µg/l	0,2		
Polyklorerte bifenyler	PCB7			mg/kg TS	0,002
Akutt toksisitet screening		TU			
TILLEGG HVERT 5. ÅR3					
Bred analyse av tungmetaller		µg/l		mg/kg TS	
Polybromerte difenyletere2	PBDE	µg/l	0,001	mg/kg TS	0,001
Heksabromcyklododekan2	HBCD	µg/l	0,01	mg/kg TS	0,01
Tetrabrom bisfenol A	TBBPA	µg/l	0,005	mg/kg TS	0,005
Bisfenol A		µg/l	0,001	mg/kg TS	0,001
Alkyfenoler og -etoksilater2		µg/l	0,5	mg/kg TS	0,05
Fenoler2		µg/l	0,5	mg/kg TS	0,5

¹ I etterdriftsfasen kan hyppigheten reduseres når overvåkingen viser at utlekkningen fra deponiet har stabilisert seg.

² Analyse må gjennomføres slik at bestemmelsesgrensen ikke er dårligere enn de angitte verdiene.

Continuation of Table 9:

Parameter	Kort-navn	Sigevann Kvartalsvis 1		Sigevannsediment 1 gang per år 1	
		Enhet	Best. gren- se2	Enhet	Best. gren- se2
Klorfenoler ²		µg/l	0,5	mg/kg TS	0,5
Tinnorganiske forbindelser		µg/l	0,01	mg/kg TS	0,01
Ftalater ²		µg/l	1	mg/kg TS	1
Klorbensener ²		µg/l	0,5	mg/kg TS	0,5
Flyktige klorerte hydrokarboner 2		µg/l	0,2		
Lineære alkylbensensulfonater	LAS	µg/l	20		
Fenoksyser ²		µg/l	0,5		
Klorerte paraffiner ²				mg/kg TS	0,001
Polyklorerte naftalener ²				mg/kg TS	0,1
Polyklorerte dibenzodioxiner/furaner ²				mg/kg TS	0,000001
Klorerte pesticider ²				mg/kg TS	0,05
Akutt toksisitet vannplanter/alge		TU			
Akutt toksisitet krepsdyr		TU			
Mutagenitetstest					

Table 10: List of Norwegian priority hazardous substances from [5], [8]

	Substance (short)
1)	Arsenic
2)	Bisphenol A
3)	Brominated flame retardants
4)	DEHP
5)	Certain surfactants (DTDMAC, DSDMAC, DHTDMAC)
6)	1,2-Dichlorethane (EDC)
7)	Dioxins and furans
8)	Cadmium
9)	Chlorinated alkyl benzenes (CABs)
10)	Chromium
11)	Hexachlorbenzene
12)	Lead
13)	Medium-chain chlorinated paraffins
14)	Mercury
15)	Musk xylenes
16)	Nonylphenol and its ethoxylates
17)	Octylphenol and its ethoxylates
18)	PAHs
19)	Pentachlorphenol (PCP)
20)	Polychlorinated biphenyls (PCBs)
21)	PFOA
22)	PFOS
23)	Short-chain chlorinated paraffins
24)	Siloxane-D4
25)	Siloxane-D5
26)	TCEP (tris(2-chloroethyl)phosphate)
27)	Tetrachloroethene (PER)
28)	Tributyl tin compounds
29)	Trichlorobenzene
30)	Trichloroethene (TRI)
31)	Triclosan
32)	2.4.6 Tri-tert-butylphenol ^l

Table 11: Complete list of parameters measured in the landfill leachate from 2006-2019

Parameter	Forkortelse	Enhet	Gjennomsnitt (2006--2019)
Surhetsgrad	pH		6,732075
Temperatur, måling pH		°C	22,35789
Ledningsevne		mS/m	245,9444
Suspendert stoff	SS	mg/l	82,64444
Sporingsstoff	Na	mg/l	186,3962
Kjemisk oksygenforbruk	KOF-Cr	mg/l	196,7593
Biokjemisk oksygenforbruk	BOF5	mg/l	15
Total organisk karbon	TOC	mg/l	55,63077
Total nitrogen	N-tot	mg/l	97,82963
Ammonium nitrogen	NH3/NH4+	mg/l	90,42296
Total fosfor	P-tot	mg/l	0,485926
Klorid	Cl	mg/l	165,8
Jern	Fe	mg/l	30,086
Mangan	Mn	mg/l	1,312113
Sink	Zn	µg/l	68,97222
Kobber	Cu	µg/l	10,12979
Bly	Pb	µg/l	1,714644
Kadmium	Cd	µg/l	0,1381
Nikkel	Ni	µg/l	15,4487
Krom	Cr	µg/l	14,60278
Arsen	As	µg/l	4,009375
Kvikksølv	Hg	µg/l	0,029688
Kalsium	Ca	mg/l	137,1176
Kalium	K	mg/l	77,47647
Magnesium	Mg	mg/l	26,47647
Aluminium	Al	µg/l	320,99
Barium	Ba	µg/l	121,975
Kobolt	Co	µg/l	4,824737
Tinn	Sn	µg/l	
Vanadium	V	µg/l	7,4
Oljeforbindelser	Upolare HC		
- fraksjon >C10-C12		µg/l	31,07
- fraksjon >C12-C16		µg/l	45,09574
- fraksjon >C16-C35		µg/l	101,1172
- fraksjon >C35-C40		µg/l	18
- olje >C10-C40		µg/l	206,075

Polysykliske arom. hydrok.	PAH16	µg/l	
- naftalen	PAH-NAF	µg/l	2,320086
- acenaftylen	PAH-ANY	µg/l	0,027556
- acenaften	PAH-ANA	µg/l	0,449882
- fluoren	PAH-FLU	µg/l	0,317388
- fenantren	PAH-FEN	µg/l	0,302318
- antracen	PAH-ANT	µg/l	0,047657
- fluoranten	PAH-FLA	µg/l	0,065065
- pyren	PAH-PYR	µg/l	0,047478
- benso(a)antracen^	PAH-BAA	µg/l	0,021111
- chrysen^	PAH-CHR	µg/l	0,034917
- benso(b)fluoranten^	PAH-BBK	µg/l	0,03
- benso(k)fluoranten^	PAH-	µg/l	0,016
- benso(a)pyren^	PAH-BAP	µg/l	0,016333
- dibenso(a,h)antracen^	PAH-DAH	µg/l	0,011
- benso(ghi)perylen	PAH-BGP	µg/l	0,016667
- indenol(123cd)pyren^	PAH-IPY	µg/l	0,017
- PAH-sum		µg/l	2,704577
- PAH-sum carciogene^			0,065364
Monosykliske aromater	BTEX	µg/l	
- benzen		µg/l	6,414444
- toluen		µg/l	8,5225
- etylbenzen		µg/l	6,552222
- o-xylen		µg/l	3,303617
- m/p-xylen		µg/l	8,742143
- sum aromater (BTEX)		µg/l	18,7213
Akutt toksisitet screening	Microtox	TU	7,582353
Fluorid		mg/l	3,91

*Analysen akkreditert fra 2009

1) Terskelverdi ut fra "Veileder om miljørisikivurdering av bunntetting og oppsamling av sigevann ved deponier" TA-1995/2003 vedlegg IV.

3) Summen av benso(b)fluoranten og benso(k)fluoranten.

N/A = not available

Sigevann - hvert 5. år

Kvartal:

Uttaksdato: 40949,44

Lab.nr.:

Parameter	Forkortelse	Enhet	average (hvert 5. år)
Polybromerte difenyletere	PBDE	µg/l	
- PBDE-99		µg/l	0,001062
- PBDE-154		µg/l	0,00041
- PBDE-203		µg/l	
- PBDE-209		µg/l	
Heksabromcyklododekan	HBCD	µg/l	
Tetrabrom bisfenol A	TBBPA	µg/l	0,039
Bisfenol A		µg/l	13,76667
Alkylfenoler og -etoksilater		µg/l	
- nonylfenolmonoetoksilat	NP1EO	µg/l	0,667333
- nonylfenoldietoksilat	NP2EO	µg/l	0,4645
- oktylfenolpolyetoksilater		µg/l	
- - OP1EO		µg/l	0,0415
- - OP2EO		µg/l	0,028
- - OP3EO		µg/l	0,047
- - OP4EO		µg/l	0,074
- - OP5EO		µg/l	
- - OP6EO		µg/l	
- 4-n-nonylfenol		µg/l	
- 4-t-oktylfenol		µg/l	0,281417
Fenoler		µg/l	
- fenol		µg/l	5,546
- o-kresol		µg/l	1,025
- m-kresol		µg/l	4,41
- p-kresol		µg/l	13,59167
- 2,3-dimetylphenol		µg/l	0,397778
- 2,4-dimetylphenol		µg/l	1,138
- 2,5-dimetylphenol		µg/l	0,295
- 2,6-dimetylphenol		µg/l	0,991818
- 3,4-dimetylphenol		µg/l	0,886667
- 3,5-dimetylphenol		µg/l	3,140833
- 2,4,6-trimetylphenol		µg/l	0,343333
- 2,3,5-trimetylphenol		µg/l	0,211667
- 2-n-propylphenol		µg/l	0,113333
- 4-n-propylphenol		µg/l	0,265
- 2-isopropylphenol		µg/l	0,880833
- 3-tert.butylphenol		µg/l	

Sum alkylfenoler		µg/l	40,1925
Klorfenoler		µg/l	
- pentaklorfenol	PCP	µg/l	
Tinnorganiske forbindelser		µg/l	
- tributyltinn	TBT	µg/l	0,00595
- trifenyлтinn	TFT	µg/l	
Ftalater		µg/l	
- diisononylftalat	DINP	µg/l	
- di-(2-etylhexyl)ftalat	DEHP	µg/l	11
- diisodekylftalat	DIDP	µg/l	
Klorbenzener		µg/l	
- 1,2,3-triklorbenzen		µg/l	0,022
- 1,2,4-triklorbenzen		µg/l	0,023875
- 1,3,5-triklorbenzen		µg/l	1,9
- hexaklorbenzen	HCB	µg/l	
Flyktige klorerte hydrokarb.		µg/l	
- 1,2-dikloreтан	EDC	µg/l	
- triklormetan		µg/l	
- 1,1,1-trikloreтан		µg/l	
- 1,1,2-trikloreтан		µg/l	
- trikloreтан	TRI	µg/l	0,11
- tetrakloreтан	PER	µg/l	
Lineæ. alkylbenz.sulfonater	LAS	µg/l	
- C9-alkyl-bensensulfonat		µg/l	
- C10-alkyl-bensensulfonat		µg/l	2,2
- C11-alkyl-bensensulfonat		µg/l	3,1
- C12-alkyl-bensensulfonat		µg/l	1,1
- C13-alkyl-bensensulfonat		µg/l	
- C14-alkyl-bensensulfonat		µg/l	
- C15-alkyl-bensensulfonat		µg/l	
Fenoksysyrer (pesticider)		µg/l	
- 2,4-D		µg/l	0,069
- MCPA		µg/l	1,0915
- MCPP		µg/l	2,05944
- 2,4,5-T		µg/l	
- 2,4,5-TP		µg/l	
- MCPB		µg/l	
- 2,4-DB		µg/l	
- 2,4-DP		µg/l	0,305182

Sum fenoksysyrer		µg/l	2,518231
Akutt toksisitet vannpl./alge	Scen.Subsp.	TU	1,875
Akutt toksisitet krepsdyr	Daphnia M.	TU	1,666667
Mutagenitetstest (AMES test)			

1) Terskelverdi ut fra "Veileder om miljørisikivurdering av bunntetting og oppsamling av sigevann ved deponier" TA-1995/2003 vedlegg IV.

2) Ikke akkrediterte analyser fram til desember 2006.

N/A = not available

Table 12: Landfill leachate composition around the world, adapted from [15]; all values except for pH [-] given in [mg/L],[118]

Age*	Landfill site	COD	BOD	BOD/ COD	pH	SS	TKN	NH ₃ -N
Y	Canada	13,800	9660	0.7	5.8	–	212	42
Y	Canada	1870	90	0.05	6.58	–	75	10
Y	China, Hong Kong	15,700	4200	0.27	7.7	–	–	2,260
Y	China, Hong Kong	17,000	7300	0.43	7.0– 8.3	>5000	3,200	3,000
Y		13,000	5000	0.38	6.8– 9.1	2000	11,000	11,000
Y		50,000	22,000	0.44	7.8– 9.0	2000	13,000	13,000
Y	China, Mainland	1900– 3180	3700–8890	0.36– 0.51	7.4– 8.5	–	–	630– 1,800
Y	Greece	70,900	26,800	0.38	6.2	950	3,400	3,100
Y	Italy	19,900	4000	0.2	8	–	–	3,917
Y	Italy	10,540	2300	0.22	8.2	1666	–	5,210
Y	South Korea	24,400	10,800	0.44	7.3	2400	1,766	1,682
Y	Turkey	16,200– 20,000 35,000– 50,000	10,800– 11,000 21,000– 25,000	0.55– 0.67 0.5–0.6	7.3– 7.8 5.6– 7.0	–	–	1,120– 2,500 2,020
Y	Turkey	35,000– 50,000	21,000– 25,000	0.5–0.6	5.6– 7.0	2630– 3930	2,370	2,020
Y	Turkey	10,750– 18,420	6380–9660	0.52– 0.59	7.7– 8.2	1013– 1540	–	1,946– 2,002
MA	Canada	3210– 9190	–	–	6.9– 9.0	–	–	–
MA	China	5800	430	0.07	7.6	–	–	–

MA	China, Hong Kong	7439	1436	0.19	8.22	784	–	–
MA	Germany	3180	1060	0.33	–	–	1,135	884
MA	Germany	4000	800	0.2	–	–	–	800
MA	Greece	5350	1050	0.2	7.9	480	1,100	940
MA	Italy	5050	1270	0.25	8.38	–	1,670	1,330
MA	Italy	3840	1200	0.31	8	–	–	–
MA	Poland	1180	331	0.28	8	–	–	743
MA	Taiwan	6500	500	0.08	8.1	–	–	5,500
MA	Turkey	9500	–	–	8.15	–	1,450	1,270
O	Brazil	3460	150	0.04	8.2	–	–	800
O	Estonia	2170	800	0.37	11.5	–	–	–
O	Finland	556	62	0.11	–	–	192	159
O	Finland	340–920	84	0.09– 0.25	7.1– 7.6	–	–	330– 560
O	France	500	7.1	0.01	7.5	130	540	430
O	France	100	3	0.03	7.7	13– 1480	5–960	0.2
O	France	1930	–	–	7	–	–	295
O	Malaysia	1533– 2580	48–105	0.03– 0.04	7.5– 9.4	159– 233	–	–
O	South Korea	1409	62	0.04	8.57	404	141	1,522
O	Turkey	10,000	–	–	8.6	1600	1,680	1,590

* Age: Y: young, MA: medium age, O: old

APPENDIX C: PERMISSIONS AND STATEMENTS



Search for Articles:

About

[For Authors](#)

[For Reviewers](#)

[For Editors](#)

[For Librarians](#)

[For Publishers](#)

[For Societies](#)

[Article Processing Charges](#)

MDPI Open Access Information and Policy

All articles published by MDPI are made immediately available worldwide under an open access license. This means:

- everyone has free and unlimited access to the full-text of *all* articles published in MDPI journals;
- everyone is free to re-use the published material if proper accreditation/citation of the original publication is given;
- open access publication is supported by the authors' institutes or research funding agencies by payment of a comparatively low [Article Processing Charge \(APC\)](#) for accepted articles.

Permissions

No special permission is required to reuse all or part of article published by MDPI, including figures and tables. For articles published under an open access Creative Common CC BY license, any part of the article may be reused without permission provided that the original article is clearly cited. Reuse of an article does not imply endorsement by the authors or MDPI.



Application of electrochemical oxidation in cold climate regions – Effect of temperature, pH and anode material on the degradation of Bisphenol A and the formation of disinfection by-products

Author: Noëmi Ambauen, Jens Muff, Franz Tscheikner-Gratl, Thuat T. Trinh, Cynthia Hallé, Thomas Meyn

Publication: Journal of Environmental Chemical Engineering

Publisher: Elsevier

Date: October 2020

© 2020 Elsevier Ltd. All rights reserved.

Please note that, as the author of this Elsevier article, you retain the right to include it in a thesis or dissertation, provided it is not published commercially. Permission is not required, but please ensure that you reference the journal as the original source. For more information on this and on your other retained rights, please visit: <https://www.elsevier.com/about/our-business/policies/copyright#Author-rights>

BACK

CLOSE WINDOW

Author reuse

Please check the Copyright Transfer Statement (CTS) or Licence to Publish (LTP) that you have signed with Springer Nature to find further information about the reuse of your content.

Authors have the right to reuse their article's Version of Record, in whole or in part, in their own thesis. Additionally, they may reproduce and make available their thesis, including Springer Nature content, as required by their awarding academic institution. Authors must properly cite the published article in their thesis according to current citation standards.

Material from: '[AUTHOR, TITLE, JOURNAL TITLE, published [YEAR], [publisher - as it appears on our copyright page]'

If you are any doubt about whether your intended re-use is covered, please contact journalpermissions@springernature.com for confirmation.

Self-Archiving

- Journal authors retain the right to self-archive the final accepted version of their manuscript. Please see our self-archiving policy for full details:

<https://www.springer.com/gp/open-access/authors-rights/self-archiving-policy/2124>

- Book authors please refer to the information on this link:

<https://www.springer.com/gp/open-access/publication-policies/self-archiving-policy>

My Account

[Shopping Cart](#)
[MySpringer](#)
[Login](#)
[SpringerAlerts](#)

About Springer

[History](#)
[Media](#)
[Compliance](#)
[Careers](#)
[Affiliate Program](#)

Help & Contact

[FAQ](#)
[Help Overview](#)
[Contact Us](#)
[Imprint](#)



SPRINGER NATURE

© 2020 Springer Nature Switzerland AG. Springer is part of [Springer Nature](#) | [General Terms & Conditions](#) • [Privacy Policy](#)


DECLARATION OF CO-AUTHORSHIP

Noëmi Ambauen applies for the evaluation of the following thesis:

Removal of organic pollutants from landfill leachate by electrochemical oxidation

Assessment of performance and applicability in Northern Norway

*)The declaration should describe the work process and division of labor, **specifically identifying the candidate's contribution**, as well as give consent to the article being included in the thesis.

<p>*) Declaration of co-authorship on the following article:</p> <p>Insights into the Kinetics of Intermediate Formation during Electrochemical Oxidation of the Organic Model Pollutant Salicylic Acid in Chloride Electrolyte <i>Water 2019, 11, 1322; doi:10.3390/w11071322</i></p> <p>Authors: Noemi Ambauen, Jens Muff, Ngoc Lan Mai, Thuat T. Trinh, Cynthia Hallé, Thomas Meyn</p> <p>I hereby declare that I am aware that the article mentioned above, of which I am co-author, will form a part of the PhD thesis by the PhD candidate Noëmi Ambauen who made a major contribution to the work in the experiments, data analysis and writing phase. I hereby consent to the article being included in the thesis.</p> <div style="display: flex; justify-content: space-between; margin-top: 20px;"> <div style="text-align: left;"> <p>24.7.2020 Esbjerg</p> <p>..... Place, date</p> </div> <div style="text-align: right;">  <p>..... Signature co-author</p> </div> </div>

*)

Declaration of co-authorship on the following article:

Insights into the Kinetics of Intermediate Formation during Electrochemical Oxidation of the Organic Model Pollutant Salicylic Acid in Chloride Electrolyte*Water* 2019, 11, 1322; doi:10.3390/w11071322**Authors: Noemi Ambauen, Jens Muff, Ngoc Lan Mai, Thuat T. Trinh, Cynthia Hallé, Thomas Meyn**

I hereby declare that I am aware that the article mentioned above, of which I am co-author, will form a part of the PhD thesis by the PhD candidate Noëmi Ambauen who made a major contribution to the work in the experiments, data analysis and writing phase. I hereby consent to the article being included in the thesis.

Hochiminh, 23.7.2020

Place, date



Signature co-author

*)

Declaration of co-authorship on the following article:

Insights into the Kinetics of Intermediate Formation during Electrochemical Oxidation of the Organic Model Pollutant Salicylic Acid in Chloride Electrolyte*Water* 2019, 11, 1322; doi:10.3390/w11071322**Authors: Noemi Ambauen, Jens Muff, Ngoc Lan Mai, Thuat T. Trinh, Cynthia Hallé, Thomas Meyn**

I hereby declare that I am aware that the article mentioned above, of which I am co-author, will form a part of the PhD thesis by the PhD candidate Noëmi Ambauen who made a major contribution to the work in the experiments, data analysis and writing phase. I hereby consent to the article being included in the thesis.

Trondheim, 23.07.2020

Place, date



Signature co-author

*)

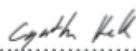
Declaration of co-authorship on the following article:

Insights into the Kinetics of Intermediate Formation during Electrochemical Oxidation of the Organic Model Pollutant Salicylic Acid in Chloride Electrolyte*Water* 2019, 11, 1322; doi:10.3390/w11071322**Authors: Noemi Ambauen, Jens Muff, Ngoc Lan Mai, Thuat T. Trinh, Cynthia Hallé, Thomas Meyn**

I hereby declare that I am aware that the article mentioned above, of which I am co-author, will form a part of the PhD thesis by the PhD candidate Noëmi Ambauen who made a major contribution to the work in the experiments, data analysis and writing phase. I hereby consent to the article being included in the thesis.

Trondheim, 08/05/2020

Place, date



Signature co-author

*)

Declaration of co-authorship on the following article:

Insights into the Kinetics of Intermediate Formation during Electrochemical Oxidation of the Organic Model Pollutant Salicylic Acid in Chloride Electrolyte*Water* 2019, 11, 1322; doi:10.3390/w11071322**Authors: Noemi Ambauen, Jens Muff, Ngoc Lan Mai, Thuat T. Trinh, Cynthia Hallé, Thomas Meyn**

I hereby declare that I am aware that the article mentioned above, of which I am co-author, will form a part of the PhD thesis by the PhD candidate Noëmi Ambauen who made a major contribution to the work in the experiments, data analysis and writing phase. I hereby consent to the article being included in the thesis.

Trondheim, 08/09/2020

Place, date



Signature co-author

DECLARATION OF CO-AUTHORSHIP

Noëmi Ambauen applies for the evaluation of the following thesis:

Removal of organic pollutants from landfill leachate by electrochemical oxidation

Assessment of performance and applicability in Northern Norway

*)The declaration should describe the work process and division of labor, **specifically identifying the candidate's contribution**, as well as give consent to the article being included in the thesis.

*)

Declaration of co-authorship on the following article:

Application of electrochemical oxidation in cold climate regions – Effect of temperature, pH and anode material on the degradation of Bisphenol A and the formation of disinfection by-products
Journal of Environmental Chemical Engineering, <https://doi.org/10.1016/j.jece.2020.104183>

Authors: Noemi Ambauen, Jens Muff, Franz Tschickner-Gratl, Thuat T. Trinh, Cynthia Hallé, Thomas Meyn

I hereby declare that I am aware that the article mentioned above, of which I am co-author, will form a part of the PhD thesis by the PhD candidate Noëmi Ambauen who made a major contribution to the work in the experiments, data analysis and writing phase. I hereby consent to the article being included in the thesis.

.....
 Place, date

.....
 Signature co-author

*)

Declaration of co-authorship on the following article:

Application of electrochemical oxidation in cold climate regions – Effect of temperature, pH and anode material on the degradation of Bisphenol A and the formation of disinfection by-products
Journal of Environmental Chemical Engineering, <https://doi.org/10.1016/j.jece.2020.104183>

Authors: Noemi Ambauen, Jens Muff, Franz Tscheickner-Gratl, Thuat T. Trinh, Cynthia Hallé, Thomas Meyn

I hereby declare that I am aware that the article mentioned above, of which I am co-author, will form a part of the PhD thesis by the PhD candidate Noëmi Ambauen who made a major contribution to the work in the experiments, data analysis and writing phase. I hereby consent to the article being included in the thesis.

Trondheim, 03.08.2020

Place, date


Signature co-author

*)

Declaration of co-authorship on the following article:


Application of electrochemical oxidation in cold climate regions – Effect of temperature, pH and anode material on the degradation of Bisphenol A and the formation of disinfection by-products
Journal of Environmental Chemical Engineering, <https://doi.org/10.1016/j.jece.2020.104183>

Authors: Noemi Ambauen, Jens Muff, Franz Tscheickner-Gratl, Thuat T. Trinh, Cynthia Hallé, Thomas Meyn

I hereby declare that I am aware that the article mentioned above, of which I am co-author, will form a part of the PhD thesis by the PhD candidate Noëmi Ambauen who made a major contribution to the work in the experiments, data analysis and writing phase. I hereby consent to the article being included in the thesis.

Trondheim, 08/05/2020

Place, date


Signature co-author

*)

Declaration of co-authorship on the following article:

Application of electrochemical oxidation in cold climate regions – Effect of temperature, pH and anode material on the degradation of Bisphenol A and the formation of disinfection by-products
Journal of Environmental Chemical Engineering, <https://doi.org/10.1016/j.jece.2020.104183>

Authors: Noemi Ambauen, Jens Muff, Franz Tschickner-Gratl, Thuat T. Trinh, Cynthia Hallé, Thomas Meyn

I hereby declare that I am aware that the article mentioned above, of which I am co-author, will form a part of the PhD thesis by the PhD candidate Noëmi Ambauen who made a major contribution to the work in the experiments, data analysis and writing phase. I hereby consent to the article being included in the thesis.

Trondheim, 06.08.2020

.....
Place, date.....
Signature co-author

*)

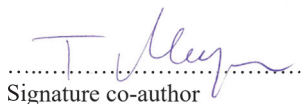
Declaration of co-authorship on the following article:

Application of electrochemical oxidation in cold climate regions – Effect of temperature, pH and anode material on the degradation of Bisphenol A and the formation of disinfection by-products
Journal of Environmental Chemical Engineering, <https://doi.org/10.1016/j.jece.2020.104183>

Authors: Noemi Ambauen, Jens Muff, Franz Tschickner-Gratl, Thuat T. Trinh, Cynthia Hallé, Thomas Meyn

I hereby declare that I am aware that the article mentioned above, of which I am co-author, will form a part of the PhD thesis by the PhD candidate Noëmi Ambauen who made a major contribution to the work in the experiments, data analysis and writing phase. I hereby consent to the article being included in the thesis.

Trondheim, 08/09/2020

.....
Place, date.....
Signature co-author

DECLARATION OF CO-AUTHORSHIP

Noëmi Ambauen applies for the evaluation of the following thesis:

Removal of organic pollutants from landfill leachate by electrochemical oxidation

Assessment of performance and applicability in Northern Norway

*)The declaration should describe the work process and division of labor, **specifically identifying the candidate's contribution**, as well as give consent to the article being included in the thesis.

*)

Declaration of co-authorship on the following article:

Electrochemical removal of Bisphenol A from Landfill Leachate under Nordic Climate Conditions
Journal of applied electrochemistry (under review)

Authors: Noemi Ambauen, Jens Muff, Cynthia Hallé, Thomas Meyn

I hereby declare that I am aware that the article mentioned above, of which I am co-author, will form a part of the PhD thesis by the PhD candidate Noëmi Ambauen who made a major contribution to the work in the experiments, data analysis and writing phase. I hereby consent to the article being included in the thesis.

22/7-2020
 Esbjørn

.....
 Place, date



 Signature co-author

*)

Declaration of co-authorship on the following article:

Electrochemical removal of Bisphenol A from Landfill Leachate under Nordic Climate Conditions*Journal of applied electrochemistry (under review)***Authors: Noemi Ambauen, Jens Muff, Cynthia Hallé, Thomas Meyn**

I hereby declare that I am aware that the article mentioned above, of which I am co-author, will form a part of the PhD thesis by the PhD candidate Noëmi Ambauen who made a major contribution to the work in the experiments, data analysis and writing phase. I hereby consent to the article being included in the thesis.

Trondheim, 08/05/2020

Place, date



Signature co-author

*)

Declaration of co-authorship on the following article:

Electrochemical removal of Bisphenol A from Landfill Leachate under Nordic Climate Conditions*Journal of applied electrochemistry (under review)***Authors: Noemi Ambauen, Jens Muff, Cynthia Hallé, Thomas Meyn**

I hereby declare that I am aware that the article mentioned above, of which I am co-author, will form a part of the PhD thesis by the PhD candidate Noëmi Ambauen who made a major contribution to the work in the experiments, data analysis and writing phase. I hereby consent to the article being included in the thesis.

Trondheim, 08/09/2020

Place, date



Signature co-author

*)

Declaration of co-authorship on the following article:

Electrochemical removal of Bisphenol A from Landfill Leachate under Nordic Climate Conditions*Journal of applied electrochemistry (under review)***Authors: Noemi Ambauen, Jens Muff, Cynthia Hallé, Thomas Meyn**

I hereby declare that I am aware that the article mentioned above, of which I am co-author, will form a part of the PhD thesis by the PhD candidate Noëmi Ambauen who made a major contribution to the work in the experiments, data analysis and writing phase. I hereby consent to the article being included in the thesis.

Trondheim, 14/09/2020

.....
Place, date

C. Weber

.....
Signature co-author

ISBN 978-82-326-5138-2 (printed ver.)
ISBN 978-82-326-5139-9 (electronic ver.)
ISSN 2703-8084 (online)
ISSN 1503-8181 (printed ver.)



NTNU

Norwegian University of
Science and Technology